

อนุภาคระดับนาโนเมตรของไทโอเลตเตดแคตไอออนิกแอมิโนเซลลูโลสที่มีสมบัติยึดติดเยื่อเมือกชนิด
ใหม่สำหรับการนำส่งยา



นางสาวกุลธิดา ทรงสุรางค์

จุฬาลงกรณ์มหาวิทยาลัย

CHULALONGKORN UNIVERSITY

บทคัดย่อและแฟ้มข้อมูลฉบับเต็มของวิทยานิพนธ์ตั้งแต่ปีการศึกษา 2554 ที่ให้บริการในคลังปัญญาจุฬาฯ (CUIR)
เป็นแฟ้มข้อมูลของนิสิตเจ้าของวิทยานิพนธ์ ที่ส่งผ่านทางบัณฑิตวิทยาลัย

The abstract and full text of theses from the academic year 2011 in Chulalongkorn University Intellectual Repository (CUIR)
are the thesis authors' files submitted through the University Graduate School.

วิทยานิพนธ์นี้เป็นส่วนหนึ่งของการศึกษาตามหลักสูตรปริญญาวิทยาศาสตรดุษฎีบัณฑิต

สาขาวิชาปิโตรเคมี

คณะวิทยาศาสตร์ จุฬาลงกรณ์มหาวิทยาลัย

ปีการศึกษา 2557

ลิขสิทธิ์ของจุฬาลงกรณ์มหาวิทยาลัย

NOVEL MUCOADHESIVE THIOLATED CATIONIC AMINOCELLULOSE NANOPARTICLES FOR
DRUG DELIVERY



A Dissertation Submitted in Partial Fulfillment of the Requirements
for the Degree of Doctor of Philosophy Program in Petrochemistry

Faculty of Science

Chulalongkorn University

Academic Year 2014

Copyright of Chulalongkorn University

Thesis Title	NOVEL MUCOADHESIVE THIOLATED CATIONIC AMINOCELLULOSE NANOPARTICLES FOR DRUG DELIVERY
By	Miss Kultida Songsurang
Field of Study	Petrochemistry
Thesis Advisor	Associate Professor Nongnuj Muangsin, Ph.D.
Thesis Co-Advisor	Krisana Siralermukul, Ph.D.

Accepted by the Faculty of Science, Chulalongkorn University in Partial Fulfillment of the Requirements for the Doctoral Degree

.....Dean of the Faculty of Science
(Professor Supot Hannongbua, Dr.rer.nat.)

THESIS COMMITTEE

.....Chairman
(Assistant Professor Warinthorn Chavasiri, Ph.D.)

.....Thesis Advisor
(Associate Professor Nongnuj Muangsin, Ph.D.)

.....Thesis Co-Advisor
(Krisana Siralermukul, Ph.D.)

.....Examiner
(Assistant Professor Varawut Tangpasuthadol, Ph.D.)

.....Examiner
(Associate Professor Nuanphun Chantarasiri, Ph.D.)

.....External Examiner
(Assistant Professor Nalena Praphairaksit, Ph.D.)

กุลธิดา ทรงสุรางค์ : อนุภาคระดับนาโนเมตรของไทโอเลตเตดแคตไอออนิกแอมิโนเซลลูโลสที่มีสมบัติยึดติดเยื่อเมือกชนิดใหม่สำหรับการนำส่งยา (NOVEL MUCOADHESIVE THIOLATED CATIONIC AMINOCELLULOSE NANOPARTICLES FOR DRUG DELIVERY) อ.ที่ปรึกษาวิทยานิพนธ์หลัก: รศ. ดร.นงนุช เหมืองสิน, อ.ที่ปรึกษาวิทยานิพนธ์ร่วม: ดร.กฤษณา ศิริเลิศมุกุล, 94 หน้า.

วัตถุประสงค์ของงานวิจัยนี้คือการออกแบบและเตรียมลักษณะตัวนำส่งยาแบบรับประทานที่มีสมบัติยึดติดเยื่อเมือกชนิดใหม่ ในงานวิจัยนี้ได้สังเคราะห์แอมฟิฟิลิกไทโอเลตเตดแคตไอออนิกแอมิโนเซลลูโลส ภายใต้สภาวะไม่รุนแรงและให้ปริมาณผลิตภัณฑ์ที่สูง การตรึงหมู่ที่มีประจุบวกและหมู่ไทออลบนเซลลูโลส ส่งผลให้ประสิทธิภาพในการยึดเกาะเยื่อเมือกเพิ่มมากขึ้นในทุกสภาวะการทดลอง (ของเหลวจำลองระบบทางเดินอาหาร: พีเอช 1.2, 6.8 และ 7.4) เซลลูโลสตัดแปรที่มีคุณสมบัติยึดติดเยื่อเมือกสามารถเกิดการรวมตัวกันเองได้ในสารละลายที่มีน้ำเป็นตัวทำละลาย ขนาดเส้นผ่านศูนย์กลางเฉลี่ยของอนุภาคอยู่ในช่วง 230-550 นาโนเมตร และค่าความต่างศักย์ระหว่างศักย์ไฟฟ้าบริเวณพื้นอยู่ในช่วง +25 ถึง +28 มิลลิโวลต์ การกระจายตัวของขนาดอนุภาคที่มีและไม่มียาแคมป์โธทีซินค่อนข้างแคบและมีประสิทธิภาพในการควบคุมการกักเก็บยาที่สูง (ประมาณ 90 เปอร์เซ็นต์) อีกทั้งสามารถควบคุมการปลดปล่อยยาของอนุพันธ์เซลลูโลสที่มีคุณสมบัติยึดเกาะเยื่อเมือกได้นานถึง 7 วัน อัตราการปลดปล่อยยาแคมป์โธทีซินจากอนุภาคระดับนาโนเมตรของตัวปลดปล่อยยาเพิ่มมากขึ้นอย่างมีนัยสำคัญโดยการเพิ่มพีเอชและปริมาณยา ดังนั้นอนุภาคระดับนาโนเมตรของอนุพันธ์เซลลูโลสที่มีคุณสมบัติยึดติดเยื่อเมือกมีแนวโน้มที่เหมาะสมเป็นตัวนำส่งในการประยุกต์ใช้ทางยาด้านต่าง ๆ โดยเฉพาะระบบการนำส่งยาที่ละลายน้ำได้ในปริมาณน้อย

สาขาวิชา ปีโตรเคมี

ลายมือชื่อนิสิต

ปีการศึกษา 2557

ลายมือชื่อ อ.ที่ปรึกษาหลัก

ลายมือชื่อ อ.ที่ปรึกษาร่วม

5373915023 : MAJOR PETROCHEMISTRY

KEYWORDS: AMPHIPHILIC THIOLATED CATIONIC AMINOCELLULOSE / MUCOADHESIVE POLYMER / CAMPTOTHECIN / DRUG DELIVERY CARRIER

KULTIDA SONGSURANG: NOVEL MUCOADHESIVE THIOLATED CATIONIC AMINOCELLULOSE NANOPARTICLES FOR DRUG DELIVERY. ADVISOR: ASSOC. PROF. NONGNUJ MUANGSIN, Ph.D., CO-ADVISOR: KRISANA SIRALERTMUKUL, Ph.D., 94 pp.

The purpose of this study was to design and prepare a novel oral mucoadhesive drug carrier. In this regard, an amphiphilic thiolated cationic aminocellulose was easily synthesized under mild homogeneous conditions with high yield. The immobilization of cationic and thiol groups onto the cellulose resulted in strongly improved mucoadhesive properties at all three tested pH values (the simulated gastrointestinal fluid: pH 1.2, 6.8 and 7.4). The mucoadhesive modified cellulose could self-assemble to form nanosized particles with a good stability in aqueous medium. The mean diameter of the particles was in the range of 230–550 nm, and zeta potential was determined to be +25 to +28 mV. The size distribution of the particles with/without camptothecin (CPT) was relatively narrow and yielded a high EE (over 90%). Moreover, the *in vitro* drug release from mucoadhesive cellulose derivatives nanoparticles could be prolonged for 7 days. The release rate of CPT from the nanocarriers was significantly accelerated by increasing pH and drug content. Therefore, mucoadhesive cellulose derivatives nanoparticles seem to be a promising carrier for various pharmaceutical applications especially for poorly water soluble drug delivery system.

Field of Study: Petrochemistry

Academic Year: 2014

Student's Signature

Advisor's Signature

Co-Advisor's Signature

ACKNOWLEDGEMENTS

Firstly and foremost I would like to express the deepest gratitude to my supervisor and co-advisor, Assoc. Prof. Nongnuj Muangsin and Dr. Krisana Siralermukul for intellectual support, supervision, and enthusiasm throughout the completion of my doctoral study. I am most grateful for their teaching and advice, not only the research methodologies but also many other methodologies in life. I appreciate all her contributions of time, ideas, and funding to make my Ph.D. experience productive and stimulating. The joy and enthusiasm she has for her research was contagious and motivational for me, even during tough times in the Ph.D. pursuit. I would not have achieved this far and this thesis would not have been completed without all the support that I have always received from her.

Secondly, I also deeply appreciate the members of my committee: Assist. Prof. Warinthorn Chavasiri, Assist. Prof. Varawut Tangpasuthadol and Assoc. Prof. Nuanphun Chantarasiri of Chulalongkorn University, and Assist. Prof. Nalena Praphiraksit of Srinakharinwirot University for their helpful comments

I am particularly very grateful to Chulalongkorn University and the Thailand Research Fund through the Royal Golden Jubilee Ph.D. Program (Grant No. PHD/0099/2554) for financial support during my doctoral study. Furthermore, I am particularly very grateful to the Doctoral Dual Degree Program (JAIST-CU) for financial support during my doctoral study. Further, I would like to show my best gratitude to my supervisor at Japan Advanced Institute of Science and Technology (JAIST), Professor Masayuki Yamaguchi for her help and valuable advice during my research at JAIST. Without these facilities and sponsorship, I would not have been able to achieve and complete my study.

Finally, I would like to express my honest thanks to my family, and my friend for their help, cheerful, love, understanding and encouragement. My thanks also given to all of those whose names have not been mentioned, for helping me to make this work complete.

CONTENTS

	Page
THAI ABSTRACT	iv
ENGLISH ABSTRACT	v
ACKNOWLEDGEMENTS	vi
CONTENTS	vii
LIST OF TABLES	x
LIST OF FIGURES	xi
LIST OF ABBREVIATIONS	xiv
CHAPTER I INTRODUCTION	1
1.1 Introduction	1
1.2 The objectives of this research	8
1.3 The scope of research	9
Chapter II THEORY AND LITERATURE REVIEWS	10
2.1 Oral administration of drugs	10
2.2 Mucoadhesive drug delivery systems	11
2.2.1 Mucoadhesion/ bioadhesion	11
2.2.2 Mechanism of Mucoadhesion	12
2.2.3 Theories of mucoadhesion	14
2.3 Polymer in pharmaceutical field	15
2.3.1 Ideal Mucoadhesive polymers	16
2.3.2 Thiolated Polymer	17
2.3.3 Cellulose and its derivatives	18
CHAPTER III EXPERIMENTAL	23

	Page
CHAPTER IV RESULTS AND DISCUSSION	34
4.1 Mucoadhesive drug carrier based on amphiphilic cationic aminocellulose	34
4.1.1 Formation and characterization of amphiphilic cationic aminocellulose	34
4.1.2 ¹³ C Nuclear Magnetic Resonance spectroscopy (NMR)	35
4.1.3 Fourier transformed infrared spectroscopy (FTIR).....	36
4.1.4 X-ray diffraction.....	38
4.1.5 Thermogravimetric analysis (TGA)	39
4.1.6 Mucoadhesion studies.....	40
4.1.7 Formation of hydrophobic cationic aminocellulose micelles.....	42
4.1.8 CMC determination	45
4.1.9 Evaluation of the EE and In vitro CPT release profiles	46
4.2.1 Formation and characterization of amphiphilic cationic thiolated aminocellulose	49
4.2.2 ¹³ C Nuclear Magnetic Resonance spectroscopy (NMR)	51
4.2.3 Fourier transformed infrared spectroscopy (FTIR).....	53
4.2.4 X-ray diffraction.....	54
4.2.5 Thermogravimetric analysis (TGA)	55
4.2.6 Determination of the thiol and disulfide groups content.....	57
4.2.7 Mucoadhesion studies.....	58
4.2.8 Spherulite growth and morphology.....	60
4.2.9 Evaluation of the EE and In vitro CPT release profiles	64
CHAPTER V CONCLUSIONS.....	68
REFERENCES	69

APPENDIX.....	80
VITA.....	94



LIST OF TABLES

Table 4.1 Comparison of the mucoadhesive property of cellulose and the modified celluloses.....	42
Table 4.2 The particle morphology, in terms of the hydrated and anhydrous spherical size, polydispersity index (PDI) and zeta potential of mucoadhesive cellulose derivative micelles with and without CPT.....	45
Table 4.3 Comparison of the mucoadhesive property in different pH solutions of cellulose and the modified celluloses and the net amount of thiol groups.....	60
Table 4.4 The particle morphology, in terms of the hydrated and anhydrous spherical size, polydispersity index (PDI) and zeta potential of mucoadhesive cellulose derivative spherulites with and without CPT.	64
Table 4.5 Encapsulation efficiency (% EE) of mucoadhesive cellulose derivative spherulites loaded with 1% (w/w) to 3 and 5% (w/w) CPT	65

LIST OF FIGURES

Figure 1.1 a) Thiolated polymers (thiomers) b) Mechanism of disulfide bond formation between thiomers and mucus glycoproteins (mucins).	2
Figure 1.2 Chemical structure of cellulose	3
Figure 1.3 Synthesis scheme of cationic aminocellulose and thiolated cationic aminocellulose.....	5
Figure 1.4 Chemical structure of camptothecin.....	6
Figure 1.5 Synthesis scheme of amphiphilic thiolated cationic aminocellulose	7
Figure 1.6 Schematic of drug loaded mucoadhesive particle.....	8
Figure 2.1 Mechanism of Mucoadhesion	13
Figure 2.2 The two stages of the mucoadhesion process	14
Figure 2.3 Mechanism of action of thiomers: drug encapsulation via disulfide formation and precise drug release with covalent binding between thiomers and mucin.	18
Figure 2.4 Chemical structure of cellulose	19
Figure 2.5 Chemical structure of a) Carboxymethylcellulose-cysteine (CMC-Cys) b) Thiolated hydroxyethylcellulose (HEC-SH) c) o-benzenedithiol-modified cellulose.....	21
Figure 2.6 Chemical structure of a) 6-Deoxy-6-trialkylammonium cellulose b) Cellulose-4-N-methylamino butyrate hydrochloride.....	22
Figure 4.1 Synthesis of the amphiphilic cationic aminocellulose	35
Figure 4.2 Representative of ^{13}C NMR spectra of (a) cellulose, (b) cationic aminocellulose, and (c) amphiphilic cationic aminocellulose	36
Figure 4.3 FTIR spectra of (a) cellulose, (b) cationic aminocellulose, and (c) amphiphilic cationic aminocellulose	37

Figure 4.4 XRD pattern of (a) cellulose, (b) cationic aminocellulose, and (c) amphiphilic cationic aminocellulose.....	39
Figure 4.5 TGA analysis (TG and DTG) of (a) cellulose, (b) cationic aminocellulose, and (c) amphiphilic cationic aminocellulose.....	40
Figure 4.6 SEM images of (a) amphiphilic cationic aminocellulose micelles (b) CPT loaded amphiphilic cationic aminocellulose.....	44
Figure 4.7 Critical micellar concentration (CMC) value of amphiphilic cationic aminocellulose in H ₂ O at room temperature.....	46
Figure 4.8 Release profiles of CPT from amphiphilic cationic aminocellulose micelles in different pH solutions. The data are shown as the mean \pm SD and are derived from three independent repeats.	48
Figure 4.9 Synthesis scheme of amphiphilic thiolated cationic aminocellulose	50
Figure 4.10 Representative of ¹³ C NMR spectra of (a) cellulose, (b) thiolated cationic aminocellulose, and (c) amphiphilic thiolated cationic aminocellulose	52
Figure 4.11 FTIR spectra of (a) cellulose, (b) thiolated cationic aminocellulose, and (c) amphiphilic thiolated cationic aminocellulose.....	54
Figure 4.12 XRD pattern of (a) cellulose, (b) thiolated cationic aminocellulose, and (c) amphiphilic thiolated cationic aminocellulose.....	55
Figure 4.13 TGA analysis (TG and DTG) of (a) cellulose, (b) thiolated cationic aminocellulose, and (c) amphiphilic thiolated cationic aminocellulose	57
Figure 4.14 SEM images of the formation of amphiphilic thiolated cationic aminocellulose spherulites	62
Figure 4.15 SEM images of amphiphilic thiolated cationic cellulose loaded with.....	63
Figure 4.16 Release profiles of CPT from 1% CPT-loaded amphiphilic cationic cellulose spherulites in different pH solutions. The data are shown as the mean \pm SD and are derived from three independent repeats.....	66

Figure 4.17 Release profiles of amphiphilic thiolated cationic cellulose loaded with 1% (w/w) to 3 and 5% (w/w) CPT in phosphate buffer solution (PBS, pH 7.4). The data are shown as the mean \pm SD and are derived from three independent repeats. 67



LIST OF ABBREVIATIONS

%	Percentage
λ	Wavelength (lambda)
μg	Microgram
μL	Microliter
μmol	Micromole
\AA	Angstrom
Aq	Aqueous
$^{\circ}\text{C}$	Degree Celsius
^{13}C NMR	^{13}C Nuclear magnetic resonance spectroscopy
cm	Centimeter
cm^{-1}	Wavenumber (unit)
CPT	Camptothecin
%DS	Degree of substitution
EA	Elemental analysis
EE	Entrapment efficiency
Eq	Equation
FTIR	Fourier transformed infrared spectroscopy
h	Hour
Hz	Hertz
kV	Kilovolt

mbar	Millibar
mg	Milligram
M	Molarity
MW	Molecular weight
MBI	5-amino-2-mercaptobenzimidazole
N	Normality
nm	Nanometer
NMP	N-methyl pyrrolidone
PAS	Periodic-Schiff
PB	Phosphate buffer
pH	A measure of the acidity or basicity of an aqueous solution
pK _a	Acid dissociation constant
ppm	One part per million
rpm	Revolutions per minute
SEM	Scanning electron microscope
SD	Standard deviation
SCF	Simulated colon buffer
SGF	Simulated gastric fluid
SIF	Simulated intestinal fluid
SM	Sulfanilamide
TGA	Thermogravimetric analysis
UV-Vis	Ultraviolet-visible spectroscopy
v/v	Volume/volume

w/v	Weight/volume
w/w	Weight/weight
XRD	X-ray diffraction



CHAPTER I

INTRODUCTION

1.1 Introduction

The oral route of drug administration is generally the most convenient and preferred means of drug delivery to systemic circulation body. However oral administration of most of the drugs in conventional dosage forms has short-term limitations due to their inability to restrain and localize the system at gastrointestinal tract [1]. To overcome this problem, a platform for drug delivery based on gastroretentive concept is required which can be effectively provided by mucoadhesive property. Mucoadhesive drug delivery system have recently been of increasing interest in pharmaceutical field to achieve improved therapeutic advantages, such as a prolongation of the residence time at the absorption site, an increase in the drug concentration gradient due to the intense contact of particles with the mucosal and a localization of drug action of the delivery system at a given target site [2-6].

A mucoadhesion promoting agent or the mucoadhesive polymer is added to the formulation which helps to promote the adhering of the active pharmaceutical ingredient to the mucus membrane. The design and selection of mucoadhesive polymers for drug delivery should possess sufficient chain flexibility, high molecular weight, hydrophilic functional groups (carboxyl (-COOH), hydroxyl (-OH) and amide (-NH₂) groups), strong anionic or positive charges and also non-toxic with biocompatibility and economically favorable. As such, these polymers would be able to interact more strongly with the mucus glycoproteins. Recent, mucoadhesive polymers which can be used in drug carrier are cationic polysaccharides, e.g., chitosan [7], pullulan [8], cationic guar [9], cationic dextrans [10] and cationic

celluloses [11, 12] because they possess excellent mucoadhesive properties and also seem to be the most commonly used in biomedical applications.

Conventionally, the attachment of mucoadhesive polymers to the mucus layer has been achieved by weak non-covalent bonds. In order to improve its mucoadhesive property, polymers introducing thiol groups, i.e., the so-called thiolated polymers (Figure 1.1a), that can form stronger covalent bonds with cysteine-rich subdomains of mucus glycoproteins via thio/disulfide exchange reaction (Figure 1.1b) has been synthesized [13-16]. A representative candidate among such thiolated polymers is thiolated chitosan.

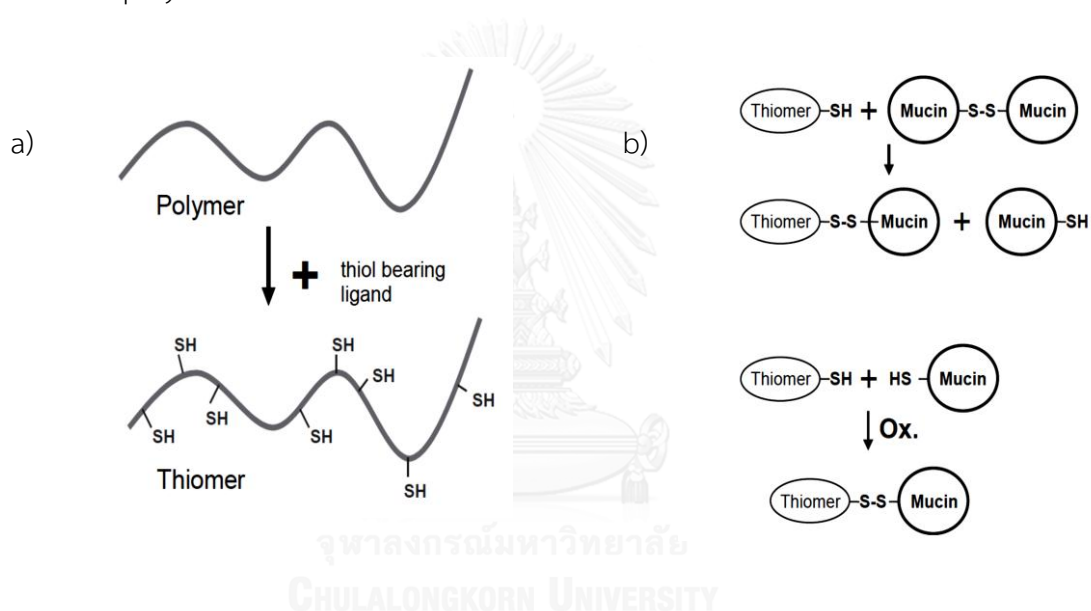


Figure 1.1 a) Thiolated polymers (thiomers) b) Mechanism of disulfide bond formation between thiomers and mucus glycoproteins (mucins).

Many studies described the usage of thiolated chitosan for various drug delivery systems such as oral, parenteral and nasal administration because it demonstrates permeation enhancing and mucoadhesive properties [17, 18]. However, chitosan and subsequently thiolated chitosans bear the disadvantage of precipitation and poor solubility in aqueous media of pH above 6.5 [19, 20]. Consequently, they do not reach their full potential as low mucosal membrane permeability where pH is above 6.5. It was, therefore, the aim of this study to design and synthesize an

alternative thiolated cationic polysaccharide showing similar properties as thiolated chitosan but being soluble over a broad pH range.

Cellulose, one of the biomass-derived materials, is useful controlled drug delivery materials and has been used in such application for many decades by virtue of their excellent biocompatibility, non-toxicity and large number of derivatizable groups [21, 22]. It is a polydisperse linear homopolymers, consisting of β -1-4-glycosidic linked D-glucopyranose units. Figure 1.2 shows the molecular structure of cellulose as a carbohydrate polymer generated from repeating β -D-glucopyranose molecules that are covalently linked through acetal functions between the equatorial OH group of C₄ and the C₁ carbon atom (β -1,4-glucan), which is, in principle, the manner in which cellulose is biogenetically formed (Marsh & Wood 1942). As a result, cellulose is an extensive, linear-chain polymer with a large number of hydroxy groups (three per anhydroglucose (AGU) unit) present in the thermodynamically preferred ⁴C₁ conformation. To accommodate the preferred bond angles of the acetal oxygen bridges, every second AGU ring is rotated 180° in the plane. In this manner, two adjacent structural units define the disaccharide cellobiose [23].

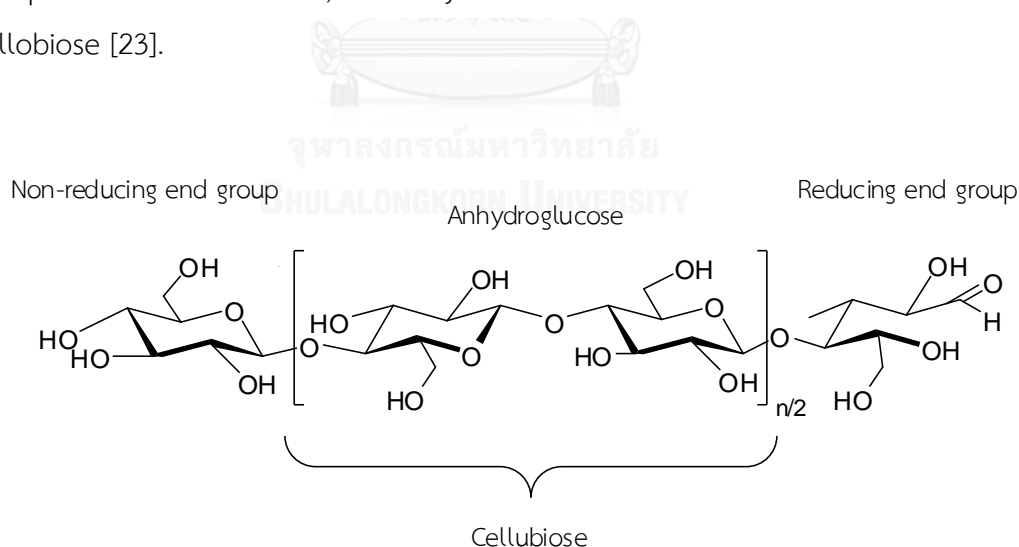


Figure 1.2 Chemical structure of cellulose

However, native cellulose has some drawbacks. It is poorly soluble in common solvents or aqueous medium due to strong intermolecular and intramolecular hydrogen bonding [24-26]. Therefore, in order to be used in drug delivery applications, it is necessary for modification of cellulose to be suitable for their role in drug delivery systems. For example, cationic charge is needed for interaction with negatively charged mucin glycoproteins and good solubility in over a broad pH range [11, 27].

The cationization of cellulose is a good candidate method to improve solubility of cellulose. Moreover, cationic polymer can selectively and efficiently deliver a gene to target cells due to they can easily complex with the anionic DNA molecules and also interact with negatively charged mucin glycoproteins, which endows it with mucoadhesive properties [28, 29]. Several methods for the synthesis of cationic group containing cellulose have been developed. Traditionally, cellulose has been modified with quaternary ammonium groups. Pasteka (1988) reported the homogeneous quaternization of regenerated cellulose with 3-chloro-2-hydroxypropyltrimethylammonium chloride in solutions of benzyltriethylammonium hydroxide. However, the degree of quaternization was as low as 0.25 [30]. Song et al. (2008) also synthesized the quaternized cellulose in a homogeneous reaction by reacting cellulose with 3-chloro-2-hydroxypropyltrimethylammonium chloride in NaOH/urea aqueous solutions. However, the solution has to be precooled at very low temperature, i.e., -12.3 °C. Furthermore, some diols were formed as a result of the side reaction [11]. In the present work, we synthesized cationic aminocellulose by ring-opening reactions of lactam under homogeneous reaction conditions. In this case, N-methyl pyrrolidone (NMP) acts both as solvent and reactant that is able to introduce the cationic ester moiety in one step without isolation and purification of intermediates. Both of cationic charge and amino groups bearing on cellulose have played an important role in the development of modern drug delivery systems.

The aim was primarily to prepare a cationic aminocellulose (cellulose-4-[N-methylamino] butyrate hydrochlorides) that would be potentially suitable for

application in a mucoadhesive drug delivery system and then conjugating with thiol groups (5-amino-2-mercaptobenzimidazole (MBI)) onto cationic aminocellulose (Figure 1.3). The amount of thiol groups immobilized on cationic aminocellulose was determined by Ellman's method, Periodic acid: Schiff (PAS) colorimetric method was used to qualify mucin-conjugated polymer bioadhesed strength in the simulated gastrointestinal fluid (pH 1.2, 6.8 and 7.4).

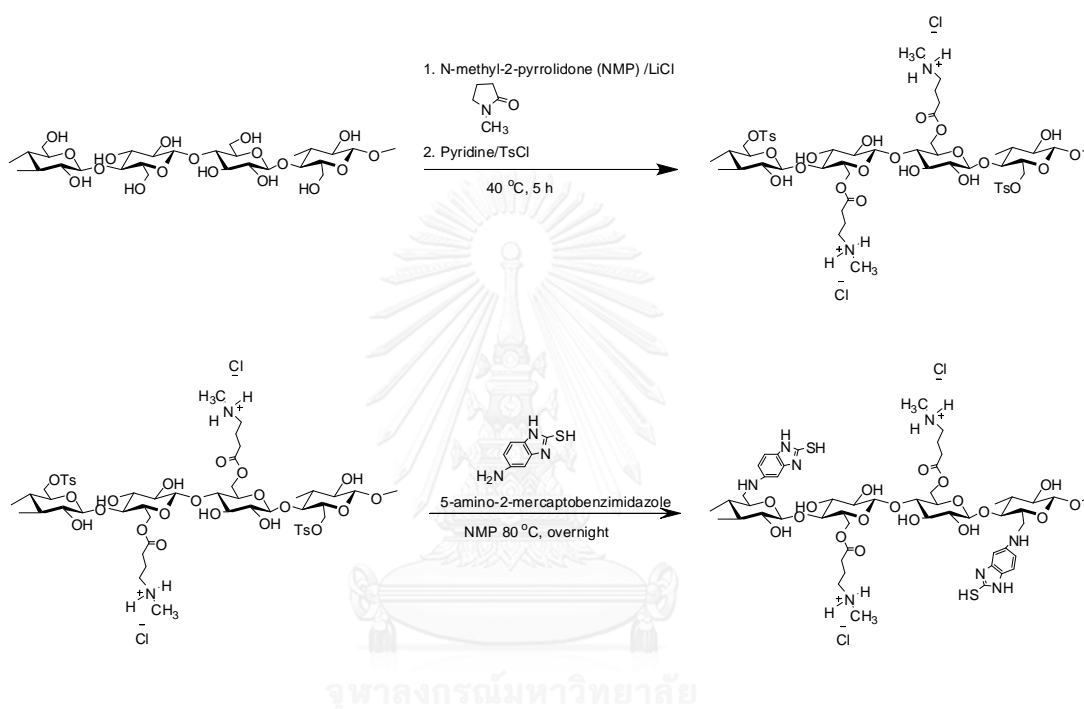


Figure 1.3 Synthesis scheme of cationic aminocellulose and thiolated cationic aminocellulose

Camptothecin (CPT) (Figure 1.4), a natural plant alkaloid extracted from *Camptotheca acuminata*, is an inhibitor of the DNA-replicating enzyme topoisomerase I [31] which is believed to act by stabilizing a topoisomerase I-induced single strand break in the phosphodiester backbone of DNA, thereby preventing religation [32, 33]. This leads to the production of a double-strand DNA break during replication, which results in cell death if not repaired. CPT and CPT analogs are increasingly in clinical use and show great utility in the treatment of various cancer including primary and metastatic colon carcinoma, small cell lung carcinoma,

ovarian, breast, pancreatic, and stomach cancer [34]. But in spite of the promise demonstrated at the pre-clinical level, clinical trials were abandoned due to unexpected toxicity and low anti-neoplastic activity [35-37]. In addition, CPT was felt to have limited clinical potential because of its low solubility and its therapeutically active lactone form. Due to these inadequacies, many types of drug delivery system have been developed in order to reduce severe systemic toxicities, improve solubility, and enhance antitumor effects by improving their pharmacokinetics [38].

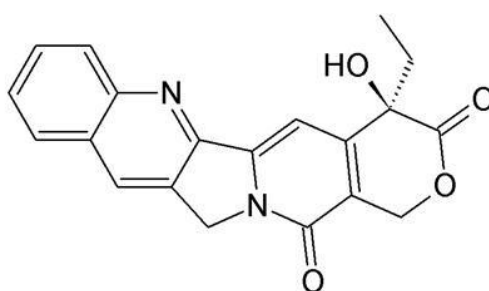


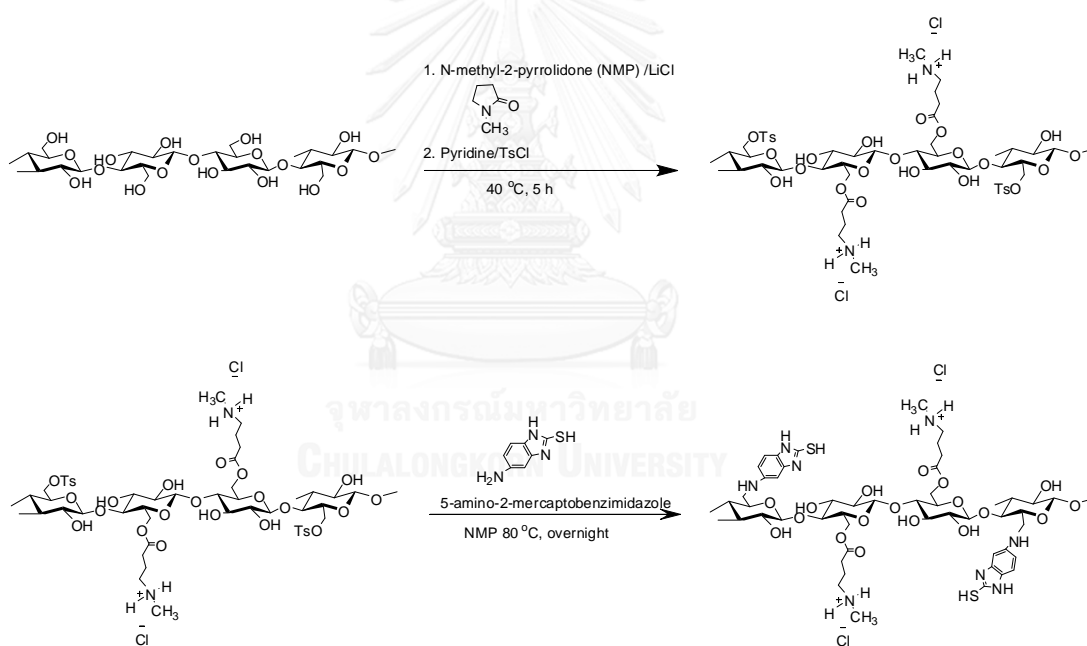
Figure 1.4 Chemical structure of camptothecin

Recently, polymeric micelles formed by self-assembly of amphiphilic block copolymers in aqueous solution have been proposed to attain effective novel drug delivery for antitumor drugs [39-43], diagnostic reagents [44], DNA [45, 46], and enzymes [47] because of their favorable characteristics of solubilization, long circulation, low toxicity, enhanced drug bioavailability, reduced side effects of drugs, etc [48]. The structure of polymeric micelles is characterized by a hydrophobic core and a hydrophilic exterior, which spontaneously forms above the critical micelle concentration (CMC) of the polymers [49, 50]. Moreover, the nano-scaled micellar carriers with incorporated drugs exhibit prolonged systemic circulation time in the body. Consequently, these features and advantages can lead to improvement in the therapeutic effect and a drastic decrease in the toxicity of drugs.

Therefore, the aim of this work was to develop the mucoadhesive polymer for application in a mucoadhesive delivery system, especially at the gastrointestinal tract (GI tract). A novel amphiphilic thiolated cationic aminocellulose (hydrophobically modified thiolated cationic cellulose) was synthesized. The new

synthetic route is illustrated in synthesis scheme Figure 1.5. The aim was primarily to prepare a mucoadhesive thiolated cationic aminocellulose would be potentially suitable for application in a mucoadhesive drug delivery system and then attaching long chain alkyl groups (octadecyl) to remaining hydroxyl groups providing the hydrophobic moieties that can achieve core-shell polymeric micelles. The novel polymer is characterized in terms of elemental analysis, ^{13}C NMR, FTIR, XRD and TGA. Degree of thiol substitution was found out using Ellman's method. Moreover, the *in vitro* mucoadhesion properties was evaluated by periodicacid schiff (PAS) method, these properties have been assessed by evaluation of the interaction between cellulose and mucin in various aqueous solution.

Step I:



Step II:

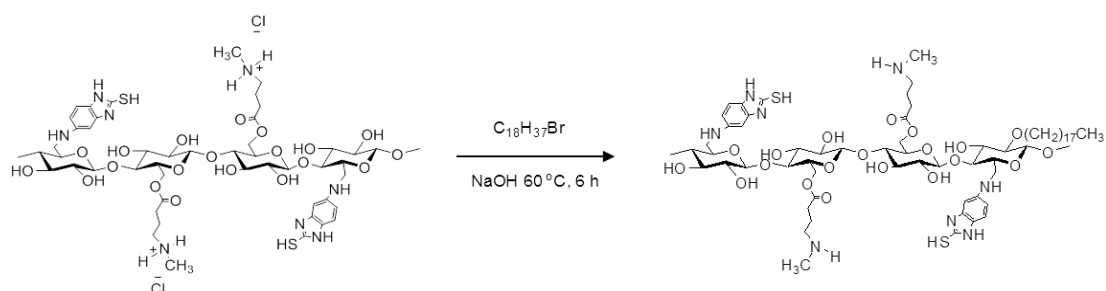


Figure 1.5 Synthesis scheme of amphiphilic thiolated cationic aminocellulose

Additionally, the utilization of self-assembled amphiphilic thiolated cationic aminocellulose micelles as a delivery carrier for poorly water-soluble drugs (CPT) was investigated (Figure 1.6). Characterization of the obtained modified cellulose micelles in terms of morphology, size and size distribution, zeta potential, critical micelle concentration, chemical analysis and thermal behavior. Study the *in vitro* release behavior of the spheres in various pH buffers (pH1.2, 6.8, and 7.4).

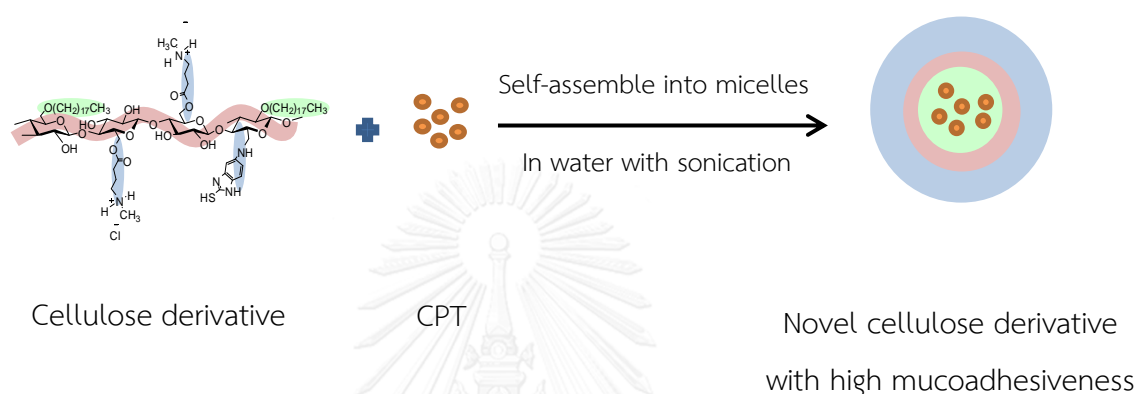


Figure 1.6 Schematic of drug loaded mucoadhesive particle

1.2 The objectives of this research

- 1) To improve mucoadhesive property of cellulose by introducing cationic charges and thiol groups
- 2) To prepare self-assembled modified cellulose micelles and investigate the possibility of using modified cellulose micelles as low water soluble drug carrier

1.3 The scope of research

The scope of this research was carried out by stepwise methodology as follows:

1) Review literature for related research work.

2) Part I: Modifying cellulose

a. Preparation of cationic aminocellulose, thiolated cationic aminocellulose, amphiphilic cationic aminocellulose and amphiphilic thiolated cationic aminocellulose

b. Characterization of the physical and chemical properties of cellulose and modified cellulose using elemental analysis, ^{13}C NMR, FTIR, XRD and TGA.

c. Determination degree of cationic group substitution.

d. Determination degree of thiol and disulfide substitution.

e. *In vitro* investigation of mucoadhesive property in simulated gastric fluid (SGF) pH 1.2, simulated intestinal fluid (SIF) pH 6.8 and simulated colon fluid (SCF) pH 7.4 by using UV-Vis method

Part II: Formation of amphiphilic cationic aminocellulose micelles and amphiphilic thiolated cationic aminocellulose micelles as a drug delivery carrier

a. Preparation of the micelles with and without drug

b. Characterization of the obtained micelles in terms of morphology, size and size distribution, zeta potential, chemical analysis and thermal behavior.

c. Determination of the drug encapsulation efficiency

d. Study the *In vitro* release behavior of the spheres in simulated gastrointestinal fluid pH 1.2, 6.8 and 7.4 using UV-Vis method.

3) Report, Discussion and Writing up thesis.

Chapter II

THEORY AND LITERATURE REVIEWS

2.1 Oral administration of drugs

Oral drug delivery has been known for decades as the most widely utilized route of administration among all the routes that have been explored for the systemic delivery of drugs via various pharmaceutical products of different dosage forms. The reasons that the oral route achieved such popularity may be in part attributed to its ease of administration as well as the traditional belief that by oral administration the drug is well absorbed as the food stuffs that are ingested daily. In fact, the development of a pharmaceutical product for oral delivery, irrespective of its physical form (solid, semi-solid or liquid dosage forms) involves varying extents of optimization of dosage forms characteristics within the inherent constraints of gastrointestinal tract (GI) physiology [51].

In the exploration of oral controlled release drug administration, one encounters three areas of potential challenge [52].

1. Development of a drug delivery system: To develop a viable oral controlled release drug delivery system capable of delivering a drug at a therapeutically effective rate to a desirable site for duration required for optimal treatment.

2. Modulation of gastrointestinal transit time: To modulate the GI transit time so that the drug delivery system developed can be transported to a target site or to the vicinity of an absorption site and reside there for prolonged period of time to maximize the delivery of a drug dose.

3. Minimization of hepatic first pass elimination: If the drug to be delivered is subjected to extensive hepatic first pass elimination, preventive measures should be devised to either bypass or minimize the extent of hepatic metabolic effect.

2.2 Mucoadhesive drug delivery systems

The pharmaceutical research is being steadily shifted from the development of new chemical entities to the development of Novel Drug Delivery System (NDDS) of existing drug molecule to maximize their effectiveness in terms of therapeutic action and patient protection. Extensive efforts have recently been focused on targeting a drug or drug delivery system in a particular region of the body for extended periods of time, not only for local targeting of drugs but also for better control of systemic drug delivery.

2.2.1 Mucoadhesion/ bioadhesion

Bioadhesion may be defined as the state in which two materials, at least one of which is biological in nature, are held together for extended period of time by interfacial forces. In pharmaceutical sciences, when the adhesive attachment is to mucus or a mucous membrane, the phenomenon is referred to as mucoadhesion [53-55]. In the early 1980s, the concept of mucoadhesives was introduced into the controlled drug delivery area. Mucoadhesives are synthetic or natural polymers that interact with the mucus layer covering the mucosal epithelial surface and main molecules constituting a major part of mucus. The concept of mucoadhesives has alerted many investigators to the possibility that these polymers can be used to overcome physiological barriers in long-term drug delivery in ocular, nasal, vagina and buccal drug delivery systems [56-59]. In addition, the development of oral mucoadhesive delivery systems was always of great interest as delivery systems capable of adhering to certain GI segments would offer various advantages. With few exceptions, however, mucoadhesive drug delivery systems have so far not reached their full potential in oral drug delivery, because the adhesion of drug delivery systems in the GI tract is in most cases insufficient to provide a prolonged residence time of delivery systems in the stomach or small intestine. The need to deliver 'challenging' molecules such as biopharmaceuticals (proteins and oligonucleotides) has increased interest in this area. Mucoadhesive materials could also be used as

therapeutic agents in their own right, to coat and protect damaged tissues (gastric ulcers or lesions of the oral mucosa) or to act as lubricating agents (in the oral cavity, eye and vagina).

Before discussing about the commonly used mucoadhesive polymers, the mechanism of mucoadhesion and the different theories which have been proposed to explain the phenomenon of mucoadhesion will be discussed.

2.2.2 Mechanism of Mucoadhesion

Mucus is a complex viscous adherent secretion which is synthesized by specialized goblet cells. Mucus is composed mainly of water (>95%) and mucins, which are glycoproteins of exceptionally high molecular weight. Furthermore, pendant sialic acid and sulphate groups located on the glycoprotein molecules result in mucin behaving as an anionic polyelectrolyte at neutral pH [60]. Other non mucin components of mucus include secretory lysozyme, lactoferrin, lipids, polysaccharides, and various other ionic species [60]. Development of novel mucoadhesive delivery systems are being undertaken so as to understand the various mechanism of mucoadhesion (Figure 2.1) and improved permeation of active agents.

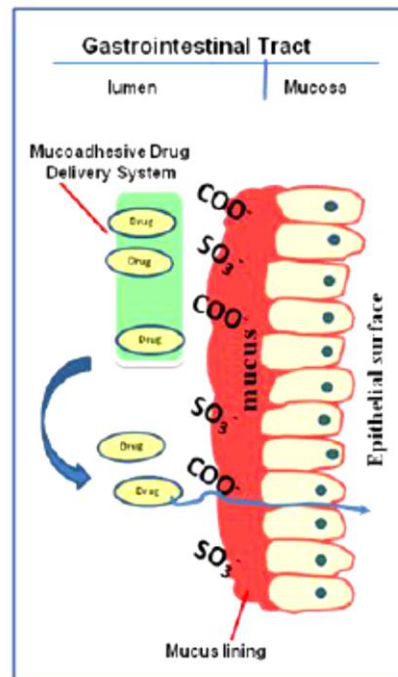


Figure 2.1 Mechanism of Mucoadhesion

As stated, mucoadhesion is the attachment of the drug along with a suitable carrier to the mucous membrane. Mucoadhesion is a complex phenomenon which involves wetting, adsorption and interpenetration of polymer chains. Mucoadhesion has the following Mechanism [61]

1. Intimate contact between a bioadhesive and a membrane (wetting or swelling phenomenon)
2. Penetration of the bioadhesive into the tissue or into the surface of the mucous membrane (interpenetration) [62]

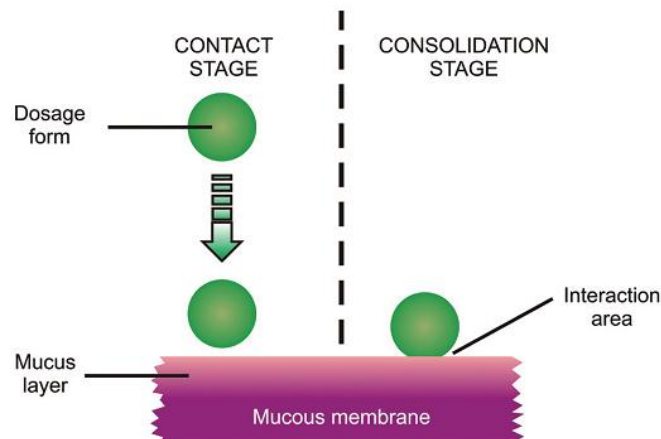


Figure 2.2 The two stages of the mucoadhesion process [63]

Residence time for most mucosal routes is less than an hour and typically in minutes, it can be increased by the addition of an adhesive agent in the delivery system which is useful to localize the delivery system and increases the contact time at the site of absorption [64]. The exact mechanism of mucoadhesion is not known but an accepted theory states that a close contact between the mucoadhesive polymer and mucin occurs which is followed by the interpenetration of polymer and mucin. The adhesion is prolonged due to the formation of van der Waals forces, hydrogen bonds and electrostatic bonds.

2.2.3 Theories of mucoadhesion

The phenomena of bioadhesion occurs by a complex mechanism. Till date, six theories have been proposed which can improve our understanding for the phenomena of adhesion and can also be extended to explain the mechanism of bioadhesion. The theories include: (a) the electronic theory, (b) the wetting theory, (c) the adsorption theory, (d) the diffusion theory, (e) the mechanical theory and (f) the cohesive theory. The electronic theory proposes transfer of electrons amongst the surfaces resulting in the formation of an electrical double layer thereby giving rise to attractive forces. The wetting theory postulates that if the contact angle of

liquids on the substrate surface is lower, then there is a greater affinity for the liquid to the substrate surface. If two such substrate surfaces are brought in contact with each other in the presence of the liquid, the liquid may act as an adhesive amongst the substrate surfaces. The adsorption theory proposes the presence of intermolecular forces, viz. hydrogen bonding and Van der Waal's forces, for the adhesive interaction amongst the substrate surfaces. The diffusion theory assumes the diffusion of the polymer chains, present on the substrate surfaces, across the adhesive interface thereby forming a networked structure. The mechanical theory explains the diffusion of the liquid adhesives into the micro-cracks and irregularities present on the substrate surface thereby forming an interlocked structure which gives rise to adhesion. The cohesive theory proposes that the phenomena of bioadhesion are mainly due to the intermolecular interactions amongst like-molecules [61, 63].

Based on the above theories, the process of bioadhesion can be broadly classified into two categories, namely chemical (electronic and adsorption theories) and physical (wetting, diffusion and cohesive theory) methods [65, 66]. The process of adhesion may be divided into two stages. During the first stage (also known as contact stage), wetting of mucoadhesive polymer and mucous membrane occurs followed by the consolidation stage, where the physico-chemical interactions prevail [67].

2.3 Polymer in pharmaceutical field

Polymers have played an integral role in the advancement of drug delivery technology by protecting an active agent during its passage through the body until its release and providing controlled release of therapeutic agents. Naturally occurring polymers are attractive as drug delivery system since they possess the biocompatibility, biodegradability and non-toxicity required for used in human [68]. Carrier technology offers an intelligent approach for drug delivery by coupling the drug to a carrier particle such as beads, microspheres, nanoparticles, liposomes. Those formulations could prolong the drug release and also generate a response in a

specific area or organ of the body requiring treatment. Moreover, a target drug, encapsulated in a polymer can be released sustainedly to improve drug therapeutic efficacy and decrease the dosing time and side effect [69].

2.3.1 Ideal Mucoadhesive polymers

A mucoadhesion promoting agent or the polymer is added to the formulation which helps to promote the adhering of the active pharmaceutical ingredient to the mucous membranes. The agent can have such additional properties like swelling so as to promote the disintegration when in contact with the saliva. As understood earlier, that various physical and chemical exchanges can affect the polymer/ mucus adhesion, so as polymer should be carefully selected with the following properties in mind [70].

1. Polymer must have a high molecular weight up to 100.00 or more this is necessary to promote the adhesiveness between the polymer and mucus.

2. Long chain polymers-chain length must be long enough to promote the interpenetration and it should not be too long that diffusion becomes a problem [71].

3. High viscosity

4. Degree of cross linking- it influences chain mobility and resistance to dissolution. Highly cross linked polymers swell in presence of water and retain their structure. Swelling favours controlled release of the drug and increases the polymer/mucus interpenetration. But as the cross linking increases, the chain mobility decreases which reduces the mucoadhesive strength [71].

5. Spatial conformation

6. Flexibility of polymer chain- this promotes the interpenetration of the polymer within the mucus network [72].

7. Concentration of the polymer- an optimum concentration is required to promote the mucoadhesive strength. It depends however, on the dosage form. For

solid dosage form the adhesive strength increases with increase in the polymer concentration. But in case of semi-solid dosage forms an optimum concentration essential beyond which the adhesive strength decreases.

8. Charge and degree of ionization- the effect of polymer charge on mucoadhesion was clearly shown by Bernkop-Schnurch and Freudl. In this work, various chemical entities were attached to chitosan and the mucoadhesive strength was evaluated. Cationic chitosan HCL showed marked adhesiveness when compared to the control. The attachment of EDTA an anionic group increased the mucoadhesive strength significantly. DTPA/chitosan system exhibited lower mucoadhesive strength than cationic chitosan and anionic EDTA chitosan complexes because of low charge. Hence the mucoadhesive strength can be attributed as anion>cation>nonionic [73].

2.3.2 Thiolated Polymer

Recently, it could be shown that polymers with thiol groups provide much higher adhesive properties than polymers generally considered to be mucoadhesive [74]. The enhancement of mucoadhesion can be explained by the formation of covalent bonds between the polymer and the mucus layer which are stronger than non-covalent bonds. These thiolated polymers, or the so-called thiomers, are supposed to interact with cysteine-rich subdomains of mucus glycoproteins via disulfide exchange reactions [14, 75]. To date, this improved mucoadhesion due to the introduction of thiol moieties has already been verified for various polymers such as chitosan, polycarbophil and carboxymethylcellulose [74].

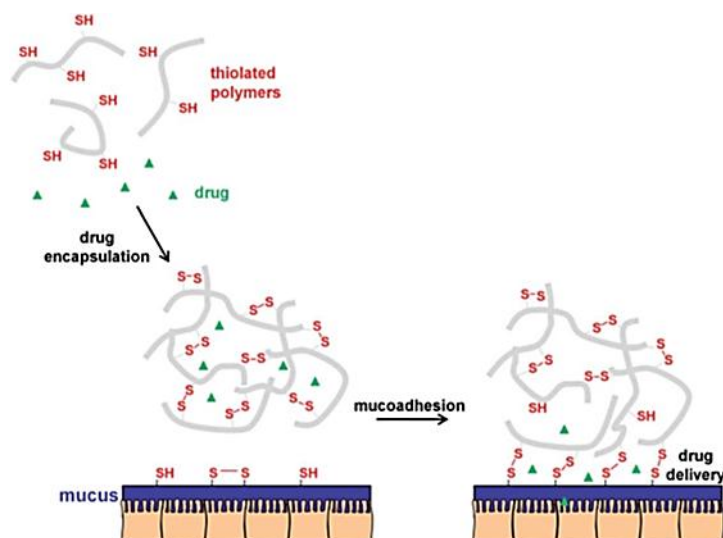


Figure 2.3 Mechanism of action of thiomers: drug encapsulation via disulfide formation and precise drug release with covalent binding between thiomers and mucin.

2.3.3 Cellulose and its derivatives

Polysaccharides, natural polymers, fabricated into hydrophilic matrices remain popular biomaterials for controlled-release dosage forms and uses of a hydrophilic polymer matrix is one of the most popular approaches in formulating an extended-release dosage forms [76]. This is due to the fact that these formulations are relatively flexible and a well-designed system usually gives reproducible release profiles.

Cellulose constitutes the most abundant and renewable polymer resource available worldwide. It is estimated that by photosynthesis, 10^{11} – 10^{12} tons of cellulose are synthesized annually in a relatively pure form or combined with lignin and other polysaccharides in the cell wall of woody plants [77, 78]. Cellulose is an organic compound with containing repeated cellobiose (disaccharide) segments with the formula of $(C_6H_{10}O_5)_n$. In nature, cellulose chains have a degree of polymerization (DP) of approximately 5,000 cellobiose units in wood cellulose and 7,500 in natural cotton cellulose [28].

Cellulose is a polydisperse linear homopolymers, consisting of β -1-4-glycosidic linked D-glucopyranose units. Figure 2.4 shows the molecular structure of cellulose as a carbohydrate polymer generated from repeating β - D-glucopyranose molecules that are covalently linked through acetal functions between the equatorial OH group of C₄ and the C₁ carbon atom (β -1,4-glucan), which is, in principle, the manner in which cellulose is biogenetically formed. As a result, cellulose is an extensive, linear-chain polymer with a large number of hydroxy groups (three per anhydroglucose (AGU) unit) present in the thermodynamically preferred ⁴C₁ conformation. The Degree of Substitution (DS) of cellulose derivatives is defined as the average number of substituted hydroxyl groups per glucose. The theoretical maximum is thus a DS of 3.0. Cellulose and its derivatives are an excellent choice as biomaterial in medicine and pharmacy due to its properties such as biocompatibility, biodegradability, non-toxicity and large number of derivatizable group. However, it is insoluble in water and most common solvents; the poor solubility is attributed primarily to the strong intramolecular and intermolecular hydrogen bonding between the individual chains. In spite of its poor solubility characteristics, cellulose is used in a wide range of applications including composites, netting, upholstery, coatings, packing, paper, etc. Chemical modification of cellulose is performed to improve process ability and to produce cellulose derivatives (cellulosics) which can be tailored for specific industrial applications. Cellulosics are used in various biomedical applications such as blood purification membranes and the like. Thus, through derivatization, cellulosics have opened a window of opportunity and have broadened the use of cellulosics.

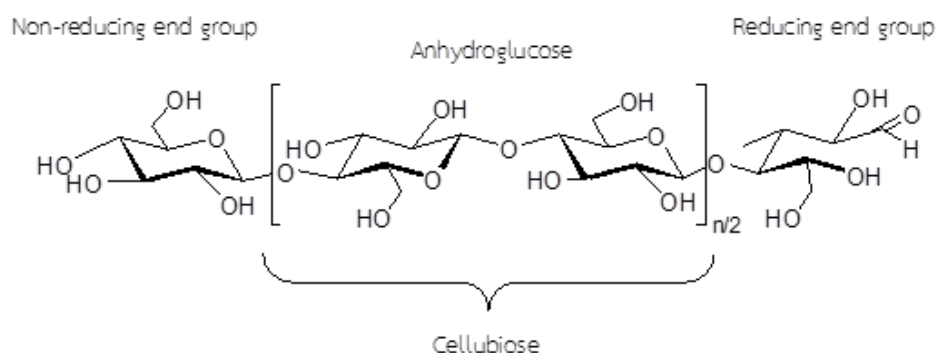


Figure 2.4 Chemical structure of cellulose

The hydroxyl (OH) groups of cellulose considered to be responsible for mucoadhesive property via non-covalent bonds, e.g. hydrogen bonds [63]. In order to improve its mucoadhesive property, cellulose bearing thiol groups that can form covalent bonds with the mucus membrane via thio/disulfide exchange reaction was synthesized and called thiolated cellulose.

In 2001, Clausen and co-worker evaluated the effect of sodium carboxymethylcellulose (NaCMC) and carboxymethylcellulose-cysteine (CMC-Cys) conjugates (Figure 2.5a) on the intestinal permeation of sodiumfluorescein (NaFlu) and model peptide drugs, bacitracin and insulin. It showed that NaCMC conjugated with cysteine further enhanced the permeation. Decreasing the amount of cysteine moieties resulted in lower permeation of NaFlu. Moreover, decreasing the concentration of CMC-Cys from 1% (m/v) to 0.5% (m/v) decreased the transport enhancement ratio (R-value) of NaFlu from 1.8 to 1.2. NaCMC at 1% (m/v) in the presence of free cysteine had no significant effect on the R-value of NaFlu compared to pure NaCMC [79].

In 2010, Sarti and co-worker modified hydroxyethylcellulose (HEC) by the replacement of hydroxyl groups on the carbohydrate structure with thiol moieties, using thiourea as thiolating reagent. Thiolated hydroxyethylcellulose (HEC-SH) (Figure 2.5b) displayed a significant permeation enhancing effect of HEC-SH and improved mucoadhesive properties in comparison with the corresponding unmodified HEC that the contact time to mucosal tissue was 4-fold increase compared with adhesion time of unmodified HEC. Moreover, MTT test showed that HEC-SH is not harmful for cells [80].

In 2011, Takagai and co-worker synthesized thio- and/or amine-modified cellulose resin materials. The o-benzenedithiol- and o-aminothiophenol-modified cellulosic resins were found to be very effective in removing mercury (II) ions from strongly acidic media (pH < 1.0). In particular, the o-benzenedithiol-modified cellulose (Figure 2.5c) material shows very good mercury selectivity and other metal ions, and has an adsorption capacity of 23 mg/g resin [81].

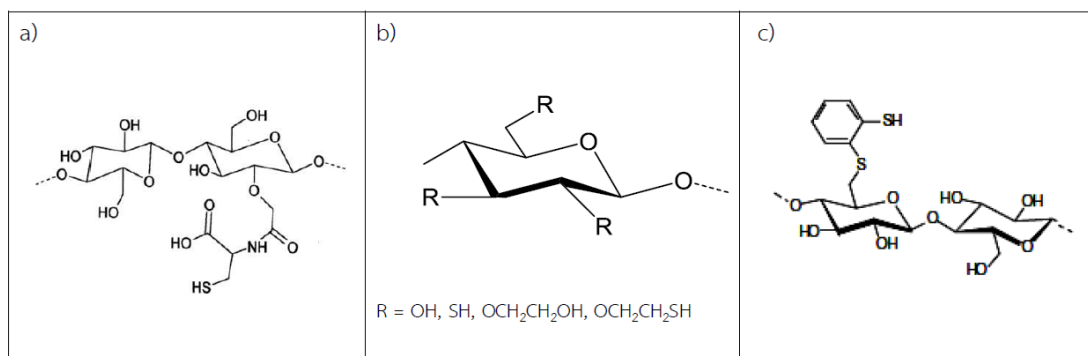


Figure 2.5 Chemical structure of a) Carboxymethylcellulose-cysteine (CMC-Cys) b) Thiolated hydroxyethylcellulose (HEC-SH) c) o-benzenedithiol-modified cellulose

Furthermore, cellulose was chemically modified to produce cationic cellulose in order to improve its physicochemical properties such as water solubility and mucoadhesive properties for using in pharmaceutical applications [82]. The cationic cellulose not only displayed relatively lower cytotoxicity, but also displayed a potent absorption enhancer for peptides and proteins, large hydrophilic compounds and is potential to be used as gene [11, 83] and protein carriers [83].

In 2008, Song and co-worker synthesized quaternized cellulose (Figure 2.6a) by reacting cellulose with 3-chloro-2-hydroxypropyl-trimethylammonium chloride (CHPTAC) in NaOH/urea aqueous solutions for the first time. Their studies showed that the quaternary aminonium groups of quaternized cellulose could form strong electrostatic attraction with the negatively charged proteins. Moreover, it displayed relatively low cytotoxicity and could be considered as promising nonviral gene carriers [11].

In 2011, Zarth and co-worker synthesized cationic aminocellulose (Figure 2.6b) by conversion of the dissolved cellulose with various lactams (N-methyl-2-pyrrolidone, ϵ -caprolactam, N-methyl- ϵ -caprolactam, and N-methyl-2-piperidone) via ring-opening reaction. It demonstrated that cationic aminocelluloses are soluble in water and DMSO. The reaction can be conducted from room temperature to 40 °C without side-reactions, using NMP/LiCl as solvent, i.e., under mild reaction conditions.

In addition, products with low degree of substitution are capable of forming polyelectrolyte complexes and might be promising compounds for the formation of capsules for drug delivery [84].

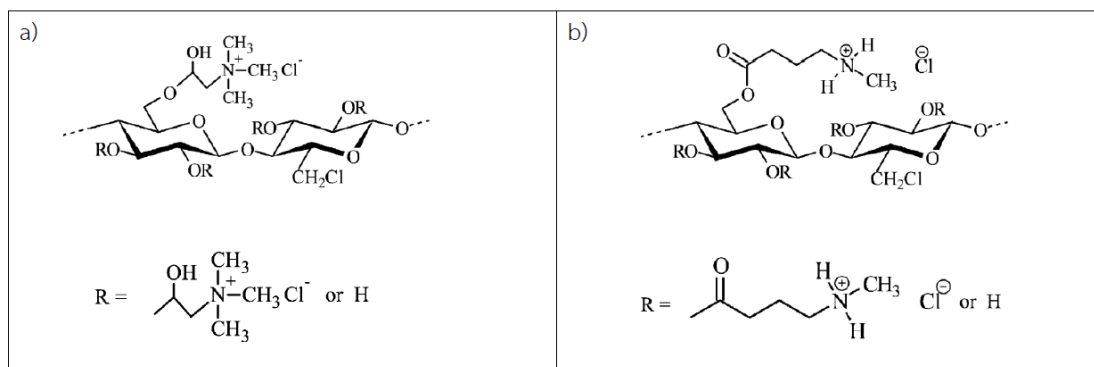
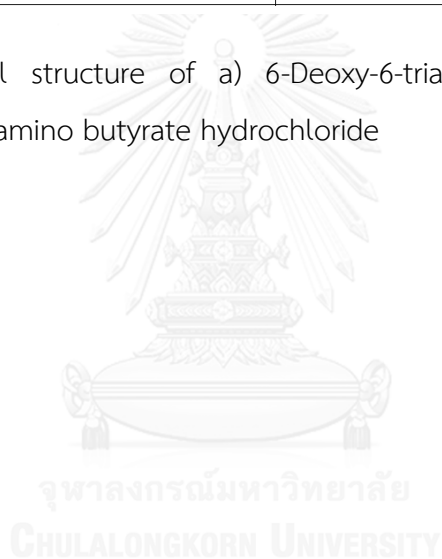


Figure 2.6 Chemical structure of a) 6-Deoxy-6-trialkylammonium cellulose b) Cellulose-4-N-methylamino butyrate hydrochloride



CHAPTER III

EXPERIMENTAL

3.1 Materials

The following materials were obtained from commercial suppliers.

3.1.1 Model drug

(S)-(+)-Camptothecin (CAS number : 7689-03-4, ~95%HPLC, powder obtained by Sigma Aldrich, USA)

3.1.2 Polymers

- Microcrystalline cellulose powder, Lot No. 435236, (Sigma-Aldrich, USA)

3.1.3 Chemicals

- 5-amino-2-mercaptobenzimidazole: analytical grade (Sigma-Aldrich, USA)
- Mucin from porcine stomach (type 2), AR grade (Sigma-Aldrich, USA)
- Basic fuchsin (pararosaniline), analytical grade (Sigma-Aldrich, USA)
- Sodium metabisulphite, analytical grade (Sigma-Aldrich, USA)
- Periodic acid, analytical grade (Sigma-Aldrich, USA)
- 5, 5'-Dithio-bis(2-nitrobenzoic acid), analytical grade (Sigma-Aldrich, USA)
- Octadecyl bromide (1-Bromooctadecane): analytical grade (Sigma-Aldrich, USA)
- *p*-Toluenesulfonyl chloride, analytical grade (Sigma-Aldrich, USA)
- Pyridine, analytical grade (Sigma-Aldrich, USA)
- Lithium chloride anhydrous, ACS reagent, $\geq 99\%$ (Sigma-Aldrich, USA)
- Pyrene for fluorescence, $\geq 99.0\%$ (Sigma-Aldrich, USA)

- Ethanol 95 %, commercial grade (Merck, Germany)
- Hydrochloric acid fuming 37%, AR grade (Merck, Germany)
- Potassium dihydrogen phosphate, AR grade (Merck, Germany)
- Potassium bromide, AR grade (Merck, Germany)
- Potassium iodide, AR grade (Merck, Germany)
- Sodium chloride, AR grade (Merck, Germany)
- Sodium hydrogen phosphate, AR grade (Merck, Germany)
- Sodium hydroxide, AR grade (Merck, Germany))
- N-methylpyrrolidone, AR grade (Merck, Germany)
- Acetone, commercial grade (Merck, Germany)
- Dialysis membrane, MW cutoff at 12,000 Da (Spectrum Laboratories Inc.)

3.2 Instruments

Instrument	Manufacture	Model
Diaphragm vacuum pump	Becthai	ME 2
Freeze dryer	Labconco	Freeze 6
Elemental Analyzer (EA)	PerkinElmer	PE2400 Series II
FTIR spectrometer	Nicolet	6700
Horizotal shaking water-bath	Lab-line instrument	3575-1
Micropipette	Mettler Toledo	Volumate
NMR spectrometer	Bruker	400 Hz
Scanning Electron Microscope	Philips	XL30CP
Particle sizer	Malvern Instruments	Zetasizer nanoseries
TGA	PerkinElmer	Pyris Diamond
UV-VIS spectrometer	PerkinElmer	Lambda 800
Fluorescence spectrometer	PerkinElmer	LS 55
Ultrasonic bath	Ney Ultrasonik	28 H

3.3 Methods

3.3.1 Synthesis of amphiphilic cellulose derivatives

3.3.1.1 Synthesis of cationic aminocellulose

Cellulose-4-[N-methylamino] butyrate hydrochlorides, which is so called cationic aminocellulose, was first prepared from the corresponding cellulose by ring-opening reactions of lactams as the procedure previously reported [84]. Cationic aminocellulose was synthesized following the route schematically summarized in Figure 3.1. Cellulose (1.00 g) was dissolved in 100 mL NMP for 2 h at 120 °C under stirring. Then, the slurry had been allowed to cool to room temperature, 9.0 g of anhydrous LiCl were added with stirring overnight. Pyridine (2.7 mL) was added to the cellulose solution at room temperature followed by stirring for 1 h. After addition of 6.47 g TsCl, the mixture was allowed to react for 6 h at 40 °C under stirring. Then, water was added dropwise. Stirring was continued for 30 min. The polymer was isolated by precipitation with 400 mL acetone/ethanol (1:1, v/v). The solid was filtered off, washed three times with acetone and aired dried. The sample was dissolved in 40 mL distilled water and dialyzed for 3 days. The water was exchanged 2 times per day. Finally, the sample was isolated by freeze-drying.

3.3.1.2 Synthesis of thiolated cationic aminocellulose

Thiolated cationic aminocellulose with a slight modification according to the procedure described above. Briefly, 1.00 g of cellulose was dissolved in 100 mL NMP. The mixture was stirred at 120 °C for 2 h and then the slurry had been allowed to cool to room temperature, 9.0 g of anhydrous LiCl were added with stirring overnight. Pyridine 2.7 mL was added to the cellulose solution at room temperature followed by stirring for 1 h. After addition of 6.47 g of TsCl, the mixture was allowed to react for 6 h at room temperature under stirring and MBI solution was added dropwise during stirring overnight at 80 °C. Then, water was added dropwise. Stirring was continued for 30 min. The polymer was isolated by precipitation with 400 mL acetone/ethanol (1:1, v/v). The solid was filtered off, washed three times with

acetone and aird dried. The sample was dissolved in 40 mL distilled water and dialyzed for 3 days. The water was exchanged 2 times per day. Finally, the sample was isolated by freeze-drying.

3.3.1.3 Synthesis of amphiphillic cationic aminocellulose or amphiphillic thiolated cationic aminocellulose

Sodium hydroxide was added into 1 wt% cationic aminocellulose or thiolated cationic aminocellulose aqueous solutions and stirred at 25 °C for 1 h and then an amount of octadecyl bromide was added drop-wise into the solutions. The mixture solutions were stirred at 60 °C for 6 h, then were precipitated and washed with ethanol, dried at 60 °C. The sample was dissolved in 40 mL distilled water and dialyzed for 2 days.

3.3.2 Chemical characterization

3.3.2.1 Elemental Analyzer, CHNS/O Analyzer (EA)

Elemental analysis was carried out with a VARIO ELIII analyzer ((CHNS/O Analyzer-Perkin Elmer, PE2400 Series II). The Degree of Substitution (DS) of cellulose derivatives is defined as the average number of substituted hydroxyl groups per glucose. The theoretical maximum is thus a DS of 3.0. The degree of substitution (DS₁) of cationic and thiol groups in first step were calculated from nitrogen content analysis by applying to the following equation:

$$DS_1 = \frac{M_{AGU} \times N_1\%}{M_N \times 100 - (M_1 \times N_1\%)}$$

where DS₁, M_{AGU}, N₁%, M_N and M₁ delegated the degree of substitution of cationic and thiol groups in first step, the molecular weight of anhydroglucose unit, the content of element nitrogen in a product step 1, the molecular weight of nitrogen and the molecular weight of summation of cationic and thiol groups, respectively.

The DS_2 value of long chain hydrocarbons (octadecyl groups) also was determined from the nitrogen content of amphiphilic cellulose derivatives e.g. amphiphilic cationic aminocellulose or amphiphilic thiolated cationic aminocellulose, and calculated according to the following equation:

$$DS_2 = \frac{\frac{M_N \times 100 \times DS_1}{N_2\%} - (M_{AGU} + (DS_1 \times M_1))}{M_2}$$

where DS_2 , $N_2\%$ and M_2 delegated the degree of substitution of octadecyl groups, the content of element nitrogen in amphiphilic cellulose derivatives and the molecular weight of the octadecyl groups, respectively.

3.3.2.2 ^{13}C Nuclear Magnetic Resonance spectroscopy (NMR)

For the characterization of cellulose and the four cellulose derivatives (cationic aminocellulose, thiolated cationic aminocellulose, amphiphilic cationic aminocellulose and amphiphilic thiolated cationic aminocellulose), about 5-8 mg of each compound were dissolved in dimethyl sulfoxide (DMSO). ^{13}C NMR spectra were recorded using Bruker NMR spectrometer operated at 400 MHz.

3.3.2.3 Fourier Transformed Infrared Spectroscopy (FTIR)

The infrared spectra of cellulose and modified celluloses were recorded on a Perkin Nicolet 6700 FTIR system in over the wavelength region of $400\text{-}4000\text{ cm}^{-1}$ at ambient temperature with a 8 cm^{-1} resolution and 16 scans. Samples were prepared using the KBr disc method.

3.3.2.4 Determination of the thiol group and disulfide group content

The degree of modification was determined by quantifying the amount of thiol groups on thiolated cationic aminocellulose was determined spectrophotometrically

with Ellman's reagent [56]. First, 0.50 mg conjugated were hydrated in 250 μL of deionized water. Then 250 μL 0.5 M phosphate buffer (pH 8.0) and 500 μL Ellman's reagent (3 mg of 5,5'-dithio-bis(2 nitrobenzoic acid) in 10 mL of 0.5 M phosphate buffer, pH 8) were added. The sample was incubated for 3 h at room temperature and the absorbance was measured at a wavelength of 450 nm with a microtitration plate reader. The amount of thiol moieties was calculated from an according standard curve obtained by cellulose solution with increasing amounts of cysteine HCl standards (Appendix A).

The amount of disulfide bonds was determined that it was formed due to the oxidation by air/atmosphere during the thiolation step. The amount of disulfide bonds within the obtained polymer was evaluated to the following test. Briefly, 0.5 mg of the thiolated polymer was hydrated in 1 mL of 50 mM phosphate buffer pH 8.0 for 30 min. 600 μL of 3% sodium-borohydride solution was added to the polymer solution, and the mixture was incubated for 2 h in an oscillating water bath. 500 μL of 1M HCl were added in order to destroy the remaining sodium-borohydride. After the addition of acetone (100 μL) the mixture was agitated for 5 min. Thereafter, 1 mL of 1M phosphate buffer pH 8.5 and 200 μL of 0.5% (w/v) DTNB dissolved in 0.5M phosphate buffer pH 8.0 was added. After incubation for 15 min at room temperature aliquots of 200 μL were transferred to a 96-well microtitration plate and the free sulfhydryl groups were determined as described above. The amount of disulfide bonds was calculated by subtracting the quantity of free thiol groups as determined by the method described above from the totality of thiol moieties present on the polymer.

3.3.2.5 X-ray powder diffraction (XRD) analysis

The X-Ray powder diffraction (XRD) pattern was performed using a Rigaku X-ray diffractometer Dmax 2200 Ultima at room temperature with a speed scan of 5°/min using CuK-alpha radiation ($\lambda = 1.54 \text{ \AA}$, 40 kV, 30 mA).

3.3.2.6 Thermogravimetric analysis (TGA)

The thermal stability of each of the samples was evaluated using TGA analysis. These experiments were performed on a PerKinElmer Pyris Diamond TG/DTA machine under a nitrogen flow at a rate of 30 mL/min. Approximately 7-10 mg of samples were placed in the alumina pan, sealed and heated at 10°C/min from 25 to 600°C.

3.3.3 In vitro bioadhesion of mucin to cellulose and the cellulose derivative polymers

3.3.3.1 Mucus glycoprotein assay

The Periodic acid schiff's (PAS) method is widely used for both the quantitative and qualitative analysis of mucins, glycoproteins, glycogen and other polysaccharides in tissues and cells [85]. The PAS colorimetric assay for the detection of glycoproteins was used as previously reported [86, 87] for the determination of the free mucin concentration, so as to evaluate the amount of mucin adsorbed onto the cellulose and its derivatives. Schiff reagent contained 100 mL of 1% (w/v) basic fuchsin (pararosaniline) in an aqueous solution and 20 mL of 1 M HCl. To this was added sodium metabisulfite (1.67% (w/v) final) just before use, and the resultant solution was incubated at 37°C until it became colorless or pale yellow. Periodic acid reagent was freshly prepared by adding 10 μ L of 50% (v/v) periodic acid solution to 7 mL of 7% (v/v) acetic acid solution.

Standard calibration curves were prepared from the four mucin standard solutions (0.2, 0.4, 0.6, 0.8 and 1.0 mg/2 mL) (Appendix 2). After adding 0.1 mL of periodic acid reagent, the solutions were incubated at 37°C for 2 h before 0.1 mL of Schiff reagent was added and incubated at room temperature for 30 min. Next 0.1 mL aliquots of the solution were transferred in triplicate into a 96-well microtiter plate and the absorbance at 555 nm was recorded. The mucin contents were then calculated by reference to the standard calibration curve.

3.3.3.2 Adsorption of mucin on cellulose and its derivatives

A 0.5% (w/v) mucin solution in each of three broadly isoosmotic solutions that differ in pH, namely simulated gastric fluid (SGF) (0.1 N HCl, pH 1.2), simulated intestinal fluid (SIF) (phosphate buffered saline (PBS), pH 6.8) and simulated colon fluid (SCF) (phosphate buffered saline (PBS), pH 7.4) media, were prepared. Cellulose and its derivatives were dispersed (at 20 mg/1.5 mL final) in the above mucin solutions, vortexed, and shaken at 37°C for 2 h. Then the dispersions were centrifuged at 12000 rpm for 2 min to pellet the cellulose-mucin or thiolated cationic aminocellulose-mucin complex and the supernatant was harvested and used for the measurement of the free mucin content. The mucin concentration was calculated by reference to the calibration curve, and the amount of mucin adsorbed to the nanoparticles was calculated as the difference between the total amount of mucin added and the free mucin content in the supernatant.

3.4.2 Characterization of the particles

3.4.2.1 Scanning Electron Microscope (SEM)

The morphology and surface appearance of the particles (before and after the drug loading) were examined by SEM. The sample was mounted onto an aluminum stub using double-sided carbon adhesive tape and coated with gold-palladium. Coating was achieved at 18 mA for at least 4 min. Scanning was performed under high vacuum and ambient temperature with beam voltage of 10-20 kV.

3.4.2.2 Particle size measurement

The particle size and size distribution of particles were evaluated with a particle size analyzer after suspension of the microspheres in an aqueous 5% (w/v) sodium tripolyphosphate solution. The particle size calculation was based on dynamic light scattering (DLS) method, as a software protocol. The scattered light

was collected at an angle of 90° through fiber optics and converted to an electrical signal by an avalanche photodiode array (APDs). All samples were sonicated and run in triplicate with the number of runs set to five and run duration set to 10 seconds.

3.4.2.3 Zeta potential

Zeta potential of the particles was determined using particle sizer. The analysis was performed at a scattering angle of 90°. All samples were sonicated and run in triplicate with the number of runs set to 5 and run duration set to 10 seconds.

3.4.2.4 Determination of critical micelle concentration

The 1000 μM of aliquot (10 mL) of pyrene solution was added into each clean test tube and dried under nitrogen, then 10 ml of amphiphilic cationic aminocellulose and amphiphilic thiolated cationic aminocellulose in water (at various concentrations of 0.01, 0.1, 0.25, 0.35, 0.5, 0.6 g/L) were added. The samples were kept at room temperature overnight for equilibration. Then the samples were subjected to fluorescence spectroscopic analysis on PerkinElmer LS 55 Luminescence Spectrometer (PerkinElmer, Massachusetts, USA). Plot between ratio of fluorescent intensity at 372 to 382 nm and concentration of amphiphilic cationic aminocellulose and amphiphilic thiolated cationic aminocellulose (g/L) was then constructed and critical micelle concentration (CMC) was estimated from the interception of curve fitting between two slopes.

3.4.3 Study of the drug behavior of the nanoparticles

3.4.3.1 Calibration curve of CPT in dimethylsulfoxide (DMSO)

The standard stock CPT solution was prepared in 1% (v/v) DMSO. CPT 5 mg was accurately weighed and dissolved with 1% (v/v) DMSO into 50 mL volumetric flask and adjusted to volume (100 ppm). The stock CPT solution was diluted to 10, 20, 30, 40, and 50 ppm with 1% (v/v) DMSO in volumetric flask. The absorbance of

standard solution was determined by UV-Vis spectrophotometer at 370 nm. The 1% (v/v) DMSO was used as a reference solution. The absorbance and calibration curve of CPT in 1% (v/v) DMSO was shown in appendix C

3.4.3.2 Calibration curve of CPT in various buffers (pH 1.2, 6.8, and 7.4)

The standard stock CPT solution was prepared in 1% (v/v) DMSO in pH 1.2, 6.8, and 7.4. CPT 5 mg was accurately weighed and dissolved with 1% (v/v) DMSO into 50 mL volumetric flask and adjusted by various buffers to volume (100 ppm). The stock CPT solution was diluted to 10, 20, 30, 40, and 50 ppm with three different buffers in volumetric flask. The absorbance of standard solution was determined by UV-Vis spectrophotometer at 370 nm. The 1% (v/v) DMSO was used as a reference solution. The absorbance and calibration curve of CPT in 1% (v/v) DMSO was shown in appendix C.

3.4.3.3 Determination of drug loading efficiency (EE)

The dried CPT immobilized onto amphiphilic cationic aminocellulose and amphiphilic thiolated cationic aminocellulose nanoparticles (2mg) were immersed in 10 mL of DMSO. The mixture was stirred at room temperature for 30 min. The supernatant of solution was collected and determined by UV-Vis spectrophotometer at 370 nm. All experiments were performed in triplicate. The percentage of encapsulation efficiency of CPT was calculated from the following equation:

$$\text{Drug encapsulation efficiency (EE)} = \frac{\text{Actual Drug Content}}{\text{Theoretical Drug Content}} \times 100$$

3.4.3.4 In vitro drug release

The CPT release from amphiphilic cationic aminocellulose and amphiphilic thiolated cationic aminocellulose nanoparticles were studied in three different buffers by dialysis bag diffusion technique. The accurate weighted quantities of 10 mg of the spheres were enclosed in a dialysis bag with a molecular weight cut off of

3500 Da and immersed into 50 mL of SGF pH 1.2, SIF pH 6.8, and SCF pH 7.4 in a flask. The flask was placed in a shaken water bath at speed of 100 rounds per minutes and incubated 37 ± 1 °C. The incubated solution was collected at designated interval of time points and equal volume of fresh medium was compensated. The released CPT amount was determined in 7 days by UV spectroscopy, detection at 370 nm. The amount of CPT released was calculated by interpolation from a calibration curves containing increasing concentrations of CPT. The percentages of cumulative CPT release were calculated from this equation

$$\% \text{ Cumulative Drug Release} = \frac{\text{Actual Drug Content}}{\text{Theoretical Drug Content}} \times 100$$



CHAPTER IV

RESULTS AND DISCUSSION

4.1 Mucoadhesive drug carrier based on amphiphilic cationic aminocellulose

4.1.1 Formation and characterization of amphiphilic cationic aminocellulose

Preliminary studies of the solubility of hydrophobic cationic aminocellulose can dissolve in distilled water and also DMSO. The solubility of cellulose derivatives is strongly influenced by their architecture and chemical composition.

Amphiphilic cationic aminocellulose were obtained by a two-step synthesis as illustrated in Figure 4.1. The frits substitution reaction by ring-opening reactions of lactam give the product with %N_a of 3.86% based on mass fractions of a cationic aminocellulose (Product step 1) and DS_C value of 0.72, which was examined by elemental analysis. Then octadecyl bromide was reacted with the remaining hydroxyl groups of cellulose in NaOH aqueous solutions. For the introducing of the long hydrophobic octadecyl chains -(CH₂)₁₇CH₃ give the product with %N_b based on mass fractions of a hydrophobic cationic aminocellulose (Product step 2) of 2.53% and DS_A value of 0.55. As the result, %N_b decreased due to C and H content increase after attaching long hydrophobic octadecyl chains implying that octadecyl groups attached to the remaining of hydroxyl groups of cellulose. The DS value of octadecyl groups can be examined by %N_b because substitution group in step 2 (octadecyl) is composed of only carbon and hydrogen atom which is similar to cellulose content, therefore it is easier to investigate the DS_A by monitor the change of nitrogen content in the second product.

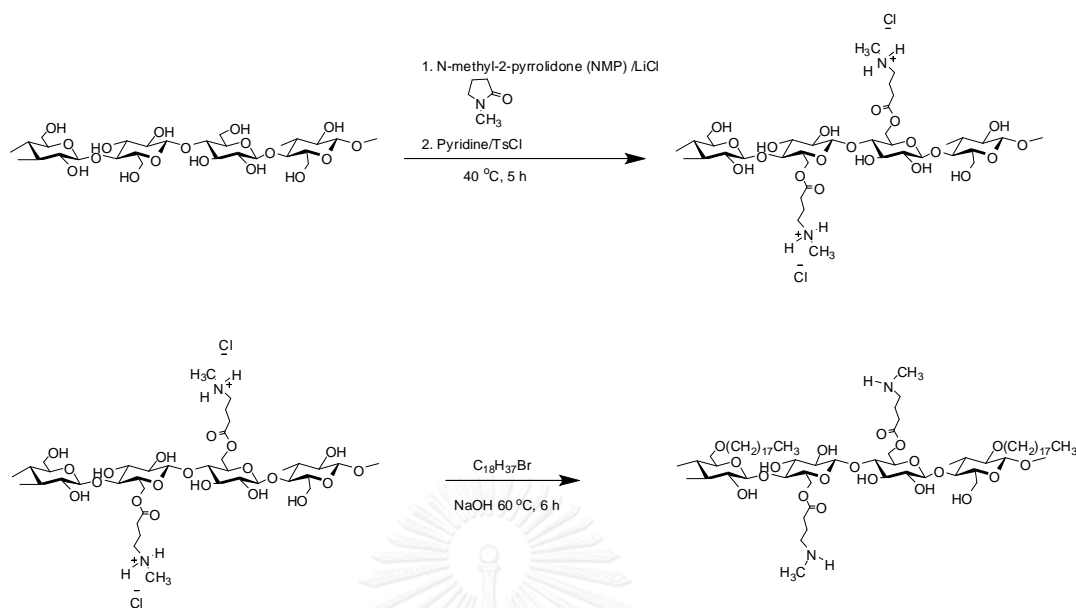


Figure 4.1 Synthesis of the amphiphilic cationic aminocellulose

4.1.2 ¹³C Nuclear Magnetic Resonance spectroscopy (NMR)

Figure 4.2 shows the ¹³C NMR spectra of cellulose and cationic aminocellulose in DMSO. In the spectra, the broad peak centered at 40.1 ppm was due to traces of the DMSO. The chemical shifts at 104.5, (74.9-77.2), 79.8 and 62.6 ppm was assigned to the C1, (C2, C3, C5), C4 and C6 of cellulose, respectively. The spectrum of cationic aminocellulose is similar to that of cellulose, except for the new high intensity peaks at around 19.8-31.6 ppm that are assigned to the C8 (CH₂), C9 (CH₂) and C11 (CH₃). In addition, the peak at 50.0 ppm is assigned to the C10 (CH₂), and the characteristic peak at 172.2 ppm is assigned to the C7 (carbonyl of ester moiety, C=O). After attaching long chain alkyl groups onto remained hydroxyl groups, a new strong signal at 12.5-34.5 ppm was assigned to the 16 methenes (-O-CH₂(CH₂)₁₆-CH₃) that was attached to the methyl group of octadecyl groups. Moreover, the methyl group of long alkyl chain (-O-CH₂(CH₂)₁₆-CH₃) has a shift at 14.7

ppm. Furthermore, FTIR method also was used to confirm if the synthesis process was a reaction completely effective.

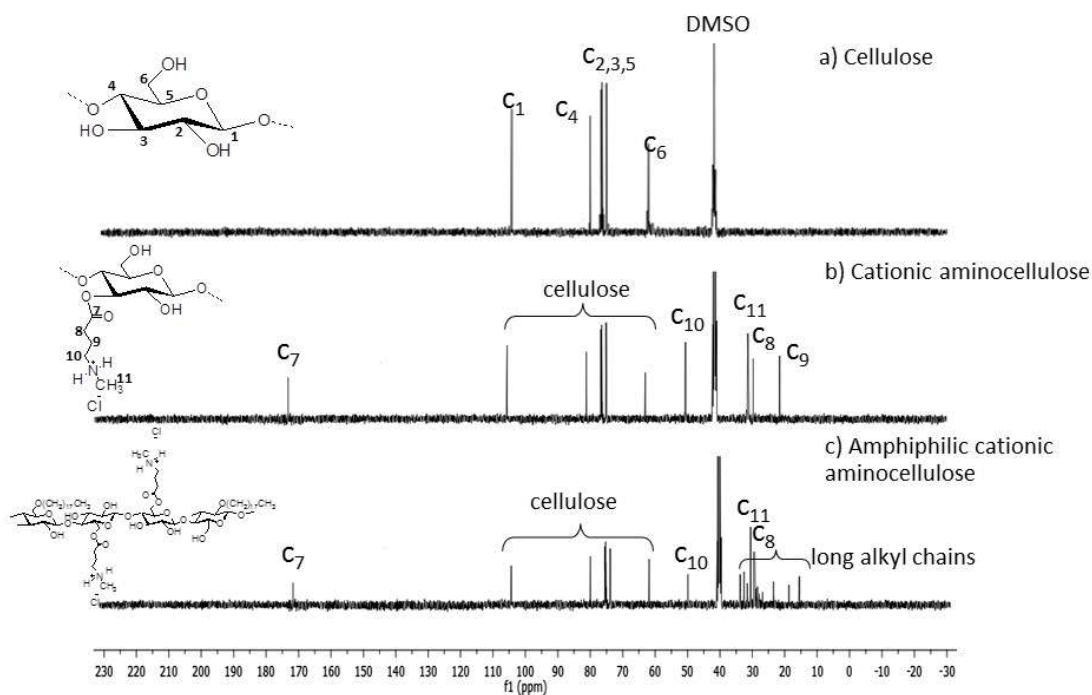


Figure 4.2 Representative of ^{13}C NMR spectra of (a) cellulose, (b) cationic aminocellulose, and (c) amphiphilic cationic aminocellulose

จุฬาลงกรณ์มหาวิทยาลัย
CHULALONGKORN UNIVERSITY

4.1.3 Fourier transformed infrared spectroscopy (FTIR)

Figure 4.3 shows the Fourier transform infrared spectra of the pure microcrystalline cellulose and its derivatives. The FTIR spectrum of the pure microcrystalline cellulose (Figure 3a) shows a strong broad band at 3400 cm^{-1} , the peak at 2900 cm^{-1} belongs to the asymmetrically stretching vibration of C-H in a pyranoid ring, a band at 1638 cm^{-1} corresponding to the stretching and bending modes of the surface hydroxyls, and the broad absorption peak at 1063 cm^{-1} is attributed to the C-O-C of cellulose. After preparation of cationic aminocellulose, the FTIR spectrum of cationic aminocellulose exhibited similar peaks compared to Figure 3a, but a new band appeared at $1,750\text{ cm}^{-1}$ and $1,268\text{ cm}^{-1}$ that are attributed to the

C=O and C-O-C of ester moiety of cationic cellulose. In addition, no unreacted NMP present because the peak at around 1670 cm^{-1} which is attributed to the C=O of NMP solvent [88] cannot be found suggesting that NMP was completely removed. Compared with that of cationic aminocellulose, the FTIR spectrum of hydrophobic cationic aminocellulose showed two new peaks at 2920 and 2851 cm^{-1} attributed to long alkyl chain and thus confirm the attachment of long chain alkyl groups to hydroxyl groups of cationic aminocellulose.

The results of the ^{13}C NMR and FTIR spectrum analyses allow us to conclude that the cationic aminocellulose and hydrophobic cationic aminocellulose were successfully prepared.

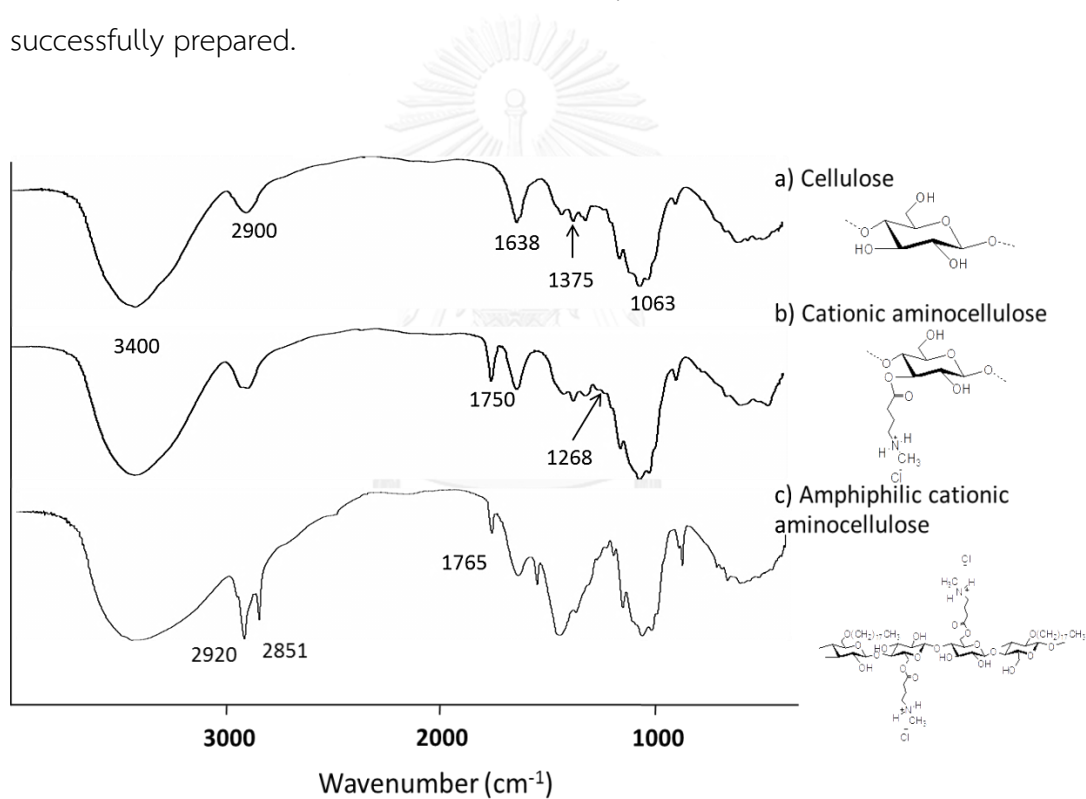


Figure 4.3 FTIR spectra of (a) cellulose, (b) cationic aminocellulose, and (c) amphiphilic cationic aminocellulose

4.1.4 X-ray diffraction

It is widely recognized that cellulose contains both crystalline and amorphous region [89]. The powder X-ray diffraction spectra of cellulose and modified samples are shown in Figure 4.4. The diffractograms of the microcrystalline cellulose samples exhibit diffraction pattern typical of cellulose I, with diffraction peaks of the 2θ angles at 15.0° , 16.6° , 22.7° and 34.1° , which can be assigned to the $11\bar{0}$, 110, 002 and 004 reflections, respectively [90]. In the diffraction spectra of cationic aminocellulose, the peak at $2\theta = 15.0^\circ$, 16.6° and 34.1° disappeared while the peak at $2\theta = 22.7^\circ$ became broader and even amorphous, moreover, a wide peak occurred near 12.8° , which demonstrates that the original crystallinity of cellulose were destroyed while recrystallization happened after providing cationic amino groups. However, after long alkyl chain substitution, a strong diffraction peak in the small-angle region ($2\theta = 5.7^\circ$ or 8.3°), a broad halo peak at around 23.4° were observed. It is possible that the present of the long alkyl chain moiety resulted in a change in the crystallinity of the cellulose and cationic aminocellulose. The results suggest that addition of long alkyl chain can enhance the crystallinity of cationic aminocellulose because of hydrophobic interaction between alkyl chains and arrangement of side groups on the backbone.

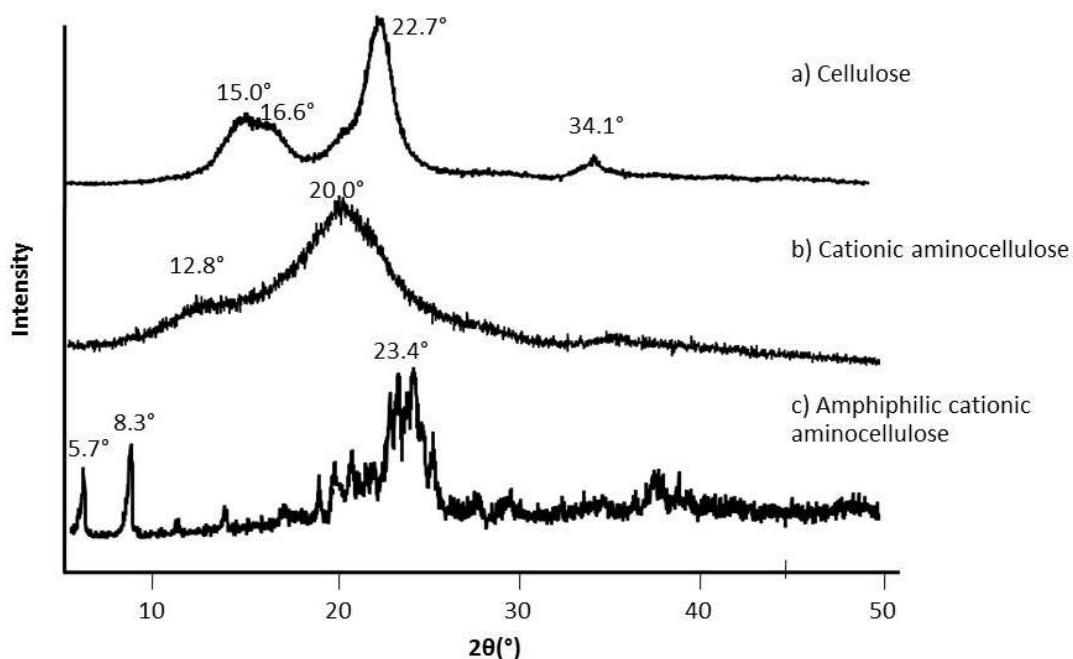


Figure 4.4 XRD pattern of (a) cellulose, (b) cationic aminocellulose, and (c) amphiphilic cationic aminocellulose

4.1.5 Thermogravimetric analysis (TGA)

Thermal analysis has been widely employed for the characterization of polymeric materials. Figure 4.5 reports thermogravimetric analysis (TGA), and derivative thermogram (DTG) curves for cellulose and the modified celluloses with a heating rate of 10 °C/min in nitrogen from 50 to 600 °C.

Thermal degradation of cellulose and modified cellulose gave an initial weight loss in the range of 50-150 °C due to the evaporation of loosely bound moisture on the surface of the samples [91-93]. For cellulose, the highest thermal decompositions stage occurred at 360 °C with a weight loss of 83% and was due to the decomposition of the cellulose backbone. The cationic aminocellulose started to degrade at a lower temperature than native cellulose with the cationic aminocellulose exhibiting their highest thermal decomposition at 345 °C, but with a

slightly lower weight loss at 63%. The decreased thermal stability of the cationic aminocellulose can be explained by the fact that after producing the cationic parts might reduce the hydrogen bonding between cellulose chains, it lead to an increase in the polymer chain mobility [94]. Furthermore, it was observed that amphiphilic cationic aminocellulose exhibited two degradation peaks at 248 and 353 °C, respectively. The first board peak weight loss at 68% could be due to degradation of cellulose backbone, while the second minor peak weight loss at 19% probably due to loss of long alkyl chains. In view of the above results, it was implied the possibility to obtain modified cellulose with good thermal stability.

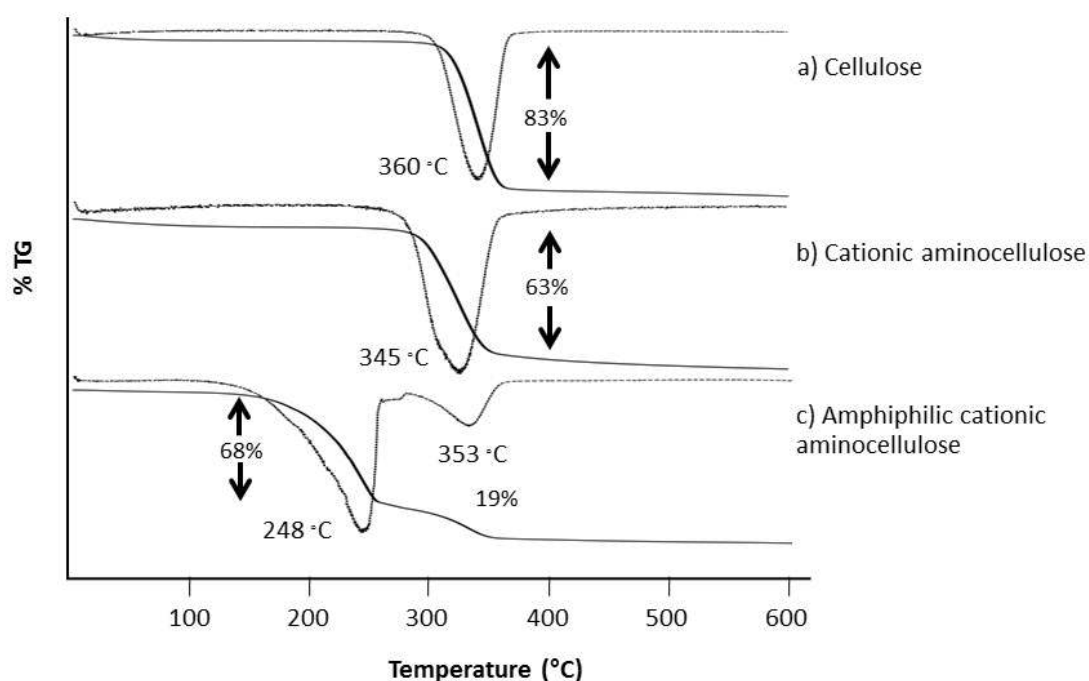


Figure 4.5 TGA analysis (TG and DTG) of (a) cellulose, (b) cationic aminocellulose, and (c) amphiphilic cationic aminocellulose

4.1.6 Mucoadhesion studies

In general, mucoadhesion is considered to occur in three major stages: wetting, penetration, and mechanical interlocking between the mucus and polymer. Several general theories have been presented to explain the mucoadhesion

phenomena. Mucoadhesive properties have traditionally been evaluated by several methods, including tensile studies, flow retention techniques and spectroscopic based analysis [3, 95]. In this study the PAS colorimetric method was used to determine the amount of free mucin and so indirectly estimate the amount of adsorbed mucin on the cellulose, cationic aminocellulose and hydrophobic cationic aminocellulose.

The amount of mucin that was adsorbed onto the polymer depend on ionization of sialic acid of the mucus glycoprotein and polymer that is to say the value of pK_a and pI for sialic acid and mucin are 2.6 and $\sim 3-5$, respectively [63]. Therefore the different forms of the glycoprotein will be influenced by the pH value of the environment. As shown in Table 4.1, the adsorption of mucin to cellulose was pH-dependent, being negligible at pH 1.2 and almost similar at pH 6.8 and pH 7.4 (about 3-fold higher than that at pH 1.2). At the low pH (pH 1.2), the mucoadhesive ability of cellulose was increased by the addition of the cationic charges or long alkyl chains because of the electrostatic and hydrophobic effects. These interactions are, however, weak in comparison with covalent bonds. The poor mucin binding at a low pH (pH 1.2) is likely to reflect the decreased density of the negative charges of sialic acid in mucin due to its protonation (pK_a 2.6). The electrostatic attraction between the negatively charged sialic acid of mucin and the cationic charges of cellulose will then be reduced leading to a reduced amount of mucin adsorption at pH 1.2. Moreover addition of the long alkyl chains (hydrophobic effects), the $-CH_2$ moieties interact in part with the $-CH_3$ groups on the mucin side chains which, lead to a high mucoadhesive adsorption.

However, at pH 6.8 or pH 7.4 a statistically stronger mucoadhesiveness was observed with the modified cellulose sample, with a ~ 2 -fold higher level of adsorbed mucin being observed that from the modified cellulose at pH 1.2. The stronger of mucoadhesiveness is also due to the electrostatic and hydrophobic effects. However at high pH, the dissolution of cellulose and modified cellulose increases, resulting in an increase in the mucoadhesive property. It can be concluded

that amphiphilic cationic aminocellulose might be a good candidate mucoadhesive polymer for drug delivery system.

Table 4.1 Comparison of the mucoadhesive property of cellulose and the modified celluloses

Formulation	Adsorbed of mucin		
	pH 1.2 (mg) (\pm SD, n=3)	pH 6.8 (mg) (\pm SD, n=3)	pH 7.4 (mg) (\pm SD, n=3)
Cellulose	0.08 \pm 0.01	0.18 \pm 0.04	0.20 \pm 0.06
Cationic aminocellulose	0.21 \pm 0.02	0.40 \pm 0.05	0.43 \pm 0.05
Amphiphilic cationic aminocellulose	0.26 \pm 0.07	0.45 \pm 0.07	0.47 \pm 0.04
Amphiphilic cationic aminocellulose-CPT 1%	0.25 \pm 0.02	0.41 \pm 0.05	0.42 \pm 0.07

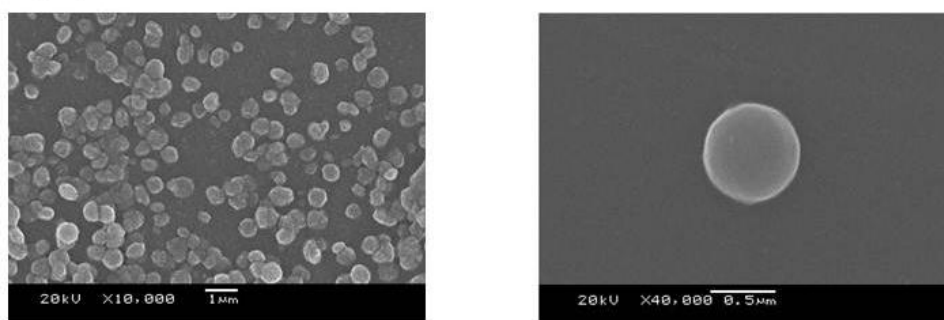
4.1.7 Formation of hydrophobic cationic aminocellulose micelles

Dialysis is one of the most extensively used methods to get the self-assembled polymer micelles. Herein the micelles of amphiphilic cationic aminocellulose samples were prepared by a dialysis method. In brief, amphiphilic cationic aminocellulose samples were dissolved in DMSO/H₂O (v/v = 1) at an initial concentration of 1 mg/mL, and then dialyzed against distilled water for 24 h using a dialysis tube (MW cutoff 12,000), and the distilled water was replaced every 4 h. The self-assembly of amphiphilic cationic aminocellulose polymer in distilled water was first fabricated based on non-polar and hydrophobic interactions between the hydrophobic core-forming chains.

To investigate the size and morphology of nanomicelles prepared in this study, SEM and DLS were used for diameter analysis. As illustrated in Figure 4.6, it was evident that the self-assembled micelles were individual nanoparticles with regular spherical shape, and dispersed homogeneously attributing to the electrostatic repulsion of the particles for their positively charged surfaces. From SEM images, the average sizes of amphiphilic cationic aminocellulose micelles were about 495 ± 54 nm, which was smaller than that observed by DLS (Figure 4.6 and Table 4.2). This is mainly attributed to the fact that the size measured by DLS is the diameter of micelles in aqueous solution, i.e., in the swollen state leading to the swelling of polymer while the size observed by SEM is the diameter of the air-dried micelles. However, the size of the drug-loaded amphiphilic cationic aminocellulose micelles (233 ± 81 nm) was slightly smaller than those of the drug-free micelles which is similar to the observation of DLS. It is probably due to the strengthened hydrophobic interaction between drug and hydrophobic moieties.

In this study, we also investigated the zeta-potential of the hydrophobic cationic aminocellulose micelles in water, and the results are listed in Table 4.2. It is found that the zeta-potential of unload and load drug micelles was 25.6 and 27.8 mV, respectively. These results suggest that amphiphilic cationic aminocellulose micelles have superficial groups with positive charge on the surface. Moreover, the micelles presented relative high zeta potentials, which mean the charged particles, could repel each other and prevent aggregation or precipitation and show a good stability [96].

a) Amphiphilic cationic aminocellulose micelles



b) CPT loaded amphiphilic cationic aminocellulose micelles

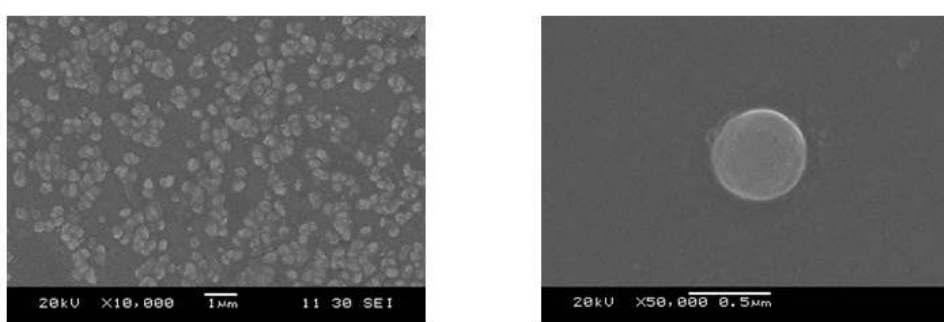


Figure 4.6 SEM images of (a) amphiphilic cationic aminocellulose micelles (b) CPT loaded amphiphilic cationic aminocellulose

Table 4.2 The particle morphology, in terms of the hydrated and anhydrous spherical size, polydispersity index (PDI) and zeta potential of mucoadhesive cellulose derivative micelles with and without CPT.

Formulation	Particle size ^a (nm ± SD)	Particle size ^b (nm ± SD)	PDI	Zeta potential (mV ± SD)
Cellulose	-	-	-	-
Cationic aminocellulose	-	-	-	-
Amphiphilic cationic aminocellulose	495±44	695±21	0.395±0.054	+25.6±0.5
Amphiphilic cationic aminocellulose -CPT 1%	233±31	410±39	0.370±0.082	+27.8±0.9

^aParticle size measured by SEM

^bParticles size measured by particle size analyzer

4.1.8 CMC determination

The synthesized amphiphilic cationic aminocellulose could easily self-assemble to form micelles in aqueous medium. The critical micelle concentration (CMC) is an important characteristic for amphiphilic materials, indicating the micelle formation ability.

CMC value of hydrophobic cationic aminocellulose in distilled water was determined by the fluorescence probe technique using pyrene as a fluorescence probe. The CMC value was defined as the concentration at an inflection point of the plot of I_{372}/I_{388} against the logarithm of the concentration of the amphiphilic cationic

aminocellulose (Figure 4.7). The CMC value of amphiphilic cationic aminocellulose was 95 mg/L. Generally, the higher degree of hydrophobic substitution to polymeric micelles can lead to a lower CMC value, which meant that amphiphilic cationic aminocellulose could easily form micelles and keep the core-shell structure even under highly diluted conditions such as body fluids.

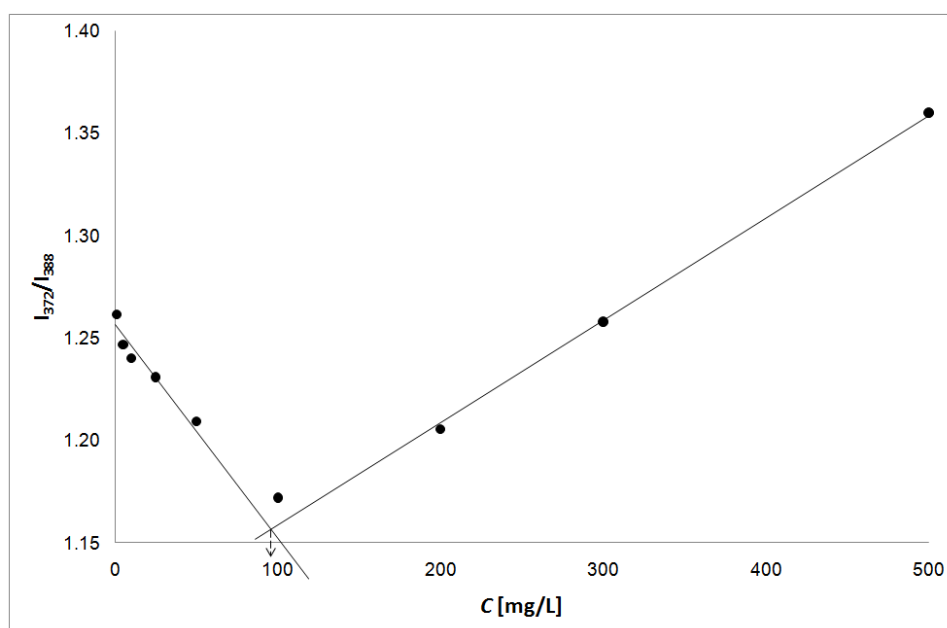


Figure 4.7 Critical micellar concentration (CMC) value of amphiphilic cationic aminocellulose in H₂O at room temperature.

4.1.9 Evaluation of the EE and In vitro CPT release profiles

CPT is a known important anti-cancer drug. However, CPT exhibits limited use because of its poor water solubility and instability. In the present study, we used CPT as a model drug by loading into aminocellulose cationic aminocellulose micelles to facilitate the use of CPT in human body. The CPT loaded aminocellulose cationic

aminocellulose showed high encapsulation efficiency (approximately 86.4%) comparing to other CPT loaded polymer micelles (e.g. 24.5%) [97, 98]. The result suggested to the entrapped CPT is more effectively stabilized in the core of the micelle.

Free CPT solution was dialyzed against PBS, pH 7.4 diffusion out of the dialysis cassette is not a limiting factor, and to establish a benchmark for assessing the performance of the micelle-based systems. The result suggested that free CPT presented a rapid release (83% released in the first 2 h) and completely diffused through the dialysis bag within 3 h, which indicated that the dialysis membrane played negligible role in the release of CPT. The in vitro release of 1% (w/w) CPT from CPT-loaded aminocellulose cationic aminocellulose micelles was performed in three different pH buffers, namely pH 1.2 (SGF), pH 6.8 (SIF) and 7.4 (SCF) at 37 °C. As shown in Figure 4.8, the in vitro release behavior of CPT showed a broadly similar sustained release trend in all three buffers, but differed in the magnitude of the release. CPT loaded polymer micelles was able to minimize the typical burst phase release of the drug in the first stage (only 20% release within 1 h) followed by a sustained release period (up to 7 days). Compared with free CPT solution, the much slower release rate of CPT from the nanocarriers than that from the free CPT solution demonstrated a sustained release of CPT from the nanocarriers.

Furthermore, the change in pH of the releasing medium could cause the drug releasing rate in Figure 4.8. The release profile of aminocellulose cationic aminocellulose micelles at pH 7.4 was faster than that of aminocellulose cationic aminocellulose micelles at pH 1.2 and pH 6.8. In the pH 7.4 medium the cumulative release ratio of CPT from the aminocellulose cationic aminocellulose micelles was approximately 72% at 24 h and then increased over the remaining time, whereas at the lower pH values (1.2 and 6.8), the cumulative CPT release level was about 46% and 62%, respectively, at the same time and then continued to increase. The differences in the CPT release kinetics are likely to be due to the swelling ratio of the particles with the changing pH of the medium. Interestingly, the burst-like release of aminocellulose cationic aminocellulose micelles at pH 1.2, 6.8, and 7.4 was not

obvious because the drug loading could be entrapped in the dense solid regions of the hydrophobic inner shell where polymer entanglement serves as a much greater impediment to drug transport. Furthermore, encapsulation of CPT into the aminocellulose cationic aminocellulose micelles caused no statistically significant ($P > 0.05$) changes in their mucoadhesive property. This phenomenon indicates that CPT was effectively encapsulated into the aminocellulose cationic aminocellulose micelles and might be a good carrier for CPT incorporation and sustained release for passive tumor targeting.

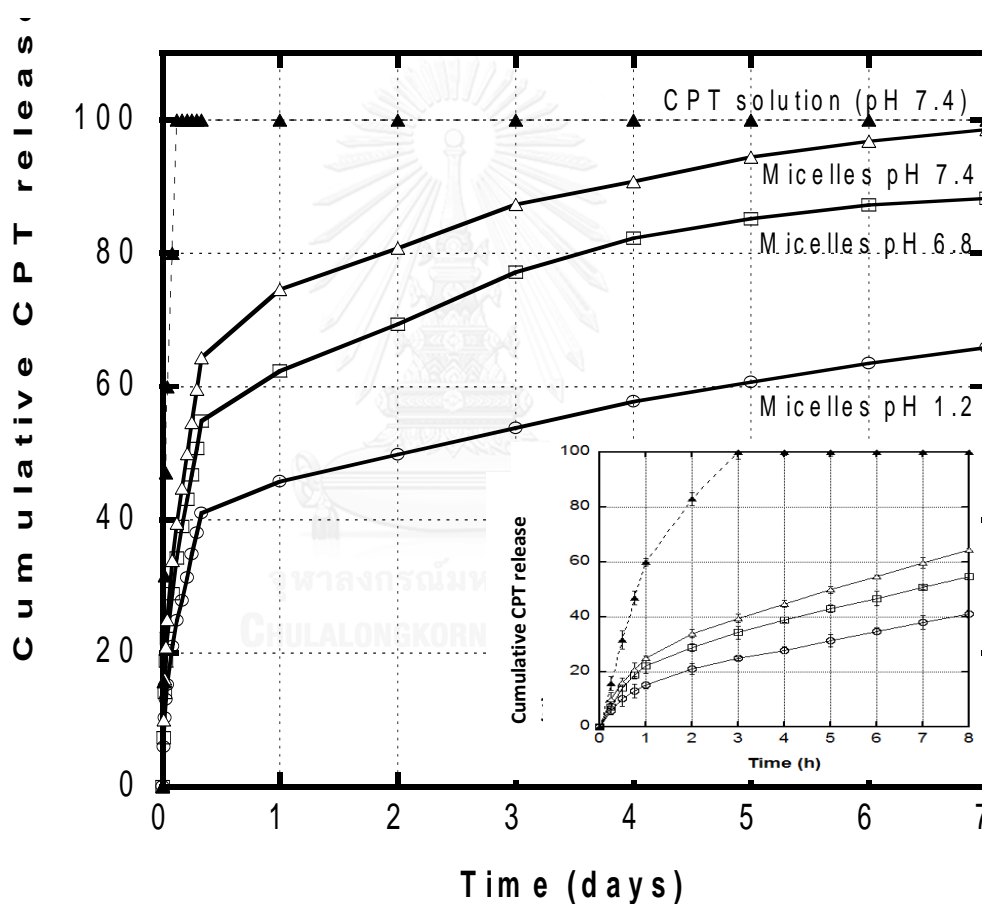


Figure 4.8 Release profiles of CPT from amphiphilic cationic aminocellulose micelles in different pH solutions. The data are shown as the mean \pm SD and are derived from three independent repeats.

4.2 Mucoadhesive drug carrier based on amphiphilic thiolated cationic aminocellulose

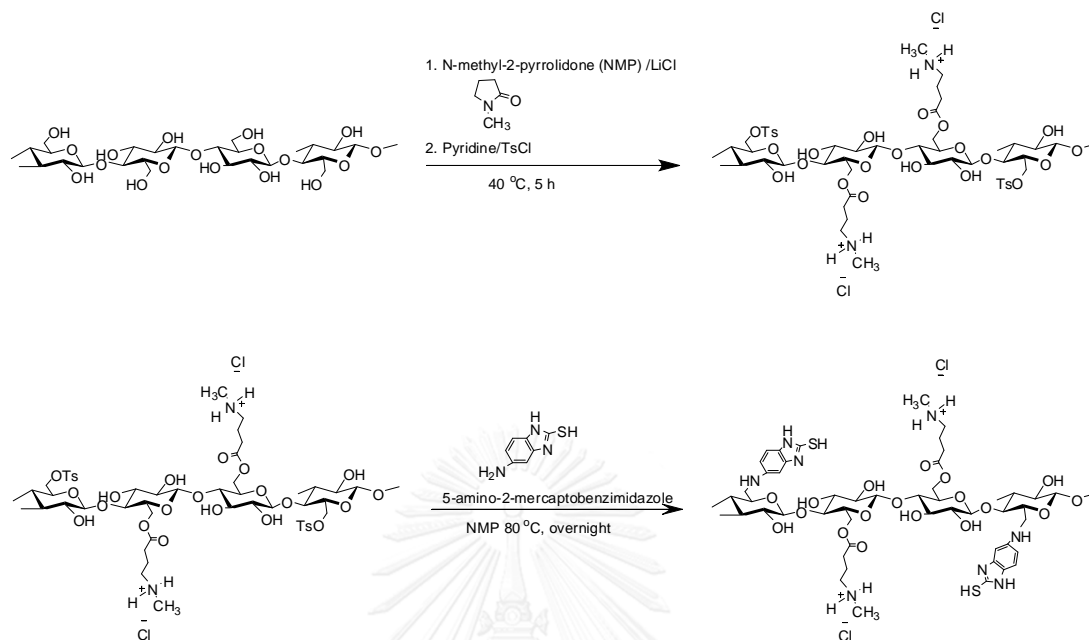
4.2.1 Formation and characterization of amphiphilic cationic thiolated aminocellulose

Amphiphilic thiolated cationic aminocellulose was synthesized. The new synthetic route is illustrated in Figure 4.9. The aim was primarily to prepare a mucoadhesive thiolated cationic aminocellulose that would be potentially suitable for application in a mucoadhesive drug delivery system and then long hydrophobic octadecyl chains $-(\text{CH}_2)_{17}\text{CH}_3$ to remaining hydroxyl groups that can achieve polymeric micelles.

Preliminary studies of the solubility of modified cellulose can fairly dissolve in distilled water and also DMSO. However, the modified cellulose shows much better solubility in mixed solvent $\text{H}_2\text{O}/\text{DMSO}$.

Amphiphilic thiolated cationic aminocellulose were obtained by a two-step synthesis as illustrated in Figure 4.9. The frits substitution reaction by attaching the cationic and thiol groups onto cellulose give the product with $\%N_a$ of 3.19% based on mass fractions of a thiolated cationic aminocellulose (Product step 1) and DS_1 value of 1.17, which was examined by elemental analysis. Then octadecyl bromide was reacted with the remaining hydroxyl groups of cellulose in NaOH aqueous solutions. For the introducing of the long hydrophobic octadecyl chains $-(\text{CH}_2)_{17}\text{CH}_3$ give the product with $\%N_b$ based on mass fractions of a amphiphilic thiolated cationic aminocellulose (Product step 2) of 2.76% and DS_2 value of 0.32. As the result, $\%N_2$ decreased due to C and H content increase after attaching long hydrophobic octadecyl chains implying that octadecyl groups attached to the remaining of hydroxyl groups of cellulose. The DS_2 value of octadecyl groups can be examined by $\%N_2$ because substitution group in step 2 (octadecyl) is composed of only carbon and hydrogen atom which is similar to cellulose content, therefore it is easier to investigate the DS_2 by monitor the change of nitrogen content in the second product.

Step I:



Step II:

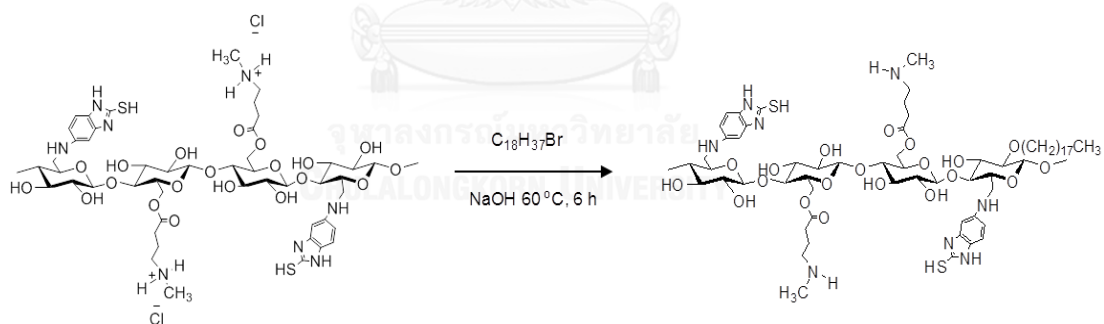


Figure 4.9 Synthesis scheme of amphiphilic thiolated cationic aminocellulose

4.2.2 ^{13}C Nuclear Magnetic Resonance spectroscopy (NMR)

Figure 4.10 shows the ^{13}C NMR spectra of cellulose and modified cellulose in DMSO. In the spectra, the broad peak centered at 40.1 ppm was due to traces of the DMSO. The chemical shifts at 104.5, (74.9-77.2), 79.8 and 62.6 ppm was assigned to the C1, (C2, C3, C5), C4 and C6 of cellulose, respectively (Figure 4.10a). Within the carbon signals in the thiolated cationic aminocellulose spectrum (Figure 4.10b), the characteristic peak of the C=O carbonyl group in ester moiety of cationic groups (C7) has a signal at 173.2 ppm and the peaks at chemical shifts at 51.9, 33.2, 31.5 and 20.3 ppm were ascribed to the C10, C11, C8 and C9 carbons in the cationic parts, respectively. In addition, the peaks at 97.1-168.3 ppm were attributed to C12-C17 of the carbons of the MBI. In order to confirm that MBI were attached to cellulose (to form thiolated cationic aminocellulose), the amount of grafted thiol groups also was evaluated by the Ellman's method. After attaching long chain alkyl groups onto remained hydroxyl groups (Figure 4.10c), the new strong signals at 14.8-33.8 ppm can be attributed to the 16 methenes ($-\text{O}-\text{CH}_2(\text{CH}_2)_{16}-\text{CH}_3$) that was attached to the methyl group of octadecyl groups. Moreover, the methyl group of long alkyl chain ($-\text{O}-\text{CH}_2(\text{CH}_2)_{16}-\text{CH}_3$) has a shift at 14.8 ppm. Furthermore, FTIR method also was used to confirm if the synthesis process was a reaction completely effective.

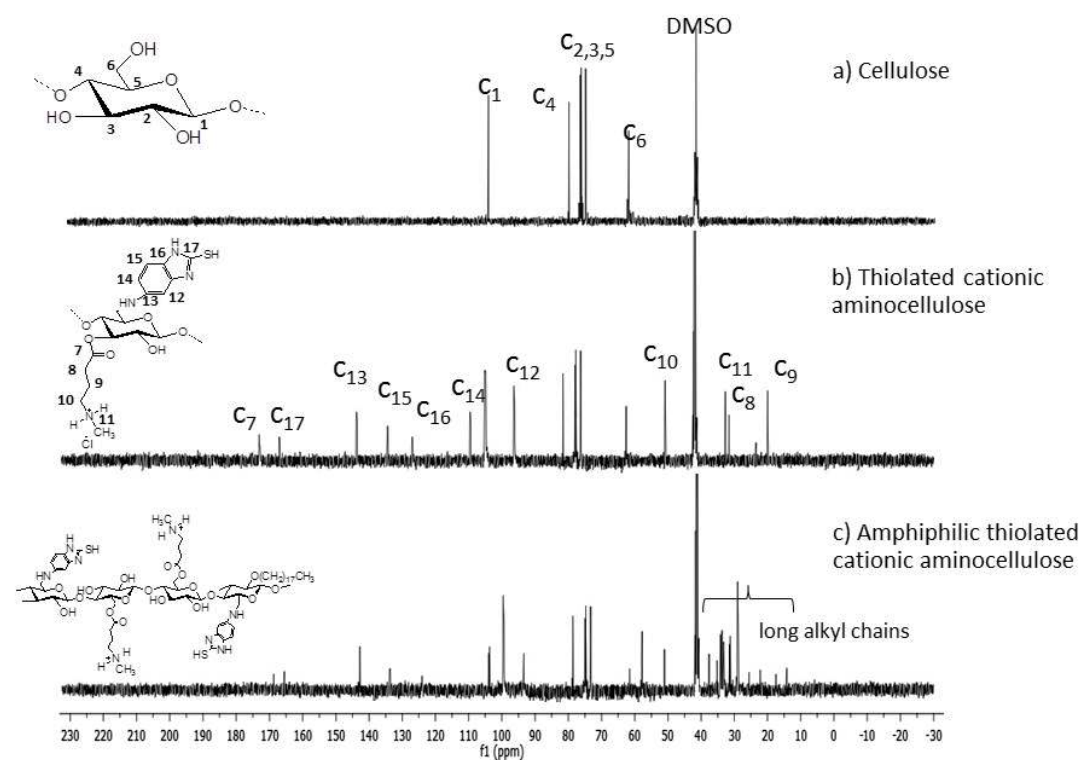


Figure 4.10 Representative of ^{13}C NMR spectra of (a) cellulose, (b) thiolated cationic aminocellulose, and (c) amphiphilic thiolated cationic aminocellulose

4.2.3 Fourier transformed infrared spectroscopy (FTIR)

Figure 4.11 shows the Fourier transform infrared spectra of the pure microcrystalline cellulose and its derivatives. The FTIR spectrum of the pure microcrystalline cellulose (Figure 4.11a) shows a strong broad band at 3400 cm^{-1} , the peak at 2900 cm^{-1} belongs to the asymmetrically stretching vibration of C-H in a pyranoid ring, a band at 1638 cm^{-1} corresponding to the stretching and bending modes of the surface hydroxyls, and the broad absorption peak at 1063 cm^{-1} is attributed to the C-O-C of cellulose. After preparation of thiolated cationic aminocellulose (Figure 4.11b), the FTIR spectrum of thiolated cationic aminocellulose exhibited similar peaks compared to Figure 3a, but a new band appeared at 1750 cm^{-1} and 1268 cm^{-1} that are attributed to the C=O and C-O-C of ester moiety of cationic parts of thiolated cationic aminocellulose. . In addition, the absorption band at 1634 and 1613 cm^{-1} were attributed to the C=N stretching vibrations of benzimidazole ring and the N-H bending of primary amine of MBI, respectively. The peaks at 618 cm^{-1} corresponded to the thiol group. Compared with that of thiolated cationic aminocellulose, the FTIR spectrum of amphiphilic thiolated cationic aminocellulose (Figure 4.11c) showed two new peaks at 2920 and 2851 cm^{-1} attributed to long alkyl chain and thus confirm the attachment of long chain alkyl groups to hydroxyl groups of thiolated cationic aminocellulose.

The results of the ^{13}C NMR and FTIR spectrum analyses allow us to conclude that the thiolated cationic aminocellulose and amphiphilic thiolated cationic aminocellulose were successfully prepared.

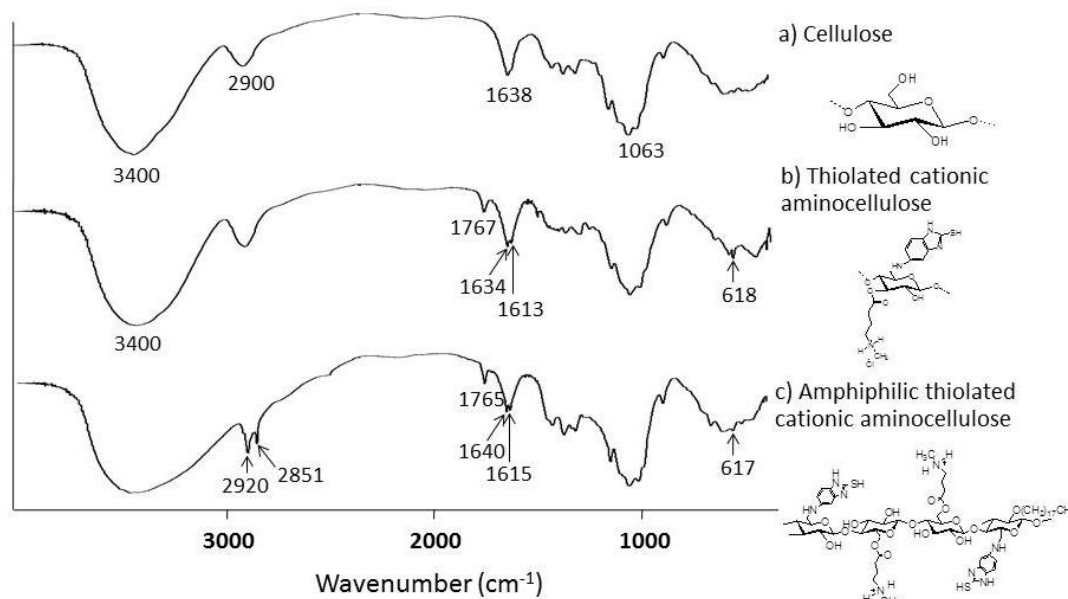


Figure 4.11 FTIR spectra of (a) cellulose, (b) thiolated cationic aminocellulose, and (c) amphiphilic thiolated cationic aminocellulose

4.2.4 X-ray diffraction

It is widely recognized that cellulose contains both crystalline and amorphous region [21]. The powder X-ray diffraction spectra of cellulose and modified samples are shown in Figure 4.12. The diffractograms of the microcrystalline cellulose samples exhibit diffraction pattern typical of cellulose I, with diffraction peaks of the 2θ angles at 15.0° , 16.6° , 22.7° and 34.1° , which can be assigned to the $1\bar{1}0$, 110, 002 and 004 reflections, respectively [90]. In the diffraction spectra of thiolated cationic aminocellulose, the characteristic peaks of cellulose at $2\theta = 15.0^\circ$, 16.6° and 34.1° disappeared while the intensity peak at $2\theta = 22.1^\circ$ decreased, moreover, a peak occurred at $2\theta = 12.2^\circ$ and 19.9° , which demonstrates that the original crystallinity of cellulose were destroyed while the degree of crystallinity on thiolation increased. However, after long alkyl chain substitution, a strong diffraction peak in the small-angle region ($2\theta = 5.5^\circ$ or 8.2°), a broad halo peak at around 24.0° were observed. It is possible that the present of the long alkyl chain moiety resulted in a change in the

crystallinity of the cellulose and thiolated cationic aminocellulose. The results suggest that addition of long alkyl chain can enhance the crystallinity of thiolated cationic aminocellulose because of hydrophobic interaction between alkyl chains and arrangement of side groups on the backbone.

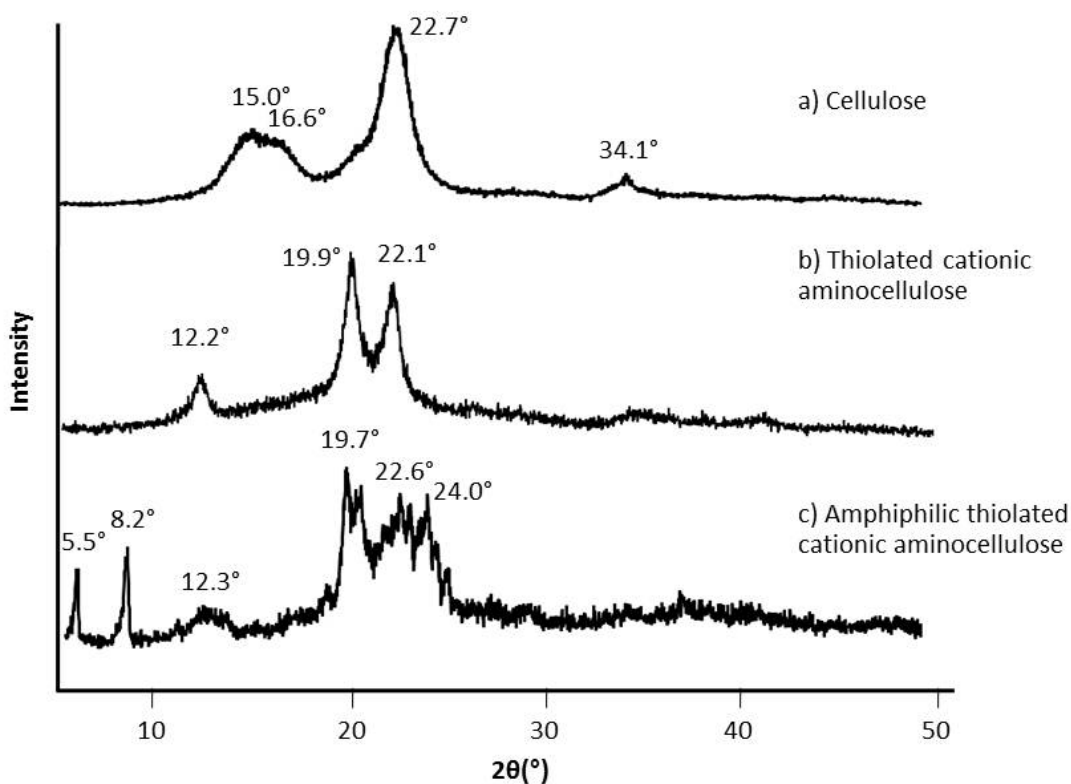


Figure 4.12 XRD pattern of (a) cellulose, (b) thiolated cationic aminocellulose, and (c) amphiphilic thiolated cationic aminocellulose

4.2.5 Thermogravimetric analysis (TGA)

Thermal analysis has been widely employed for the characterization of polymeric materials. Figure 4.13 shows thermogravimetric analysis (TGA), and derivative thermogram (DTG) curves for cellulose and the modified celluloses with a heating rate of 10 °C/min in nitrogen from 50 to 600 °C.

Thermal degradation of cellulose and modified cellulose gave an initial weight loss in the range of 50-150 °C due to the evaporation of loosely bound moisture on the surface of the samples and volatile products [91-93]. For cellulose, the highest thermal decompositions stage occurred at 360 °C with a weight loss of 83% and was due to the decomposition of the cellulose backbone. The thiolated cationic aminocellulose started to degrade at a lower temperature than native cellulose with the thiolated cationic aminocellulose exhibiting their highest thermal decomposition at 339 °C, but with a slightly lower weight loss at 70%. The decreased thermal stability of the thiolated cationic aminocellulose can be explained by the fact that after producing the cationic and thiol groups might reduce the hydrogen bonding between cellulose chains, it lead to an increase in the polymer chain mobility [94]. Furthermore, it was observed that amphiphilic thiolated cationic aminocellulose exhibited two degradation peaks at 232 and 335 °C, respectively. The first board peak weight loss at 47% probably due to loss of long alkyl chains, while the second peak weight loss at 37% could be due to degradation of cellulose backbone. It is implied that introduction of cationic groups, thiol groups and long alkyl side chains reflects the change in the crystalline structure of cellulose. In view of the above results, it was implied the possibility to obtain modified cellulose with good thermal stability.

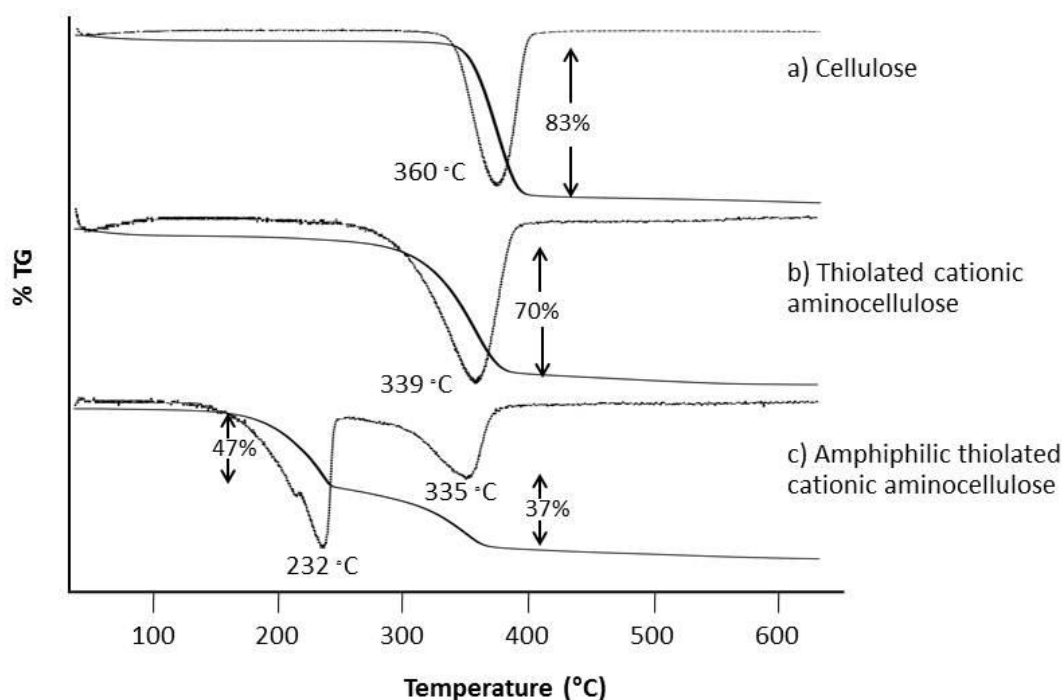


Figure 4.13 TGA analysis (TG and DTG) of (a) cellulose, (b) thiolated cationic aminocellulose, and (c) amphiphilic thiolated cationic aminocellulose

จุฬาลงกรณ์มหาวิทยาลัย
CHULALONGKORN UNIVERSITY

4.2.6 Determination of the thiol and disulfide groups content

One of the important factors of these modified polymers is the level (density) of free thiol groups and disulfide bonds, which cannot be evaluated by NMR. Thus, the degree of modification was determined spectrophotometrically with Ellman's reagent (5,5'-dithiobis(2-nitrobenzoic acid, DTNB). The amount of thiol moieties was calculated from a standard curve obtained by the thiolated cationic aminocellulose solutions with increasing amount of cysteine standard at a wavelength of 450 nm. As already shown by many reports, thiomers are subject to oxidation of thiol groups to disulfide bonds, therefore, disulfide content of samples also was measured after reduction with NaBH_4 . The amount of disulfide bonds was calculated by subtracting the quantity of free thiol groups, as determined above, from the total number of

thiol moieties present on the polymer. The amount of free thiol groups and disulfide bonds immobilized on of thiolated cationic aminocellulose were quantified to be $47.23 \pm 0.16 \mu\text{mol/g}$ and $6.79 \pm 0.12 \mu\text{mol/g}$ polymer, respectively, whilst neither were detected in the pure cellulose (Table 4.3). Furthermore, formation of amphiphilic thiolated cationic aminocellulose with/without CPT slightly decreased the amount of thiol groups. However, these decreases were not statistically significant ($p > 0.05$).

4.2.7 Mucoadhesion studies

The mucoadhesive properties of cellulose, thiolated cationic aminocellulose and amphiphilic thiolated cationic aminocellulose were evaluated in terms of their *in vitro* binding to mucin in solution, and the results are summarized in Table 4.3.

The amount of mucin that was adsorbed onto the polymer depend on ionization of sialic acid of the mucus glycoprotein and polymer that is to say the value of pK_a and pI for sialic acid and mucin are 2.6 and $\sim 3-5$, respectively. Therefore the different forms of the glycoprotein will be influenced by the pH value of the environment.

At pH 1.2 cellulose showed poor mucoadhesive ability but those for thiolated cationic aminocellulose and amphiphilic thiolated cationic aminocellulose were about 3.4- and 3.6-fold higher, respectively, (Table 4.3). Cellulose cannot be dissolved and still perfectly has hydroxyl groups on the cellulose backbone, but the sialic acid on the mucin would also be protonated and so uncharged (-COOH and -SO₃H groups) leading to no electrostatic interaction with cellulose but only hydrogen bonds and van der Waal's interactions. When the cellulose was introduced with cationic and thiol groups, the solubility of cellulose increased. The thiolated cationic aminocellulose contained cationic and thiol (-SH) groups exhibited a slightly stronger mucoadhesiveness compared to pure cellulose. The -SH groups on the thiolated cationic aminocellulose can react with the -SH/-S-S (cysteine and cystine) groups on

the mucin to form disulfide bridges via oxidation. For the amphiphilic thiolated cationic aminocellulose, the aliphatic side chain of long alkyl chains provided further hydrophobic interactions with the CH_2/CH_3 groups of the mucin side chain, whilst the carboxylic group of the MA side chain can form strong hydrogen bonds with the $-\text{COOH}$ and $-\text{SO}_3\text{H}$ groups of the mucus glycoprotein leading to an increased mucoadhesiveness. Therefore, the effect of electrostatic, hydrogen and hydrophobic effects impact on the mucoadhesion of cellulose and the modified cellulose at low pH values.

At pH 6.8 and 7.4, cellulose partially dissolved leading to enhanced the surface area to contact with mucin and so the ~ 2.3 -fold higher mucoadhesion than at pH 1.2. The mucoadhesiveness of thiolated cationic aminocellulose and amphiphilic thiolated cationic aminocellulose were also increased (~ 2.5 -fold) over that at pH 1.2 and so remained higher (~ 3.7 -fold) than that for cellulose. This is because the sialic acid groups of mucin are mostly deprotonated and so charged ($-\text{COO}^-$ and $-\text{SO}^{-3}$), leading to increased ionic interactions between mucin and cationic charge in thiolated cationic aminocellulose and amphiphilic thiolated cationic aminocellulose. In addition, the thiolate anions ($-\text{S}^-$; $\text{p}K_a \sim 2.6$) would lead to a greater extent of oxidation and nucleophilic attack forming covalent disulfide bonds between the thiol group of thiolated cationic aminocellulose and the cysteine-rich subdomains of the mucus glycoprotein [2,27]. Therefore, the effect of electrostatic, the hydrogen bonding, hydrophobic and covalent effects impact more on the mucoadhesion of cellulose and the modified cellulose at the higher pH.

Moreover, loading of the amphiphilic thiolated cationic aminocellulose with CPT at 1% (w/w) decreased their mucoadhesiveness, although the magnitude of this decrease was least for cellulose over the three pH values. Overall, it can be concluded that thiolated cationic aminocellulose and amphiphilic thiolated cationic aminocellulose might be a good candidate mucoadhesive polymer for drug delivery system.

Table 4.3 Comparison of the mucoadhesive property in different pH solutions of cellulose and the modified celluloses and the net amount of thiol groups.

Formulation	Total thiol groups ($\mu\text{mol/g}$)	Total disulfide groups ($\mu\text{mol/g}$)	Adsorbed of mucin		
			pH 1.2 (mg) ($\pm\text{SD}, n=3$)	pH 6.8 (mg) ($\pm\text{SD}, n=3$)	pH 7.4 (mg) ($\pm\text{SD}, n=3$)
Cellulose	-	-	0.08 ± 0.01	0.18 ± 0.04	0.20 ± 0.06
Thiolated cationic aminocellulose	47.23 ± 0.16	6.79 ± 0.12	0.27 ± 0.04	0.67 ± 0.03	0.73 ± 0.08
Amphiphilic thiolated cationic aminocellulose	45.69 ± 0.08	14.54 ± 0.06	0.29 ± 0.04	0.69 ± 0.10	0.75 ± 0.07
Amphiphilic thiolated cationic aminocellulose-CPT 1%	44.82 ± 0.05	11.33 ± 0.03	0.29 ± 0.11	0.61 ± 0.10	0.70 ± 0.06

4.2.8 Spherulite growth and morphology

Due to the fact that the functionalities of materials can be tuned efficiently through operating their structures, diverse strategies have been developed successfully to produce materials with well-defined structures. Spherulites, also known as “sea-urchin” crystal morphology, crystalline morphologies, are an important crystal form that commonly appears in macromolecule systems. They appeared to be interesting systems for controlled release and protection of encapsulated substances [99, 100] because they have a very high surface area to volume ratio. Spherulite formation is a very common form of self-assembly observed during polymer crystallization [101, 102], particularly from synthetic polymer solution

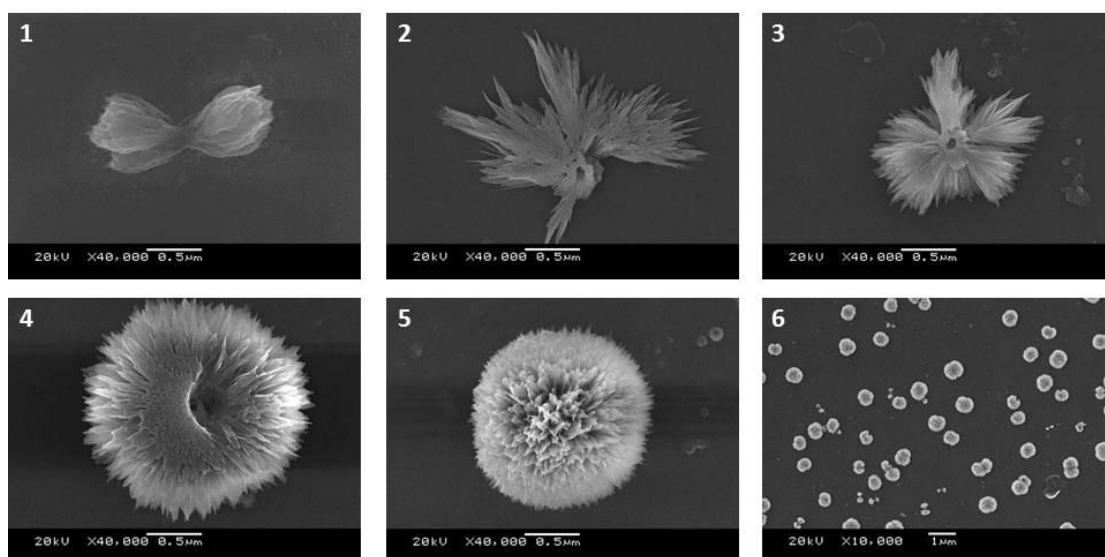
or polymer melt. In order to improve further the performances of drug delivery systems, it is highly desirable to fabricate materials with not only a mucoadhesive property, but also a large specific surface area for high activity with excellent ability of therapeutic value of various medicinal drugs and bioactive molecules.

Self-assembly of amphiphilic thiolated cationic aminocellulose spherulites were prepared by a dialysis method. In brief, amphiphilic thiolated cationic aminocellulose samples were dissolved in DMSO/H₂O (v/v = 1) at an initial concentration of 1 mg/mL, and then dialyzed against distilled water for 24 h using a dialysis tube (MW cutoff 12,000), and the distilled water was replaced every 4 h. The self-assembly of amphiphilic thiolated cationic aminocellulose in distilled water was first fabricated based on non-polar and hydrophobic interactions between the hydrophobic core-forming chains.

The whole process of formation of spherulites was clearly observed under SEM. Figures 4.14 showed a series of SEM images showing the formation of a spherulite. As seen in the figure, the process of a lamellar sheaf developed into a spherulite skeleton upon further growth of the lamellae (stack of lamellae). During the growth process, the stacked lamellae splay apart continually and branch occasionally due to the repulsion of the amorphous materials between the lamellae are the general features of polymer spherulites [28,29]. The continuous growth of the primary lamellae forms a spherical skeleton, and the secondary lamellae fill up the space between the primary lamellae. Also, it has been noted that the spherulites were fairly spherical structure with an average diameter of about 547 nm. From the SEM images, it can be found that the surface of the obtained nanospheres consist of highly oriented nanofibers of about 50 nm in diameter and 100-200 nm in length, which is similar to the structure of a sea urchin. The diameter values for drug loaded micelles were in the range of 421–498 nm (Figure 4.15), which slightly increased with increasing of drug content.

In this study, we also investigated the zeta-potential and polydispersity index (PDI) of the amphiphilic cellulose spherulites in water, and the results are listed in Table 4.4. All formulations had a narrow size distribution, with a polydispersity index

of 0.3-0.4. These results are in agreement with the SEM images (Figure 4.14) that show fairly spherical spherulites or sea-urchin like structures in dehydrated condition. However, the structure in hydrated condition did not study yet. The measurement of the zeta potential allows predictions about the storage stability in suspension by means of electrostatic repulsion between the particles. Unload and load drug spherulites exhibited a positive zeta potential of about +25.1 and +27.8 mV, respectively. The results suggested that the colloidal suspension was stable with less aggregation [30].



CHULALONGKORN UNIVERSITY

Figure 4.14 SEM images of the formation of amphiphilic thiolated cationic aminocellulose spherulites

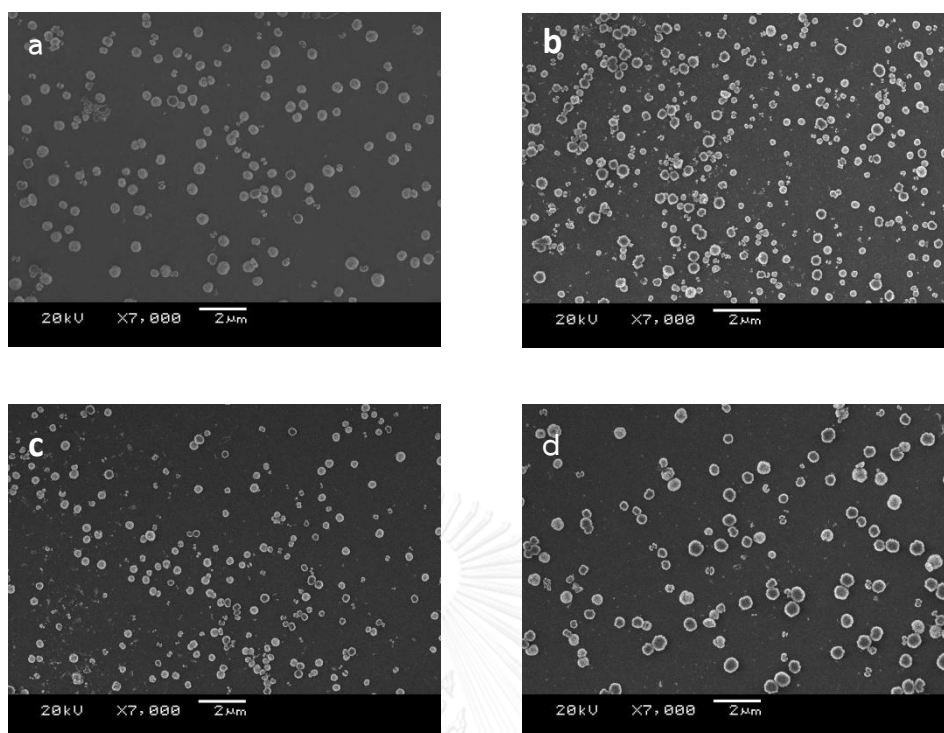


Figure 4.15 SEM images of amphiphilic thiolated cationic cellulose loaded with 0%, 1%, 3 and 5% (w/w) CPT, respectively

Table 4.4 The particle morphology, in terms of the hydrated and anhydrous spherical size, polydispersity index (PDI) and zeta potential of mucoadhesive cellulose derivative spherulites with and without CPT.

Formulation	Particle size ^a (nm ± SD)	Particle size ^b (nm ± SD)	PDI	Zeta potential (mV±SD)
Cellulose	-	-	-	-
Thiolated cationic aminocellulose	-	-	-	-
Amphiphilic thiolated cationic aminocellulose	547 ± 31	713 ± 44	0.374 ± 0.074	25.1 ± 0.7
Amphiphilic thiolated cationic aminocellulose-CPT 1%	421 ± 45	587 ± 55	0.316 ± 0.065	27.8 ± 1.1
Amphiphilic thiolated cationic aminocellulose-CPT 3%	469 ± 34	598 ± 63	0.338 ± 0.035	26.7 ± 0.6
Amphiphilic thiolated cationic aminoellulose-CPT 5%	498 ± 53	644 ± 43	0.363 ± 0.020	26.8 ± 1.6

^aParticle size measured by SEM

^bParticles size measured by particle size analyzer

4.2.9 Evaluation of the EE and In vitro CPT release profiles

CPT is a known important anti-cancer drug. However, CPT exhibits limited use because of its poor water solubility and instability. In the present study, we used CPT as a model drug by loading into amphiphilic thiolated cationic aminocellulose

spherulites to facilitate the use of CPT in human body. The CPT loaded amphiphilic cationic aminocellulose spherulites showed high encapsulation efficiency (over 90% (Table 4.5)). Increasing the CPT loading level in the amphiphilic thiolated cationic aminocellulose from 1% (w/w) to 3 and 5% (w/w) CPT increased the EE of CPT, with an EE of 94.9% being attained at a 5% (w/w) CPT loading. The result suggested to the entrapped CPT is more effectively stabilized in the amphiphilic thiolated cationic aminocellulose spherulites.

Table 4.5 Encapsulation efficiency (% EE) of mucoadhesive cellulose derivative spherulites loaded with 1% (w/w) to 3 and 5% (w/w) CPT

Formulation	EE (%)
Amphiphilic thiolated cationic aminocellulose-CPT 1%	91.2 ± 3.1
Amphiphilic thiolated cationic aminocellulose-CPT 3%	93.6 ± 3.9
Amphiphilic thiolated cationic aminoellulose-CPT 5%	94.9 ± 2.9

Figure 4.16 shows the *in vitro* release of free CPT solution in pH 7.4 and 1% (w/w) CPT from CPT-loaded amphiphilic cationic aminocellulose spherulites in three different pH buffers, namely pH 1.2 (SGF), pH 6.8 (SIF) and 7.4 (SCF) at 37 °C. From the release profiles, free CPT without any formulation showed a rapid release (83% released in the first 2 h) and completely diffused within 3 h. In addition, the *in vitro* release behavior of CPT loaded polymer spherulites showed a broadly similar sustained release trend in all three pH mediums, but differed in the magnitude of the release. It was able to minimize the typical burst phase release of the drug in the first stage (about 10% release within 1 h) followed by a sustained release period (up

to 7 days). However, the release rate of CPT from the polymer spherulites at pH 1.2 was much slower than at either pH 6.8 or 7.4 because the difficult dissolution of spherulites in the acid media limited the release of the drug effectively. In the pH 1.2 medium the cumulative release ratio of CPT from the spherulites was approximately 48% at 1 day and then increased over the remaining time, whereas at the higher pH values (6.8 or 7.4), the cumulative CPT release level was about 63% and 78%, respectively, at the same time and then increased over the remaining time and continued to sustained drug release up to 7 days. The differences in the CPT release kinetics are likely to be due to the swelling ratio of the particles with the changing pH of the medium. The higher swelling ratios of the polymer creates a larger surface area and looser matrix for the CPT to diffuse out of [31] and so led to its quick release from the particles at higher pH (pH 6.8, 7.4) and correspondingly the slower release kinetics at low pH (pH 1.2). Thus, the CPT release behavior was dominated by the swelling ratio of the amphiphilic cationic aminocellulose spherulites.

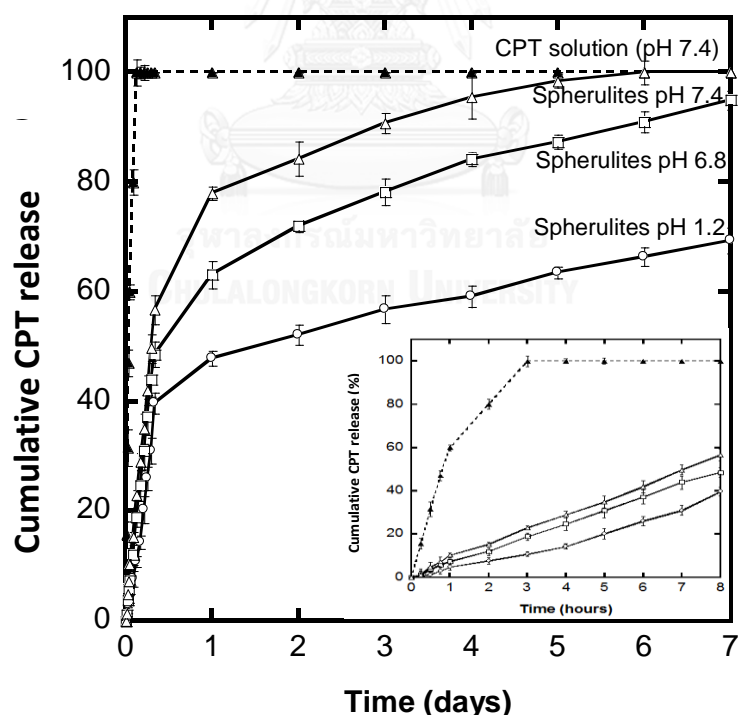


Figure 4.16 Release profiles of CPT from 1% CPT-loaded amphiphilic cationic cellulose spherulites in different pH solutions. The data are shown as the mean \pm SD and are derived from three independent repeats.

The *in vitro* release profiles of amphiphilic thiolated cationic aminocellulose loaded with 1% (w/w) to 3 and 5% (w/w) CPT in phosphate buffer solution (PBS, pH 7.4) are shown in Figure 4.17. With increasing the amount of CPT loading on the spherulites (from 1% to 3 and 5% (w/w)), resulted in a faster release profile of CPT of the higher loading of CPT, however, still displayed a sustained released thereafter over the 24 h period. It was obvious that the cumulative release of CPT enhanced with the amount of CPT in the formulation because the higher level of drug corresponding to a lower level of the polymer in the formulation. Moreover, higher drug levels in the formulation produced a higher drug concentration gradient between the polymers and dissolution medium, and thus the cumulative release of drug was also increased [103].

This phenomenon indicates that CPT was effectively encapsulated into the amphiphilic cationic aminocellulose spherulites and might be better alternative option to available drug carriers for cancer treatment.

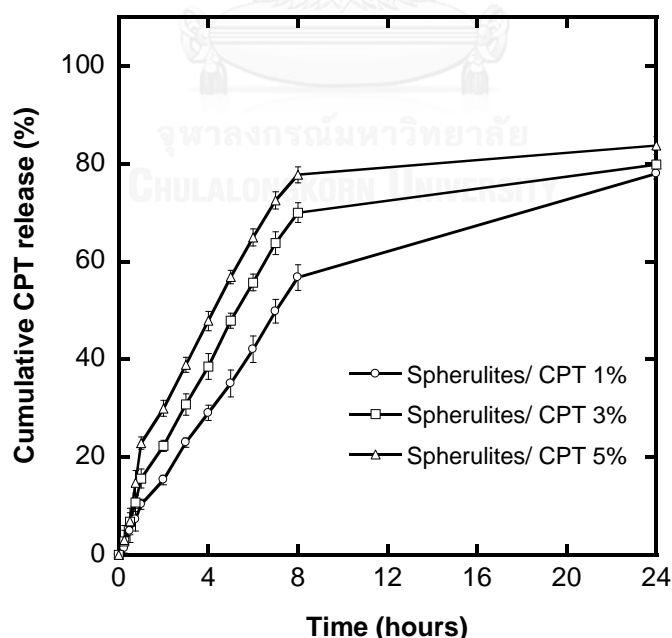


Figure 4.17 Release profiles of amphiphilic thiolated cationic cellulose loaded with 1% (w/w) to 3 and 5% (w/w) CPT in phosphate buffer solution (PBS, pH 7.4). The data are shown as the mean \pm SD and are derived from three independent repeats.

CHAPTER V

CONCLUSIONS

Amphiphilic thiolated cationic aminocellulose containing thiomers and positive charges was successfully synthesized as a drug delivery carrier in order to improve the mucoadhesive property and to release the capacity of the drug. The resulting amphiphilic thiolated cationic aminocellulose displayed 45.69 μmol immobilized free thiol groups and 14.54 μmol disulfide bonds per gram of polymer and also had a stronger mucoadhesive property compared to unmodified cellulose for all three different pH (pH 1.2, 6.8 and 7.2). In addition, the amphiphilic cationic aminocellulose and amphiphilic thiolated cationic aminocellulose were able to self-assemble in aqueous solution. On the SEM image of amphiphilic cationic aminocellulose, morphology of spherical shape stability of 233-495 nm in diameter and low particle size distribution were observed. On the other hand, the amphiphilic thiolated cationic aminocellulose showed a unique morphology of spherulites (urchin-like structure). An average spherulites size was in the range of 420-550 nm with a good stability in aqueous medium. Modified cellulose nanoparticles could be loaded with camptothecin (CPT), employed as a model anti-cancer drug, at an over 90% EE, and revealed both a reduced burst effect and a prolonged release of CPT over 7 days. The release rate of CPT from the nanocarriers was significantly accelerated by increasing pH and drug content. According to these results, CPT loaded amphiphilic thiolated cationic aminocellulose spherulites would be better alternative option to available drug carriers for cancer treatment.

REFERENCES

1. Khan, G.M. *Controlled release oral dosage forms: Some recent advances in the matrix type drug delivery systems*. Journal of Medical Sciences, 2001. **1**(5): p. 350-354.
2. Ludwig, A. *The use of mucoadhesive polymers in ocular drug delivery*. Advanced Drug Delivery Reviews, 2005. **57**(11): p. 1595-1639.
3. Salamat-Miller, N., Chittchang, M., and Johnston, T.P. *The use of mucoadhesive polymers in buccal drug delivery*. Advanced Drug Delivery Reviews, 2005. **57**(11): p. 1666-1691.
4. Kharenko, E.A., Larionova, N.I., and Demina, N.B. *Mucoadhesive drug delivery systems (Review)*. Pharmaceutical Chemistry Journal, 2009. **43**(4): p. 200-208.
5. Boddupalli, B.M., Mohammed, Z.N.K., Nath, R.A., and Banji, D. *Mucoadhesive drug delivery system: An overview*. Journal of Advanced Pharmaceutical Technology & Research, 2010. **1**(4): p. 381-387.
6. Shaikh, R., Raj Singh, T., Garland, M., Woolfson, A., and Donnelly, R. *Mucoadhesive drug delivery systems*. Journal of Pharmacy & Bioallied Sciences, 2011. **3**(1): p. 89-100.
7. Juntapram, K., Praphairaksit, N., Siraleartmukul, K., and Muangsin, N. *Electrosprayed polyelectrolyte complexes between mucoadhesive N,N,N-trimethylchitosan-homocysteine thiolactone and alginate/carrageenan for camptothecin delivery*. Carbohydrate Polymers, 2012. **90**(4): p. 1469-1479.
8. Ferreira, S., Coutinho, P.J.G., and Gama, F.M. *Synthesis and Characterization of Self-Assembled Nanogels Made of Pullulan*. Materials, 2011. **4**(4): p. 601-620.
9. Singh, M., Tiwary, A.K., and Kaur, G. *Investigations on interpolymer complexes of cationic guar gum and xanthan gum for formulation of bioadhesive films*. Research in Pharmaceutical Sciences, 2010. **5**(2): p. 79-87.
10. Zheng, C., Liu, X., Zhu, J., and Zhao, Y. *Preparation of cationic biodegradable dextran microspheres loaded with BSA and study on the mechanism of*

- protein loading*. Drug Development and Industrial Pharmacy, 2012. **38**(6): p. 653-658.
11. Song, Y., Sun, Y., Zhang, X., Zhou, J., and Zhang, L. *Homogeneous Quaternization of Cellulose in NaOH/Urea Aqueous Solutions as Gene Carriers*. Biomacromolecules, 2008. **9**(8): p. 2259-2264.
 12. Rahmat, D., Sakloetsakun, D., Shahnaz, G., Perera, G., Kaindl, R., and Bernkop-Schnürch, A. *Design and synthesis of a novel cationic thiolated polymer*. International Journal of Pharmaceutics, 2011. **411**(1-2): p. 10-17.
 13. Bernkop-Schnürch, A. and Steininger, S. *Synthesis and characterisation of mucoadhesive thiolated polymers*. International Journal of Pharmaceutics, 2000. **194**(2): p. 239-247.
 14. Bernkop-Schnürch, A., Scholler, S., and Biebel, R.G. *Development of controlled drug release systems based on thiolated polymers*. Journal of Controlled Release, 2000. **66**(1): p. 39-48.
 15. Bernkop-Schnürch, A. *Thiomers: A new generation of mucoadhesive polymers*. Advanced Drug Delivery Reviews, 2005. **57**(11): p. 1569-1582.
 16. Albrecht, K., Zirm, E.J., Palmberger, T.F., Schlocker, W., and Bernkop-Schnürch, A. *Preparation of Thiomers Microparticles and In Vitro Evaluation of Parameters Influencing Their Mucoadhesive Properties*. Drug Development and Industrial Pharmacy, 2006. **32**(10): p. 1149-1157.
 17. Sakloetsakun, D., Perera, G., Hombach, J., Millotti, G., and Bernkop-Schnürch, A. *The Impact of Vehicles on the Mucoadhesive Properties of Orally Administrated Nanoparticles: a Case Study with Chitosan-4-Thiobutylamidine Conjugate*. AAPS PharmSciTech, 2010. **11**(3): p. 1185-1192.
 18. Roldo, M., Hornof, M., Caliceti, P., and Bernkop-Schnürch, A. *Mucoadhesive thiolated chitosans as platforms for oral controlled drug delivery: synthesis and in vitro evaluation*. European Journal of Pharmaceutics and Biopharmaceutics, 2004. **57**(1): p. 115-121.
 19. Mourya, V.K. and Inamdar, N. *Trimethyl chitosan and its applications in drug delivery*. Journal of Materials Science: Materials in Medicine, 2009. **20**(5): p. 1057-1079.

20. Lee, W.J., Cha, S., Shin, M., Jung, M., Islam, M.A., Cho, C.S., and Yoo, H.S. *Efficacy of thiolated eudragit microspheres as an oral vaccine delivery system to induce mucosal immunity against enterotoxigenic Escherichia coli in mice*. European Journal of Pharmaceutics and Biopharmaceutics, 2012. **81**(1): p. 43-48.
21. Klemm, D., Heublein, B., Fink, H.P., and Bohn, A. *Cellulose: Fascinating Biopolymer and Sustainable Raw Material*. Angewandte Chemie International Edition, 2005. **44**(22): p. 3358-3393.
22. Chang, C. and Zhang, L. *Cellulose-based hydrogels: Present status and application prospects*. Carbohydrate Polymers, 2011. **84**(1): p. 40-53.
23. Kontturi, E., Tammelin, T., and Osterberg, M. *Cellulose-model films and the fundamental approach*. Chemical Society Reviews, 2006. **35**(12): p. 1287-1304.
24. Malm, C.J., Fordyce, C.R., and Tanner, H.A. *Properties of Cellulose Esters of Acetic, Propionic, and Butyric Acids*. Industrial & Engineering Chemistry, 1942. **34**(4): p. 430-435.
25. Edgar, K.J., Buchanan, C.M., Debenham, J.S., Rundquist, P.A., Seiler, B.D., Shelton, M.C., and Tindall, D. *Advances in cellulose ester performance and application*. Progress in Polymer Science, 2001. **26**(9): p. 1605-1688.
26. Mohanty, A.K., Wibowo, A., Misra, M., and Drzal, L.T. *Development of renewable resource-based cellulose acetate bioplastic: Effect of process engineering on the performance of cellulosic plastics*. Polymer Engineering & Science, 2003. **43**(5): p. 1151-1161.
27. Song, Y., Zhang, L., Gan, W., Zhou, J., and Zhang, L. *Self-assembled micelles based on hydrophobically modified quaternized cellulose for drug delivery*. Colloids and Surfaces B: Biointerfaces, 2011. **83**(2): p. 313-320.
28. Fayazpour, F., Lucas, B., Alvarez-Lorenzo, C., Sanders, N.N., Demeester, J., and De Smedt, S.C. *Physicochemical and Transfection Properties of Cationic Hydroxyethylcellulose/DNA Nanoparticles*. Biomacromolecules, 2006. **7**(10): p. 2856-2862.

29. Mazoniene, E., Joceviciute, S., Kazlauske, J., Niemeyer, B., and Liesiene, J. *Interaction of cellulose-based cationic polyelectrolytes with mucin*. Colloids and Surfaces B: Biointerfaces, 2011. **83**(1): p. 160-164.
30. Pašteka, M. *Quaternization of regenerated cellulose under homogeneous reaction conditions*. Acta Polymerica, 1988. **39**(3): p. 130-132.
31. Herben, V.M., ten Bokkel Huinink, W., and Beijnen, J. *Clinical Pharmacokinetics of Topotecan*. Clinical Pharmacokinetics, 1996. **31**(2): p. 85-102.
32. Hsiang, Y.H., Hertzberg, R., Hecht, S., and Liu, L.F. *Camptothecin induces protein-linked DNA breaks via mammalian DNA topoisomerase I*. Journal of Biological Chemistry, 1985. **260**(27): p. 14873-14878.
33. Liu, L.F. *DNA Topoisomerase Poisons as Antitumor Drugs*. Annual Review of Biochemistry, 1989. **58**(1): p. 351-375.
34. Min, K.H., Park, K., Kim, Y.S., Bae, S.M., Lee, S., Jo, H.G., Park, R.W., Kim, I.S., Jeong, S.Y., Kim, K., and Kwon, I.C. *Hydrophobically modified glycol chitosan nanoparticles-encapsulated camptothecin enhance the drug stability and tumor targeting in cancer therapy*. Journal of Controlled Release, 2008. **127**(3): p. 208-218.
35. Gottlieb, J.A. and Luce, J.K. *Treatment of malignant melanoma with camptothecin (NSC-100880)*. Cancer chemotherapy reports, 1972. **56**(1): p. 103-105.
36. Moertel, C.G., Schutt, A.J., Reitemeier, R.J., and Hahn, R.G. *Phase II study of camptothecin (NSC-100880) in the treatment of advanced gastrointestinal cancer*. Cancer chemotherapy reports. **56**(1): p. 95-101.
37. Muggia, F.M., Creaven, P.J., Hansen, H.H., Cohen, M.H., and Selawry, O.S. *Phase I clinical trial of weekly and daily treatment with camptothecin (NSC-100880): correlation with preclinical studies*. Cancer chemotherapy reports, 1972. **56**(4): p. 515-521.
38. Opanasopit, P., Ngawhirunpat, T., Chaidedgumjorn, A., Rojanarata, T., Apirakaramwong, A., Phongying, S., Choochottiros, C., and Chirachanchai, S. *Incorporation of camptothecin into N-phthaloyl chitosan-g-mPEG self-*

- assembly micellar system*. European Journal of Pharmaceutics and Biopharmaceutics, 2006. **64**(3): p. 269-276.
39. Yokoyama, M., Okano, T., Sakurai, Y., Ekimoto, H., Shibazaki, C., and Kataoka, K. *Toxicity and Antitumor Activity against Solid Tumors of Micelle-forming Polymeric Anticancer Drug and Its Extremely Long Circulation in Blood*. Cancer Research, 1991. **51**(12): p. 3229-3236.
 40. Yokoyama, M., Satoh, A., Sakurai, Y., Okano, T., Matsumura, Y., Kakizoe, T., and Kataoka, K. *Incorporation of water-insoluble anticancer drug into polymeric micelles and control of their particle size*. Journal of Controlled Release, 1998. **55**(2-3): p. 219-229.
 41. Yokoyama, M., Okano, T., Sakurai, Y., Fukushima, S., Okamoto, K., and Kataoka, K. *Selective Delivery of Adiramycin to a Solid Tumor Using a Polymeric Micelle Carrier System*. Journal of Drug Targeting, 1999. **7**(3): p. 171-186.
 42. Mizumura, Y., Matsumura, Y., Hamaguchi, T., Nishiyama, N., Kataoka, K., Kawaguchi, T., Hrushesky, W.J., Moriyasu, F., and Kakizoe, T. *Cisplatin-incorporated polymeric micelles eliminate nephrotoxicity, while maintaining antitumor activity*. Japanese Journal of Cancer Research, 2001. **92**(3): p. 328-336.
 43. Torchilin, V.P., Lukyanov, A.N., Gao, Z., and Papahadjopoulos-Sternberg, B. *Immunomicelles: Targeted pharmaceutical carriers for poorly soluble drugs*. Proceedings of the National Academy of Sciences, 2003. **100**(10): p. 6039-6044.
 44. Torchilin, V.P. *PEG-based micelles as carriers of contrast agents for different imaging modalities*. Advanced Drug Delivery Reviews, 2002. **54**(2): p. 235-252.
 45. Vinogradov, S.V., Bronich, T.K., and Kabanov, A.V. *Self-Assembly of Polyamine-Poly(ethylene glycol) Copolymers with Phosphorothioate Oligonucleotides*. Bioconjugate Chemistry, 1998. **9**(6): p. 805-812.
 46. Liaw, J., Chang, S.F., and Hsiao, F.C. *In vivo gene delivery into ocular tissues by eye drops of poly(ethylene oxide)-poly(propylene oxide)-poly(ethylene oxide) (PEO-PPO-PEO) polymeric micelles*. Gene Therapy, 2001. **8**(13): p. 999-1004.

47. Harada, A. and Kataoka, K. *Pronounced activity of enzymes through the incorporation into the core of polyion complex micelles made from charged block copolymers*. *Journal of Controlled Release*, 2001. **72**(1-3): p. 85-91.
48. Ahmad, Z., Shah, A., Siddiq, M., and Kraatz, H.-B. *Polymeric micelles as drug delivery vehicles*. *RSC Advances*, 2014. **4**(33): p. 17028-17038.
49. Blanz, A., Armes, S.P., and Ryan, A.J. *Self-Assembled Block Copolymer Aggregates: From Micelles to Vesicles and their Biological Applications*. *Macromolecular Rapid Communications*, 2009. **30**(4-5): p. 267-277.
50. Xiao, M., Xia, G., Wang, R., and Xie, D. *Controlling the self-assembly pathways of amphiphilic block copolymers into vesicles*. *Soft Matter*, 2012. **8**(30): p. 7865-7874.
51. Davis, S.S. *The design and evaluation of controlled release systems for the gastrointestinal tract*. *Journal of Controlled Release*, 1985. **2**(0): p. 27-38.
52. Chien, Y.W., *Novel drug delivery systems*, in *Oral drug delivery and delivery systems*, Chien, Y.W., Editor. 1992, Marcel Dekker Inc; : New York. p. 139-196.
53. Kaelble, D.H. and Moacanin, J. *A surface energy analysis of bioadhesion*. *Polymer*, 1977. **18**: p. 475-481.
54. Gu, J.M., Robinson, J.R., and Leung, S.H. *Binding of acrylic polymers to mucin/epithelial surfaces: structure-property relationships*. *Critical Reviews in Therapeutic Drug Carrier Systems*, 1988. **5**(1): p. 21-67.
55. Duchêne, D., Touchard, F., and Peppas, N.A. *Pharmaceutical and Medical Aspects of Bioadhesive Systems for Drug Administration*. *Drug Development and Industrial Pharmacy*, 1988. **14**(2-3): p. 283-318.
56. Hornof, M., Weyenberg, W., Ludwig, A., and Bernkop-Schnürch, A. *Mucoadhesive ocular insert based on thiolated poly(acrylic acid): development and in vivo evaluation in humans*. *Journal of Controlled Release*, 2003. **89**(3): p. 419-428.
57. Tafaghodi, M., Tabassi, S.A.S., Jaafari, M.-R., Zakavi, S.R., and Momen-nejad, M. *Evaluation of the clearance characteristics of various microspheres in the human nose by gamma-scintigraphy*. *International Journal of Pharmaceutics*, 2004. **280**(1-2): p. 125-135.

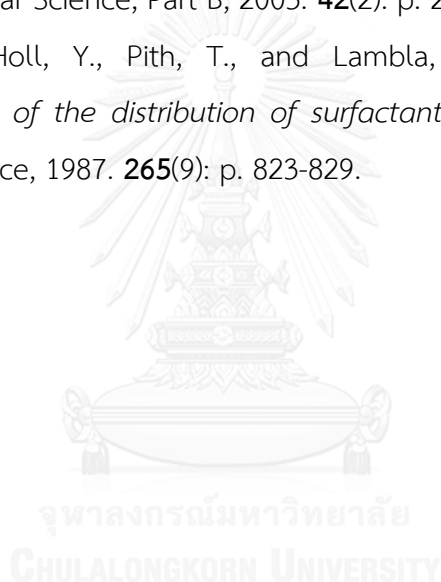
58. Bernkop-Schnürch, A. and Hornof, M. *Intravaginal drug delivery systems*. American Journal of Drug Delivery, 2003. **1**(4): p. 241-254.
59. Korbonits, M., Slawik, M., Cullen, D., Ross, R.J., Stalla, G., Schneider, H., Reincke, M., Bouloux, P.M., and Grossman, A.B. *A Comparison of a Novel Testosterone Bioadhesive Buccal System, Striant, with a Testosterone Adhesive Patch in Hypogonadal Males*. The Journal of Clinical Endocrinology & Metabolism, 2004. **89**(5): p. 2039-2043.
60. Tilloo, S.K., Rasala, T.M., and Kale, V.V. *Mucoadhesive microparticulate drug delivery system*. Journal of Pharmaceutics and Biopharmaceutics, 2011. **9**(1): p. 52-56.
61. Andrews, G.P., Lavery, T.P., and Jones, D.S. *Mucoadhesive polymeric platforms for controlled drug delivery*. European Journal of Pharmaceutics and Biopharmaceutics, 2009. **71**(3): p. 505-518.
62. Chowdary, K.P.R. and Srinivas, L. *Mucoadhesive drug delivery systems: A review of current status*. Indian Drugs, 2000. **37**(9): p. 400-406.
63. Smart, J.D. *The basics and underlying mechanisms of mucoadhesion*. Advanced Drug Delivery Reviews, 2005. **57**(11): p. 1556-1568.
64. Yang, X. and Robinson, J.R., *Bioadhesion in mucosal drug delivery*, in *Biorelated Polymers and Gels: Controlled Release and Applications in Biomedical Engineering*, T., O., Editor. 1998, Academic Press: San Diego, CA. p. 135-192.
65. Hubbell, J.A. *Biomaterials in tissue engineering*. Biotechnology, 1995. **13**(6): p. 565-576.
66. Peppas, N.A. and Sahlin, J.J. *Hydrogels as mucoadhesive and bioadhesive materials: a review*. Biomaterials, 1996. **17**(16): p. 1553-1561.
67. Wu, S., *Formation of adhesive bond*, in *Polymer Interface and Adhesion*. 1982, Marcel Dekker Inc: New York. p. 359-447.
68. Oh, H., Kim, K., and Kim, S. *Characterization of deposition patterns produced by twin-nozzle electrospray*. Journal of Aerosol Science, 2008. **39**(9): p. 801-813.

69. Kweon, D.K., Song, S.B., and Park, Y.Y. *Preparation of water-soluble chitosan/heparin complex and its application as wound healing accelerator*. *Biomaterials*, 2003. **24**(9): p. 1595-1601.
70. Allur, H.H., Johnston, T.P., and Mitra, A.K., *Encyclopedia of Pharmaceutical Technology*, Swarbrick, J. and Boylan, J.C., Editors. 1990, Marcel Dekker: NewYork. p. 193-218.
71. Huang, Y., Leobandung, W., Foss, A., and Peppas, N.A. *Molecular aspects of muco- and bioadhesion:: Tethered structures and site-specific surfaces*. *Journal of Controlled Release*, 2000. **65**(1-2): p. 63-71.
72. Sudhakar, Y., Kuotsu, K., and Bandyopadhyay, A.K. *Buccal bioadhesive drug delivery — A promising option for orally less efficient drugs*. *Journal of Controlled Release*, 2006. **114**(1): p. 15-40.
73. Ugwoke, M.I., Agu, R.U., Verbeke, N., and Kinget, R. *Nasal mucoadhesive drug delivery: Background, applications, trends and future perspectives*. *Advanced Drug Delivery Reviews*, 2005. **57**(11): p. 1640-1665.
74. Bernkop-Schnürch, A., Schwarz, V., and Steininger, S. *Polymers with Thiol Groups: A New Generation of Mucoadhesive Polymers?* *Pharmaceutical Research*, 1999. **16**(6): p. 876-881.
75. Snyder, G.H., Reddy, M.K., Cennerazzo, M.J., and Field, D. *Use of local electrostatic environments of cysteines to enhance formation of a desired species in a reversible disulfide exchange reaction*. *Biochim Biophys Acta.* , 1983. **749**(3): p. 219-226.
76. Alderman, D.A.A. *Review of cellulose ethers in hydrophilic matrices for oral controlled-release dosage forms*. *International Journal of Pharmaceutical Technology and Product Manufacture*, 1984. **5**: p. 1-9.
77. Sun Y., Lin L., Deng H., Li J., He B., Sun R., and P., O. *Structural changes of bamboo cellulose in formic acid*. *Bioresources*, 2008. **3**(2): p. 297-315.
78. Reier, C.E. and Shangraw, R.F. *Microcrystalline cellulose in tableting*. *Journal of Pharmaceutical Sciences*, 1966. **55**(5): p. 510-515.
79. Clausen, A.E. and Bernkop-Schnürch, A. *Thiolated carboxymethylcellulose: in vitro evaluation of its permeation enhancing effect on peptide drugs*.

- European Journal of Pharmaceutics and Biopharmaceutics, 2001. **51**(1): p. 25-32.
80. Sarti, F., Staaf, A., Sakloetsakun, D., and Bernkop-Schnürch, A. *Thiolated hydroxyethylcellulose: Synthesis and in vitro evaluation*. European Journal of Pharmaceutics and Biopharmaceutics, 2010. **76**(3): p. 421-427.
81. Takagai, Y., Shibata, A., Kiyokawa, S., and Takase, T. *Synthesis and evaluation of different thio-modified cellulose resins for the removal of mercury (II) ion from highly acidic aqueous solutions*. Journal of Colloid and Interface Science, 2011. **353**(2): p. 593-597.
82. Hu, H., Yu, L., Tan, S., Tu, K., and Wang, L.Q. *Novel complex hydrogels based on N-carboxyethyl chitosan and quaternized chitosan and their controlled in vitro protein release property*. Carbohydrate Research, 2010. **345**(4): p. 462-468.
83. Song, Y., Zhou, J., Li, Q., Guo, Y., and Zhang, L. *Preparation and Characterization of Novel Quaternized Cellulose Nanoparticles as Protein Carriers*. Macromolecular Bioscience, 2009. **9**(9): p. 857-863.
84. Zarth, C., Koschella, A., Pfeifer, A., Dorn, S., and Heinze, T. *Synthesis and characterization of novel amino cellulose esters*. Cellulose, 2011. **18**(5): p. 1315-1325.
85. Matsuda, A., Kobayashi, H., Itoh, S., Kataoka, K., and Tanaka, J. *Immobilization of laminin peptide in molecularly aligned chitosan by covalent bonding*. Biomaterials, 2005. **26**(15): p. 2273-2279.
86. Saboktakin, M.R., Tabatabaie, R.M., Maharramov, A., and Ramazanov, M.A. *Development and in vitro evaluation of thiolated chitosan-Poly(methacrylic acid) nanoparticles as a local mucoadhesive delivery system*. International Journal of Biological Macromolecules, 2011. **48**(3): p. 403-407.
87. Juntapram, K., Praphairaksit, N., Siraleartmukul, K., and Muangsin, N. *Synthesis and characterization of chitosan-homocysteine thiolactone as a mucoadhesive polymer*. Carbohydrate Polymers, 2012. **87**(4): p. 2399-2408.
88. Ponzio, E.A., Echevarria, R., Morales, G.M., and Barbero, C. *Removal of N-methylpyrrolidone hydrogen-bonded to polyaniline free-standing films by*

- protonation-deprotonation cycles or thermal heating*. Polymer International, 2001. **50**(11): p. 1180-1185.
89. Klemm, D., Heublein, B., Fink, H.-P., and Bohn, A. *Cellulose: Fascinating Biopolymer and Sustainable Raw Material*. Angewandte Chemie International Edition, 2005. **44**(22): p. 3358-3393.
 90. Isogai, I., *Allomorphs of cellulose and other polysaccharides*. Cellulosic Polymers, Blends and Composites, ed. Gilbert, R.D. 1994, Munich: Hanser Publishing.
 91. Liu, Y. and Hu, H. *X-ray diffraction study of bamboo fibers treated with NaOH*. Fibers and Polymers, 2008. **9**(6): p. 735-739.
 92. Das, K., Ray, D., Bandyopadhyay, N.R., Ghosh, T., Mohanty, A., and Misra, M. *A study of the mechanical, thermal and morphological properties of microcrystalline cellulose particles prepared from cotton slivers using different acid concentrations*. Cellulose, 2009. **16**(5): p. 783-793.
 93. Rosa, S.M.L., Rehman, N., de Miranda, M.I.G., Nachtigall, S.M.B., and Bica, C.I.D. *Chlorine-free extraction of cellulose from rice husk and whisker isolation*. Carbohydrate Polymers, 2012. **87**(2): p. 1131-1138.
 94. Jandura, P., Riedl, B., and Kokta, B.V. *Thermal degradation behavior of cellulose fibers partially esterified with some long chain organic acids*. Polymer Degradation and Stability, 2000. **70**(3): p. 387-394.
 95. Khutoryanskiy, V.V. *Advances in Mucoadhesion and Mucoadhesive Polymers*. Macromolecular Bioscience, 2011. **11**(6): p. 748-764.
 96. Honary, S. and Zahir, F. *Effect of Zeta Potential on the Properties of Nano-Drug Delivery Systems - A Review*. Tropical Journal of Pharmaceutical Research 2013. **12**(2): p. 255-264.
 97. McCarron, P.A., Marouf, W.M., Quinn, D.J., Fay, F., Burden, R.E., Olwill, S.A., and Scott, C.J. *Antibody Targeting of Camptothecin-Loaded PLGA Nanoparticles to Tumor Cells*. Bioconjugate Chemistry, 2008. **19**(8): p. 1561-1569.
 98. Luo, Y.L., Yang, X.L., Xu, F., Chen, Y.S., and Zhang, B. *Thermosensitive PNIPAM-b-HTPB block copolymer micelles: Molecular architectures and camptothecin drug release*. Colloids and Surfaces B: Biointerfaces, 2014. **114**(0): p. 150-157.

99. Bernheim-Grosswasser, A., Ugazio, S., Gauffre, F., Viratelle, O., Mahy, P., and Roux, D. *Spherulites: A new vesicular system with promising applications. An example: Enzyme microencapsulation*. The Journal of Chemical Physics, 2000. **112**(7): p. 3424-3430.
100. Freund, O., Amédee, J., Roux, D., and Laversanne, R. *In vitro and in vivo stability of new multilamellar vesicles*. Life Sciences, 2000. **67**(4): p. 411-419.
101. Magill, J.H. *Review Spherulites: A personal perspective*. Journal of Materials Science, 2001. **36**(13): p. 3143-3164.
102. Bassett, D.C. *Polymer Spherulites: A Modern Assessment*. Journal of Macromolecular Science, Part B, 2003. **42**(2): p. 227-256.
103. Zhao, C.L., Holl, Y., Pith, T., and Lambla, M. *FTIR-ATR spectroscopic determination of the distribution of surfactants in latex films*. Colloid and Polymer Science, 1987. **265**(9): p. 823-829.





APPENDIX

จุฬาลงกรณ์มหาวิทยาลัย
CHULALONGKORN UNIVERSITY

APPENDIX A

Standard curve of *L*-cysteine Hydrochloride

The concentrations versus peak absorbance of *L*-cysteine are presented in Table 1A. The plot of calibration curve of *L*-cysteine hydrochloride is illustrated in Figure 1A.

Table 1A Absorbance of various concentrations of *L*-cysteine Hydrochloride by UV Spectrometer

Concentration ($\mu\text{mol/L}$)	Abs.	Abs.	Abs.	AVG \pm SD
15.2582	0.0337	0.0341	0.0346	0.0341 ± 0.0005
30.5164	0.0680	0.0692	0.0697	0.0690 ± 0.0009
76.2911	0.1211	0.1210	0.1205	0.1209 ± 0.0003
152.5822	0.1920	0.1930	0.1940	0.1930 ± 0.0010
305.1643	0.3106	0.3100	0.3200	0.3135 ± 0.0056
509.6244	0.5350	0.5380	0.5370	0.5367 ± 0.0015
762.9108	0.7550	0.7560	0.7510	0.7540 ± 0.0026

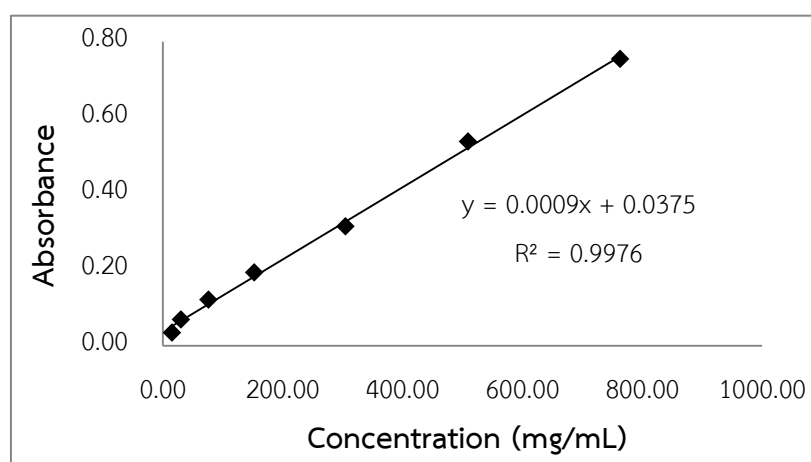


Figure 1A Standard curve of *L*-cysteine Hydrochloride by UV spectrometer

Table 2A Absorbance thiol groups by UV spectrometer

	Abs.	Abs.	Abs.	AVG	Thiol \pm SD (μ M)
Thiolated cationic aminocellulose	0.468	0.475	0.457	0.467	47.23 \pm 0.16
Amphiphilic thiolated cationic aminocellulose	0.445	0.439	0.435	0.443	45.69 \pm 0.38

Table 3A Absorbance disulfide groups by UV spectrometer

	Abs.	Abs.	Abs.	AVG	Disulfide \pm SD (μ M)
Thiolated cationic aminocellulose	0.222	0.229	0.210	0.220	6.79 \pm 0.06
Amphiphilic thiolated cationic aminocellulose	0.250	0.274	0.267	0.264	14.54 \pm 0.12

APPENDIX B

Calibration curve of mucin (type II)

The concentration versus peak absorbance mucin glycoprotein (type II) determined by UV is presented in Table 1B. The plot of calibration curve of mucin is illustrated in Figure 1B.

Table 1B Absorbance concentrations of mucin (type II) at pH 1.2, 6.8 and 7.4 by UV spectrometer

Concentration (mg/ 2mL)	HCl (pH 1.2)	PBS (PH 6.8)	PBS (PH 7.4)
0.2	0.063	0.260	0.236
0.4	0.131	0.527	0.609
0.6	0.184	0.766	0.869
0.8	0.224	1.000	1.122
1.0	0.275	1.29	1.371

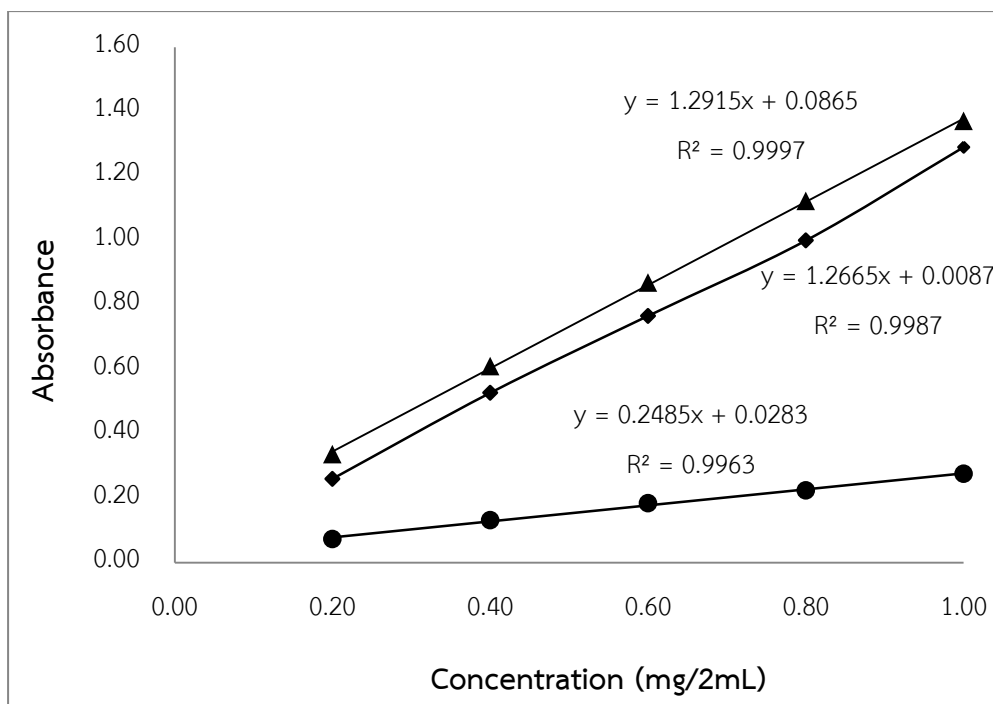


Figure 1B Standard curve of mucin at pH 1.2, 6.8, and 7.4

Table 2B Absorbance of various concentrations of mucin (type II) at pH 1.2

	Abs.	Abs.	Abs.	Absorbed mucin (mg) ± SD
Cellulose	0.111	0.104	0.118	0.08 ± 0.01
Cationic aminocellulose	0.082	0.104	0.095	0.21 ± 0.02
Thiolated cationic aminocellulose	0.087	0.089	0.080	0.27 ± 0.04
Amphiphilic thiolated cationic aminocellulose	0.083	0.078	0.088	0.29 ± 0.04

Table 3B Absorbance of various concentrations of mucin (type II) at pH 6.8

	Abs.	Abs.	Abs.	Absorbed mucin (mg) \pm SD
Cellulose	0.792	0.781	0.778	0.18 \pm 0.04
Cationic aminocellulose	0.547	0.544	0.539	0.40 \pm 0.05
Thiolated cationic aminocellulose	0.234	0.226	0.235	0.67 \pm 0.03
Amphiphilic thiolated cationic aminocellulose	0.214	0.215	0.203	0.69 \pm 0.10

Table 4B Absorbance of various concentrations of mucin (type II) at pH 7.4

	Abs.	Abs.	Abs.	Absorbed mucin (mg) \pm SD
Cellulose	0.666	0.653	0.683	0.20 \pm 0.06
Cationic aminocellulose	0.498	0.491	0.487	0.43 \pm 0.05
Thiolated cationic aminocellulose	0.262	0.255	0.265	0.73 \pm 0.08
Amphiphilic thiolated cationic aminocellulose	0.250	0.272	0.211	0.75 \pm 0.07

APPENDIX C

Calibration curve of CPT

Table 1C Absorbance of CPT drug in DMSO determined in 370 nm

Concentration (ppm)	Abs.	Abs.	Abs.	AVG \pm SD
5	0.2612	0.2662	0.2767	0.2680 \pm 0.0082
10	0.5959	0.6116	0.5892	0.5989 \pm 0.0112
15	0.8930	0.8770	0.9428	0.9043 \pm 0.0039
20	1.2187	1.2235	1.2430	1.2284 \pm 0.0130
25	1.5258	1.5390	1.4919	1.5189 \pm 0.0247

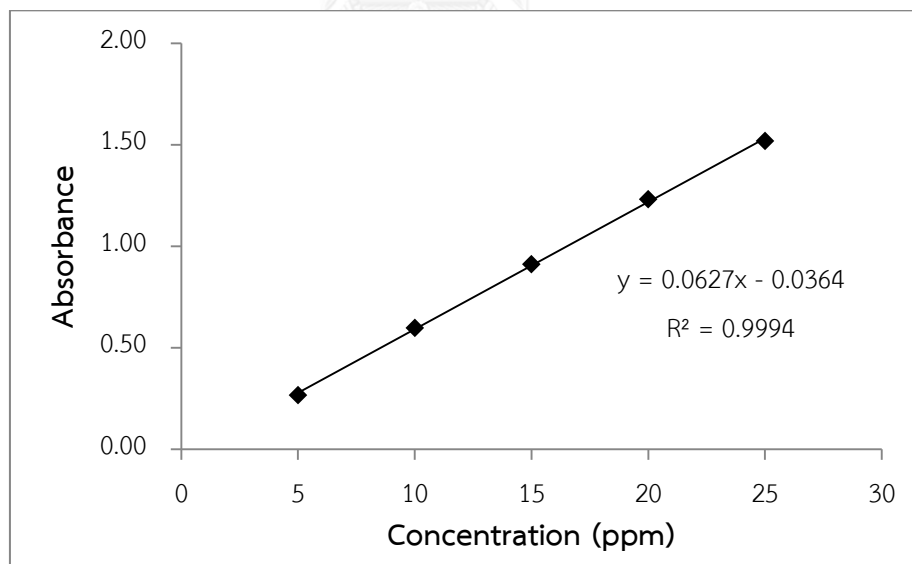
**Figure 1C** Calibration curve of CPT in DMSO determined in 370 nm.

Table 2C Absorbance of CPT drug in pH 1.2 determined in 370 nm

Concentration (ppm)	Abs.	Abs.	Abs.	AVG \pm SD
5	0.2412	0.2554	0.2436	0.2467 \pm 0.0076
10	0.5863	0.6023	0.5740	0.5875 \pm 0.0142
15	0.9126	0.9013	0.9116	0.9085 \pm 0.0063
20	1.2319	1.1420	1.2440	1.2060 \pm 0.0557
25	1.5422	1.5186	1.5010	1.5206 \pm 0.0207

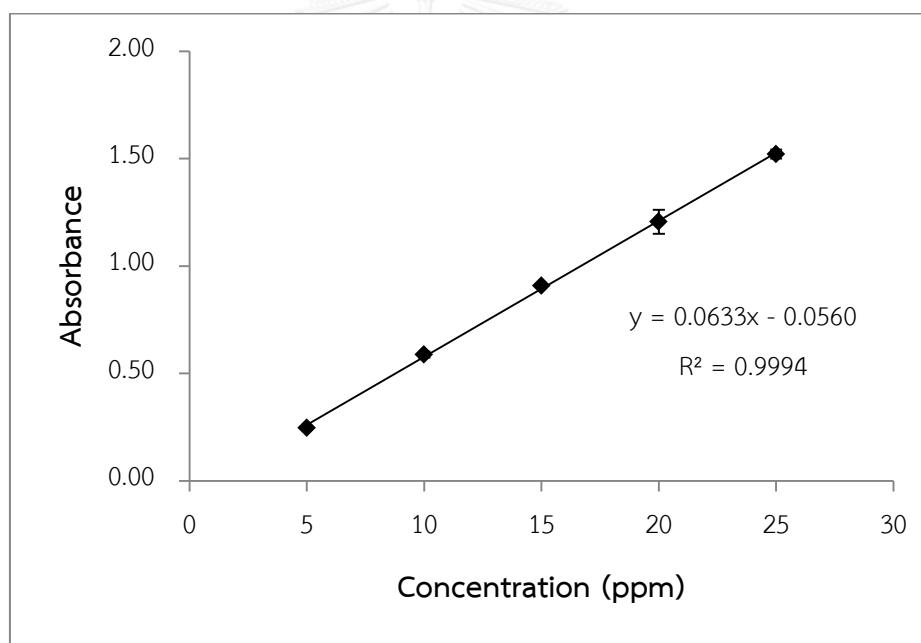
**Figure 2C** Calibration curve of CPT in pH 1.2 determined in 370 nm.

Table 3C Absorbance of CPT drug in pH 6.8 determined in 370 nm

Concentration (ppm)	Abs.	Abs.	Abs.	AVG \pm SD
5	0.2589	0.2717	0.2675	0.2660 \pm 0.0065
10	0.5940	0.6000	0.5975	0.5972 \pm 0.0030
15	0.9114	0.9096	0.9123	0.9111 \pm 0.0014
20	1.2313	1.2325	1.2297	1.2312 \pm 0.0014
25	1.5233	1.5157	1.5140	1.5177 \pm 0.0050

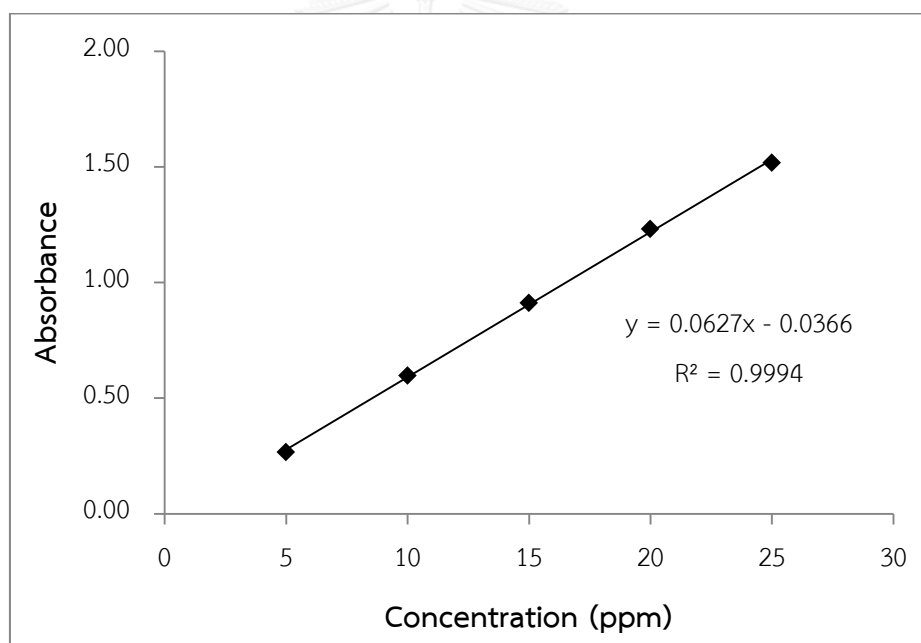
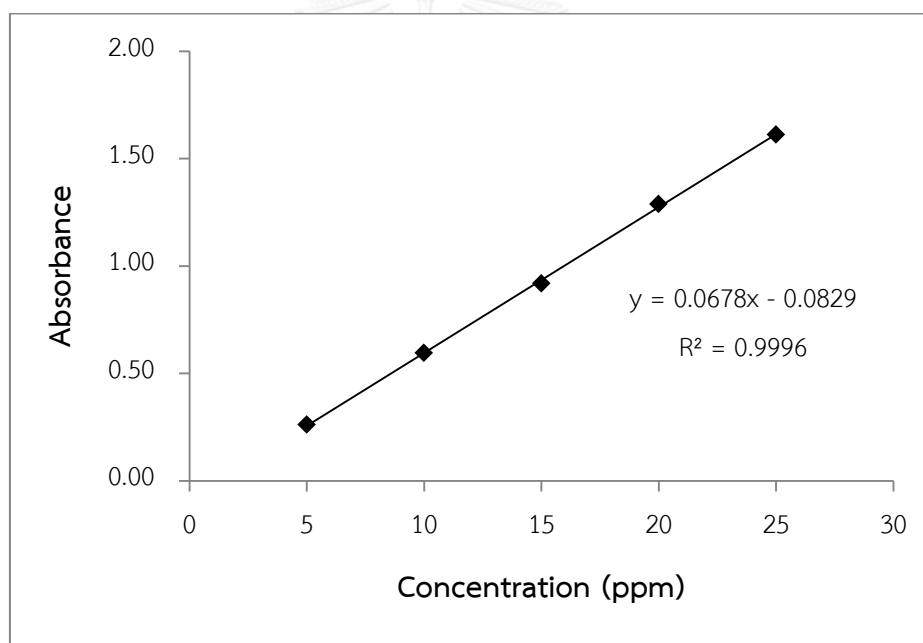
**Figure 3C** Calibration curve of CPT in pH 6.8 determined in 370 nm.

Table 4C Absorbance of CPT drug in pH 7.4 determined in 370 nm

Concentration (ppm)	Abs.	Abs.	Abs.	AVG \pm SD
5	0.2512	0.2647	0.2676	0.2612 \pm 0.0088
10	0.5911	0.5968	0.5992	0.5957 \pm 0.0042
15	0.9220	0.9198	0.9126	0.9181 \pm 0.0049
20	1.2871	1.3050	1.2712	1.2878 \pm 0.0169
25	1.6240	1.6157	1.5942	1.6113 \pm 0.0154

**Figure 4C** Calibration curve of CPT in pH 7.4 determined in 370 nm.

APPENDIX D

Cumulative CPT Release

Table 1D Cumulative 1% CPT release from amphiphilic cationic aminocellulose micelles in pH 1.2, 6.8 and 7.4

Times (days)	Amount of CPT release			
	Pure CPT pH 7.4	Micelles pH 1.2	Micelles pH 6.8	Micelles pH 7.4
0.00	0.00 ± 0.00	0.00 ± 0.00	0.00 ± 0.00	0.00 ± 0.00
0.01	15.76 ± 2.46	5.98 ± 1.58	7.35 ± 1.19	9.99 ± 2.41
0.02	31.64 ± 3.35	10.35 ± 2.77	14.14 ± 1.17	16.25 ± 1.58
0.03	47.04 ± 2.46	13.03 ± 2.55	18.88 ± 1.24	20.94 ± 2.46
0.04	60.03 ± 1.35	15.27 ± 1.27	22.23 ± 2.64	25.08 ± 0.88
0.08	80.02 ± 2.35	21.03 ± 1.92	28.95 ± 1.47	33.96 ± 1.57
0.13	100.00 ± 2.35	24.93 ± 0.67	34.34 ± 2.44	39.56 ± 1.46
0.17	100.00 ± 1.04	27.90 ± 1.23	39.02 ± 0.89	44.78 ± 1.22
0.21	100.00 ± 1.35	31.35 ± 2.30	43.14 ± 1.43	49.96 ± 1.21
0.25	100.00 ± 0.00	34.85 ± 1.21	46.75 ± 2.57	54.64 ± 0.76
0.29	100.00 ± 0.00	38.05 ± 2.50	50.76 ± 0.70	59.64 ± 1.98
0.33	100.00 ± 0.00	41.04 ± 1.37	54.85 ± 0.88	64.35 ± 0.77
1.00	100.00 ± 0.00	45.75 ± 2.70	62.34 ± 2.41	74.56 ± 2.85
2.00	100.00 ± 0.00	49.84 ± 1.76	69.33 ± 1.39	80.77 ± 1.71
3.00	100.00 ± 0.00	53.82 ± 1.34	77.16 ± 0.88	87.35 ± 1.91
4.00	100.00 ± 0.00	57.75 ± 1.94	82.33 ± 1.65	90.76 ± 1.24

Times (days)	Amount of CPT release			
	Pure CPT pH 7.4	Micelles pH 1.2	Micelles pH 6.8	Micelles pH 7.4
5.00	100.00 ± 0.00	60.66 ± 2.23	85.21 ± 1.42	94.47 ± 1.46
6.00	100.00 ± 0.00	63.45 ± 1.33	87.25 ± 1.99	96.78 ± 1.54
7.00	100.00 ± 0.00	65.85 ± 1.32	88.24 ± 2.11	98.55 ± 2.14



Table 2D Cumulative 1% CPT release from amphiphilic thiolated cationic aminocellulose micelles in pH 1.2, 6.8 and 7.4

Times (days)	Amount of CPT release			
	Pure CPT pH 7.4	Spherulites pH 1.2	Spherulites pH 6.8	Spherulites pH 7.4
0.00	0.00 ± 0.00	0.00 ± 0.00	0.00 ± 0.00	0.00 ± 0.00
0.01	15.76 ± 2.46	0.73 ± 2.35	1.13 ± 2.83	1.39 ± 1.34
0.02	31.64 ± 3.35	1.38 ± 2.56	3.83 ± 0.85	4.86 ± 2.34
0.03	47.04 ± 2.46	2.99 ± 1.57	5.87 ± 0.73	7.25 ± 2.36
0.04	60.03 ± 1.35	4.85 ± 1.45	7.42 ± 1.35	10.36 ± 1.03
0.08	80.02 ± 2.35	7.75 ± 1.45	12.09 ± 1.83	15.34 ± 0.95
0.13	100.00 ± 2.35	10.85 ± 0.98	18.94 ± 1.75	22.98 ± 0.98
0.17	100.00 ± 1.04	14.35 ± 1.22	24.73 ± 2.85	29.05 ± 1.57
0.21	100.00 ± 1.35	20.35 ± 2.45	31.02 ± 3.35	35.04 ± 2.76
0.25	100.00 ± 0.00	26.03 ± 2.11	37.29 ± 3.32	42.05 ± 2.74
0.29	100.00 ± 0.00	31.05 ± 2.33	43.98 ± 3.11	49.85 ± 2.42
0.33	100.00 ± 0.00	39.75 ± 1.93	48.63 ± 2.34	56.74 ± 2.64
1.00	100.00 ± 0.00	47.92 ± 1.37	63.14 ± 2.45	78.03 ± 1.21
2.00	100.00 ± 0.00	52.21 ± 1.84	72.04 ± 1.10	84.27 ± 3.12
3.00	100.00 ± 0.00	56.82 ± 2.53	78.23 ± 2.43	90.75 ± 1.82
4.00	100.00 ± 0.00	59.21 ± 1.92	84.20 ± 1.22	95.48 ± 3.87
5.00	100.00 ± 0.00	63.56 ± 1.03	87.34 ± 1.25	98.44 ± 1.16
6.00	100.00 ± 0.00	66.42 ± 1.73	91.00 ± 1.89	100.00 ± 2.19
7.00	100.00 ± 0.00	69.37 ± 2.35	94.92 ± 1.74	100.00 ± 0.44

Table 3D Cumulative 1%, 3% and 5% CPT release from amphiphilic thiolated cationic aminocellulose micelles in pH 7.4

Times (days)	Amount of CPT release in pH 7.4			
	Pure CPT	Spherulites/ CPT 1%	Spherulites/ CPT 3%	Spherulites/ CPT 5%
0.00	0.00 ± 0.00	0.00 ± 0.00	0.00 ± 0.00	0.00 ± 0.00
0.01	15.76 ± 2.46	1.39 ± 1.34	4.73 ± 2.34	5.08 ± 2.95
0.02	31.64 ± 3.35	4.86 ± 2.34	8.83 ± 1.84	8.87 ± 2.73
0.03	47.04 ± 2.46	7.25 ± 2.36	13.74 ± 1.85	14.74 ± 2.53
0.04	60.03 ± 1.35	10.36 ± 1.03	18.64 ± 1.93	19.87 ± 1.28
0.08	80.02 ± 2.35	15.34 ± 0.95	25.34 ± 1.12	26.97 ± 1.65
0.13	100.00 ± 2.35	22.98 ± 0.98	33.76 ± 2.19	34.87 ± 1.53
0.17	100.00 ± 1.04	29.05 ± 1.57	40.53 ± 2.64	42.86 ± 1.98
0.21	100.00 ± 1.35	35.04 ± 2.76	48.87 ± 1.54	48.84 ± 1.36
0.25	100.00 ± 0.00	42.05 ± 2.74	55.74 ± 1.74	58.97 ± 1.76
0.29	100.00 ± 0.00	49.85 ± 2.42	63.76 ± 2.37	67.53 ± 1.76
0.33	100.00 ± 0.00	56.74 ± 2.64	70.02 ± 2.03	76.76 ± 1.63
1.00	100.00 ± 0.00	78.03 ± 1.21	79.87 ± 2.85	83.73 ± 1.85
2.00	100.00 ± 0.00	84.27 ± 3.12	88.00 ± 2.32	90.27 ± 1.74
3.00	100.00 ± 0.00	90.75 ± 1.82	94.82 ± 2.10	94.08 ± 2.05
4.00	100.00 ± 0.00	95.48 ± 3.87	98.14 ± 2.87	99.28 ± 2.10
5.00	100.00 ± 0.00	98.44 ± 1.16	100.00 ± 1.98	100.00 ± 2.84
6.00	100.00 ± 0.00	100.00 ± 2.19	100.00 ± 1.09	100.00 ± 1.04
7.00	100.00 ± 0.00	100.00 ± 0.44	100.00 ± 1.66	100.00 ± 1.32

VITA

Name: Kultida Songsurang

Date of birth: July 28, 1985

Nationality: Thai

Address: 32/72 Prachasuk City Village, Pracha Uthid 58/1 Road, Thungkru, Bangkok 10140

University Education: Bachelor's Degree from Department of Chemistry, Faculty of Science, Chulalongkorn University, 2004-2008

Master's Degree from Program of Petrochemistry and Polymer Science, Faculty of Science, Chulalongkorn University, 2008-2010

Doctoral's Degree from School of Materials Science, Japan Advanced Institute of Science and Technology, 2011-2014

Conference attendance: Up to 14 international and domestic conferences

- Publication:
1. K. Songsurang, et al., AAPS PharmSciTech, 2011, 12, 35-45.
 2. K. Songsurang, N. et al., Archives of Pharmacal Research, 2011, 34, 583-592.
 3. K. Songsurang, et al., Carbohydrate Polymers, 2013, 98, 1335-1342.
 4. K. Songsurang, et al., Cellulose, 2013, 20, 83-96.
 5. K. Songsurang, et al., European Polymer Journal, 2014, 59, 105-112.
 6. K. Songsurang, et al., Handbook of Sustainable Polymers: Processing and Applications, to be published by Stanford publisher –Singapore. Accepted
 8. K. Songsurang, et al., Carbohydrate Polymers, Revised.
 9. K. Songsurang, et al., Journal of Microencapsulation, Submitted.